Flake graphite prospects in the Fennoscandian Shield

Jenny Palosaari

Licentiate thesis

ÅBO AKADEMI UNIVERSITY

Geology and Mineralogy

April 2021

ÅBO AKADEMI UNIVERSITY

Geology and Mineralogy

JENNY PALOSAARI: Flake graphite prospects in the Fennoscandian Shield

Licentiate thesis, 50 p.

Geology and Mineralogy

April 2021

Abstract

Natural graphite is listed among the critical raw materials for the European Union because of its economic importance and supply risk. Natural graphite is needed in batteries and energy storage and the demand is growing continuously. This thesis describes two flake graphite occurrences in Fennoscandia and is motivated by the importance of graphite for the future. The flake graphite occurrences in Sortland (Norway) and in Piippumäki (Finland) were studied. Sampled graphite-bearing rocks and liberated graphite flakes were examined and analyzed with petrographic microscopy, scanning electron microscopy (SEM), X-ray diffraction (XRD) and Raman spectroscopy.

The precursor of flake graphite is amorphous graphite, which is formed from organic matter that has usually deposited in sediments offshore. Flake graphite is formed during increasing metamorphic conditions when the graphene layers in graphite are arranged parallel to one another, the spacing between the graphene layers decreases, and the remaining impurities are removed. The bedrock in Fennoscandia, especially in Finland, is mostly metamorphosed at high grade. There are also many occurrences of metamorphosed black shales (which contain graphite) in these areas, which increases the potential of finding high-quality flake graphite.

The results of this study show that the flake graphite found in both Sortland and Piippumäki are of high quality with minor or no defects. The flakes are up to 1 mm in size and the obtained Raman spectra show that the graphite often lacks the defect band. The characteristic bands shown by the Raman spectra indicate conditions in which the graphite formed, including additional bands formed by defects, which decrease with a higher degree of metamorphism. The results also show that the graphite is unaffected by retrograde metamorphism.

The interest in graphite exploration and the refinement of battery anode technology is increasing in Fennoscandia. The results from this study indicate that the studied graphite is of high quality, that similar graphite deposits of high quality are found in Fennoscandia, and that high-quality graphite can also be found in areas affected by retrograde metamorphism.

Abstrakt på svenska

Europeiska Unionen har listat naturlig grafit som ett kritiskt material, grundat på dess ekonomiska betydelse och att det inte produceras inom EU. Naturlig grafit behövs inom batteriindustrin och lagring av energi och efterfrågan ökar kontinuerligt. Denna avhandling beskriver två förekomster av flakgrafit i den Fennoskandiska skölden: Sortland i Norge och Piippumäki i Finland, och studien är motiverad av grafitens betydelse för framtiden. De provtagna grafitförande bergarterna och de frigjorda grafitflaken studerades och analyserades med petrografiskt mikroskop, svepelektronmikroskop (SEM), röntgendiffraktion (XRD) och Ramanspektroskopi.

Flakgrafit utvecklas från amorf grafit, som i sin tur härstammar från organiskt material som har avlagrats i sediments på havsbottnen. Flakgrafit formas under stigande metamorfa förhållanden genom att grafenlagren i grafit ordnas parallellt i relation till varandra, mellanrummet mellan grafenlagren minskar och att föroreningar försvinner. Berggrunden i Fennoskandien, och speciellt i Finland, är till stor del genomgått metamorfos av hög grad. Dessa områden innefattar även förekomster av svartskiffrar (som innehåller grafit), vilket ökar möjligheten till att hitta flakgrafit av hög kvalitet.

Resultaten som erhållits i denna studie visar att flakgrafiten är av hög kvalitet med få eller inga defekter. Grafitflaken är upp till 1 mm i storlek och de erhållna Raman spektran visar de karakteristiska banden för grafit och att grafiten oftast saknar defektbandet. Defekter i grafiten minskar och försvinner med ökande metamorfosgrad. Resultaten visar också att grafitens kvalitet inte har påverkats av retrograd metamorfos, som kan observeras i tunnslip.

Prospektering av grafit och satsningar kring batteriproduktion är för tillfället på hög nivå i Fennoskandien. Resultaten från denna studie tyder att den studerade flakgrafiten är av hög kvalitet, att liknande grafitförekosmter har påträffats på andra håll i Fennoskandien, och att det även i områden påverkade av retrograd metamorfos kan hittas grafit av hög kvalitet.

Contents

1 Introduction

Natural graphite has been listed as a critical raw material for the European Union since 2011 (European Commission, 2020). According to the World Bank (2020), the production of natural graphite has to increase by up to 500 % to meet the growing demand in energy storage by 2050. The aim of this research is to characterize flake graphite of high quality in Fennoscandia. Two different areas have been studied and are described in this thesis: Sortland in Vesterålen, Norway, and Piippumäki in eastern Finland. These areas are also compared to other occurrences of natural graphite in the Fennoscandian Shield. In this study, high-quality flake graphite is defined as being free from defects and impurities.

Natural graphite can be divided into three different types: amorphous, flake and vein graphite. Amorphous graphite can be found in low-grade metamorphic areas, while flake graphite is formed during increasing metamorphic conditions. During graphitization, the sheets of graphene are arranged parallel to one another, which results in the flakiness of graphite. The amount of impurities in graphite also decreases during this process (Beyssac and Rumble, 2014). The graphitization process is progressive and an irreversible transformation of organic matter to graphite (Buseck and Beyssac, 2014). Vein graphite is formed when carbon-rich fluids precipitate in fractures in igneous rocks and granulite facies terrains (Luque et al., 2014).

Raman spectroscopy is a suitable analytical instrument for characterizing graphite, since graphite shows characteristic bands in the obtained Raman spectra. Raman spectroscopy can also be used to determine the peak metamorphic temperature in graphite (Beyssac et al., 2002), which can be used as a reference, alongside other geothermometers, to determine metamorphic degree through petrographic analysis of thin sections. X-ray diffraction (XRD) and scanning electron microscopy (SEM) were also utilized to analyze the quality of the sampled graphite, as well as petrographic studies of thin sections of the graphite-bearing and surrounding rocks.

1.1 Scope

This licentiate thesis focuses on identifying flake graphite occurrences in Fennoscandia and aims to answer the following questions:

- Are the flake graphite occurrences in Fennoscandia of high quality?
- Which factors contribute to the formation of high-quality flake graphite?
- Can retrograde metamorphism affect the quality of graphite?

To answer these questions, this study required the following steps:

- Determination of what high-quality graphite is
- Finding potential graphite occurrences in Fennoscandia by reviewing existing research
- Field work and sampling of graphite-bearing rocks
- Sample preparation for analyses and use of SEM, XRD and Raman spectroscopy

This work is part of the project FennoFlakes, which aims at creating a uniform value chain for Finnish flake graphite: from raw material to applications (see Lund et al., 2021). FennoFlakes is a collaboration between Geology and Mineralogy, and the Laboratory of Molecular Science and Engineering at Åbo Akademi University. The field work is done in collaboration with the exploration company Fennoscandian Resources Oy, and sample fragmentation and pseudosection construction together with the Geological Survey of Finland.

1.2 Publications

Two peer-reviewed articles were published during this work:

- Palosaari, J., Latonen, R-M., Smått, J-H., Blomqvist, R. & Eklund, O. (**2016**) *High-quality flake graphite in a high-grade metamorphic region in Sortland, Vesterålen, northern Norway.* Norwegian Journal of Geology, vol 96, 19-26.
- Palosaari, J., Latonen, R-M., Smått, J-H., Raunio, S. & Eklund, O. (**2020**) *The flake graphite prospect of Piippumäki – an example of a high-quality graphite occurrence in a retrograde metamorphic terrain in Finland.* Mineralium Deposita, 55, 1647–1660.

2 Graphite

Graphite is a mineral consisting only of carbon with a hexagonal crystal structure. Graphite is built up by layers of graphene, which are one atom thick layers of carbon atoms. The graphene layers are stacked in an ABAB-sequence in a hexagonal structure with 0.3354 nm distance between the layers (Fig. 1). There are three different types of natural graphite: amorphous, flake, and vein graphite.
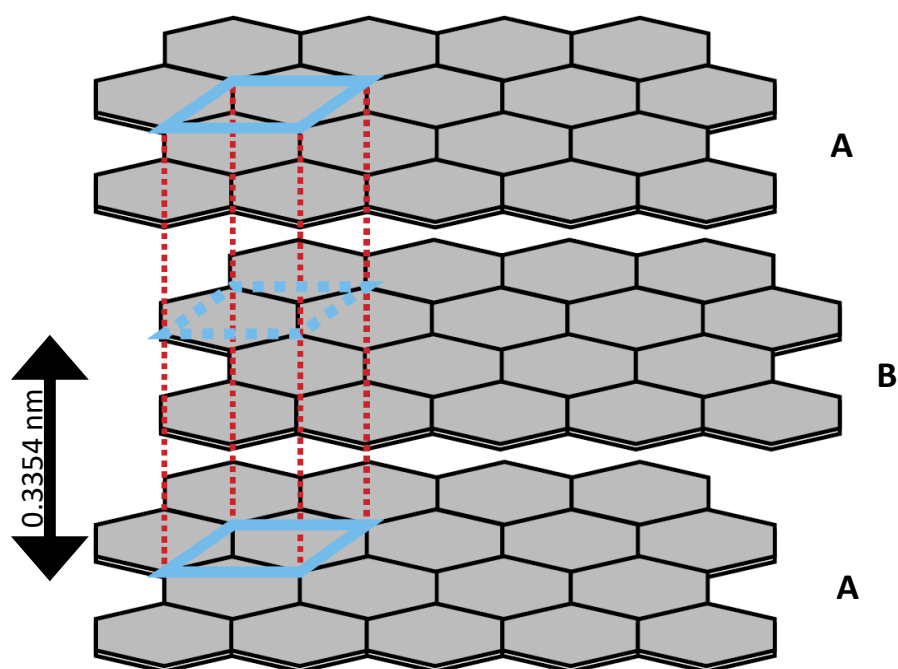

Figure 1. Crystal structure and the unit cell of graphite. The distance between the graphene sheets (in gray) is 0.3354 nm. Modified from Beyssac and Rumble (2014).

Amorphous graphite, or microcrystalline graphite, is found in low-grade metamorphic rocks and consists of small grains of graphite. Crystalline flake graphite is found in high-grade metamorphic rocks and is flaky, soft, and silvery in appearance and usually up to 1 cm in crystal size (Fig. 2) (Beyssac & Rumble, 2014; Robinson et al., 2017). Commercially, flake graphite is classified based on diameter, namely coarse (150-850 µm) and fine flakes (45-150 µm). The fine flakes can be further divided into 100-150 µm, 75-100 µm and <75 µm (Chelgani et al., 2016). Vein graphite is precipitated from carbon-rich fluids (Luque et al., 2014), and appears as coarse flakes called lump or chip and has the highest value on the market (Robinson et al., 2017). Graphite can be used in a range of different applications owing to its properties of both metals and nonmetals, such as high electrical and thermal conductivity, high thermal resistance, lubricity, and chemical inertness. The biggest producers of natural graphite are China, India, and Brazil (Robinson et al., 2017).

Figure 2. Graphite sample collected in Piippumäki, eastern Finland.

2.1 Formation

Graphite originates from organic matter and the process forming graphite is called graphitization, preceded by a carbonization process. During the carbonization process organic matter transforms to a carbonaceous solid residue, which can be graphitized during metamorphism. During the graphitization process, the spacing between the graphene layers is decreased, the graphene layers are organized parallel to one another, and the lattice structure is improved (Landis, 1971; Buseck and Beyssac, 2014). Landis (1971) shows the formation of graphite is temperature dependent, and that fully ordered graphite is encountered at upper greenschist-lower amphibolite facies. Flake graphite is formed during upper amphibolite and granulite facies metamorphism (Simandl et al., 2015). The graphitization process is irreversible, and graphite can be used as an indicator for metamorphic grade (Buseck and Beyssac, 2014).

Vein graphite is formed through precipitation of carbon-rich fluids in fractures, but the source of the carbon differs between deposits hosted in granulite and igneous rocks. The graphite in vein deposits is characterized as flaky with high crystallinity and purity. Granulite rocks usually host monomineralic graphite veins, while those in igneous rocks are often associated with hydrous minerals or magmatic sulfides (Luque et al., 2014).

2.2 Applications

Due to its properties of both metals and nonmetals, graphite is suitable for many different applications. For example, natural graphite is used for example in fuel cells, batteries, brakes, refractories, carbon brushes, and lubricants, and is therefore important within energy production and energy storage applications. Amorphous graphite is mainly used in refractories, while coarser flake graphite is used, for example, in lubricants for high temperatures and battery applications (Robinson et al., 2017). Graphite from vein deposits is mainly used by the refractory and lubricant industry. Based on the high purity and crystallinity in vein graphite, it could be suitable for use in high-quality fuel cells and Li-ion batteries (Luque et al., 2014; Robinson et al. 2017). Due to the increasing demand for graphite, it is listed among the critical raw materials for the European Union (European Commission, 2020). The production of natural graphite should also increase by more than 500 % by 2050 to meet the demands of energy storage technology (World Bank, 2020).

3 Materials and methods

Flake graphite has been examined at two different locations for this study: Sortland in Vesterålen, northern Norway (Palosaari et al., 2016) and Piippumäki in eastern Finland (Palosaari et al., 2020). Both areas have been studied to some extent previously by others, for example, Gautneb and Tveten (2000), and Simonen (1982). Historical mining of graphite has also been conducted in the areas. All analyzed samples are presented in Appendix I showing which method has been applied.

3.1 Sortland, Vesterålen

Three different areas were studied ca. 10 km from the town of Sortland in Vesterålen: Hornvatnet, Lamarkvatnet, and Vikeid (Fig. 3). The areas include historical graphite mines and were studied in the 19th and 20th centuries. The first memorandum is from 1820 and first commercial mining was done during 1899-1914 (Gautneb and Tveten, 2000). Field work consisted of geological mapping and sampling of graphite-bearing rocks and surrounding lithologies. The graphite-bearing rocks were poorly exposed and encountered in old excavations and ditches in the area (Fig. 4). The flake graphite is found disseminated in pyroxene gneiss, and as thicker layers of graphite schist. The amount of graphite in the area ranges from ca. 10 to 30 %, with an average graphite content of ca. 19 % (Gautneb and Tveten, 1992).
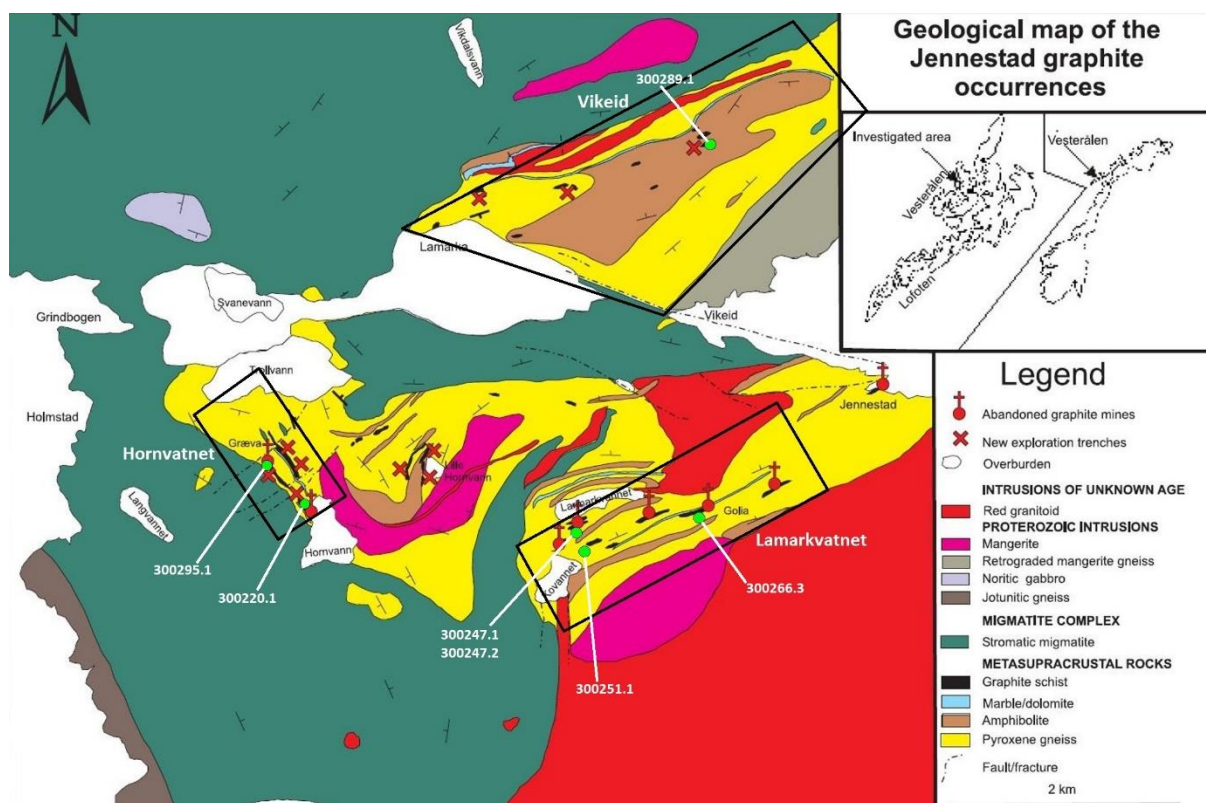

Figure 3. Geological map of the studied area in Vesterålen, adapted from Gautneb and Tveten (2000). The study areas are indicated by black lines, the graphite-bearing rocks as black veins, and sample collection sites as green dots.

The graphite-bearing rocks are of Palaeoproterozoic age and belong to a group of metasupracrustal rocks, which may originate from sediments in shallow marine environments (Griffin et al., 1978; Gautneb and Tveten, 2000). The metamorphic degree in the area is increasing from amphibolite to granulite facies towards the west, which is indicated by orthopyroxene found in the Hornvatnet area that is the westernmost of the studied areas (Ekholm, 2015).

6

Figure 4. Blackish graphite schist next to a forest road in the area of Vikeid, Sortland.

3.2 Piippumäki

The Piippumäki prospect is located ca. 50 km SW of the town of Mikkeli, in the northern part of the Southern Finland Subprovince of the Svecofennian Province (Fig. 5) (Nironen et al., 2016). The regional metamorphism reached upper amphibolite and granulite facies 1.88–1.79 Ga ago (Hölttä and Heilimo, 2017). Not far from Piippumäki (ca. 5 km) lies the abandoned graphite mine Kärpälä, which was in production until the 1940s. The Piippumäki area has previously been studied by Suomen Malmi Oy in the 1960s and by Rautaruukki Oy in the 1980s (Nurmela, 1989). Strong electromagnetic anomalies appear in the area (airborne geophysical low altitude surveys), and continuing towards Kärpälä. The anomalies are interpreted as black shales (Mineral Deposits and Exploration, n.d., Geological Survey of Finland; Arkimaa et al., 2000; Hyvönen et al., 2013). The graphite-bearing rocks were easily encountered in old trenches during field work.
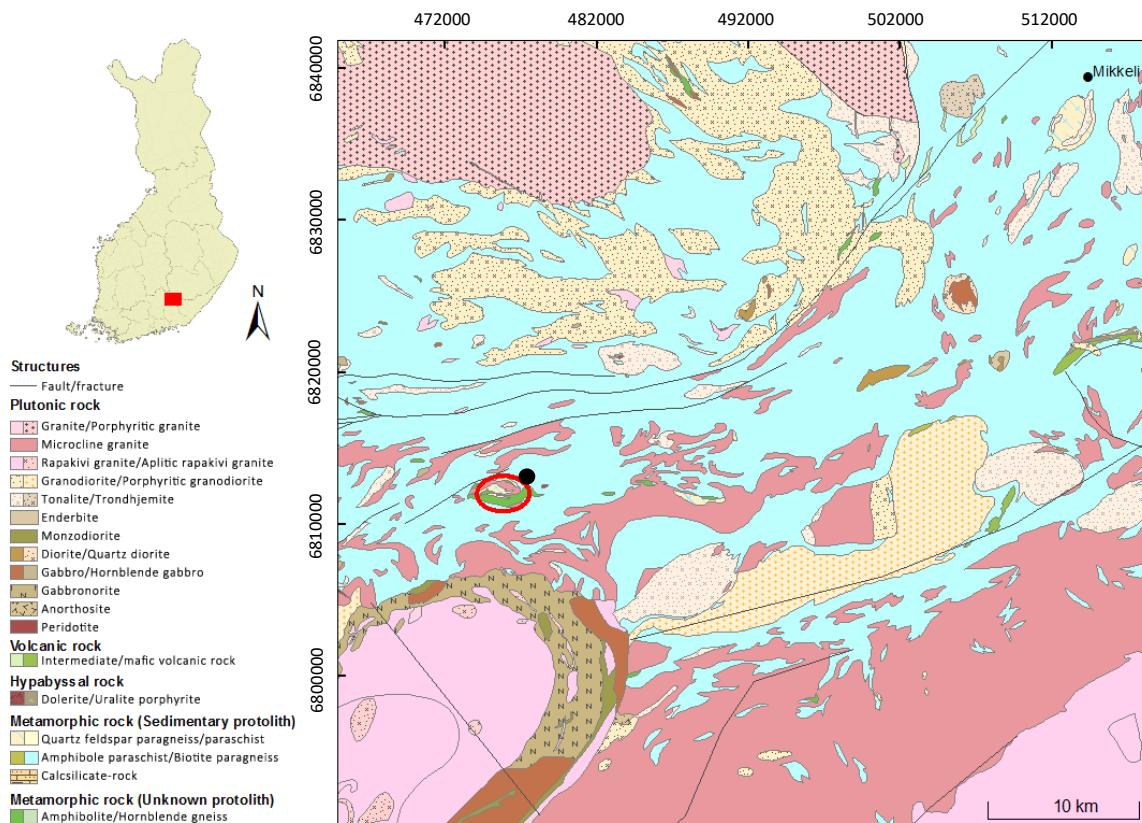
Figure 5. Geological map showing the overview of the regional geology and the location for Piippumäki (red circle). Piippumäki is located ca. 50 km from Mikkeli. The black dot indicates the location of the abandoned Kärpälä mine. Modified from the digital geological map database of Finland (DigiKP, Geological Survey of Finland 2017).

The dominating rocks in the Piippumäki area are quartz-feldspar gneiss and amphibolite (Fig. 6). Diopside amphibolite is also found in the area. The quartz-feldspar gneiss is of sedimentary origin and the protolith of the amphibolite is unknown. Graphite-bearing layers in the gneiss can be up to few meters thick (Simonen, 1982). The gneiss consists principally of medium-grained quartz and feldspar, where plagioclase is more abundant than microcline. Biotite is also present along with accessory minerals apatite, zircon, garnet, and sillimanite. Sulfides are found in the layers that are rich in mica and graphite. Cordierite is also present in the area, predominantly in the surrounding mica gneisses. Limestone associations are found within the mica gneisses in small quantities (Simonen, 1982). The amphibolite is fine-grained and banded with the main minerals hornblende, diopside, quartz, and plagioclase. The measured structures in Piippumäki are steeply dipping at 75-85° and strike W-E, and the fold axis dips 60° towards NW, NE, and SW. These measured structures correspond to the assumption by Simonen (1982) that the quartz-feldspar gneiss and amphibolite are part of an anticline.
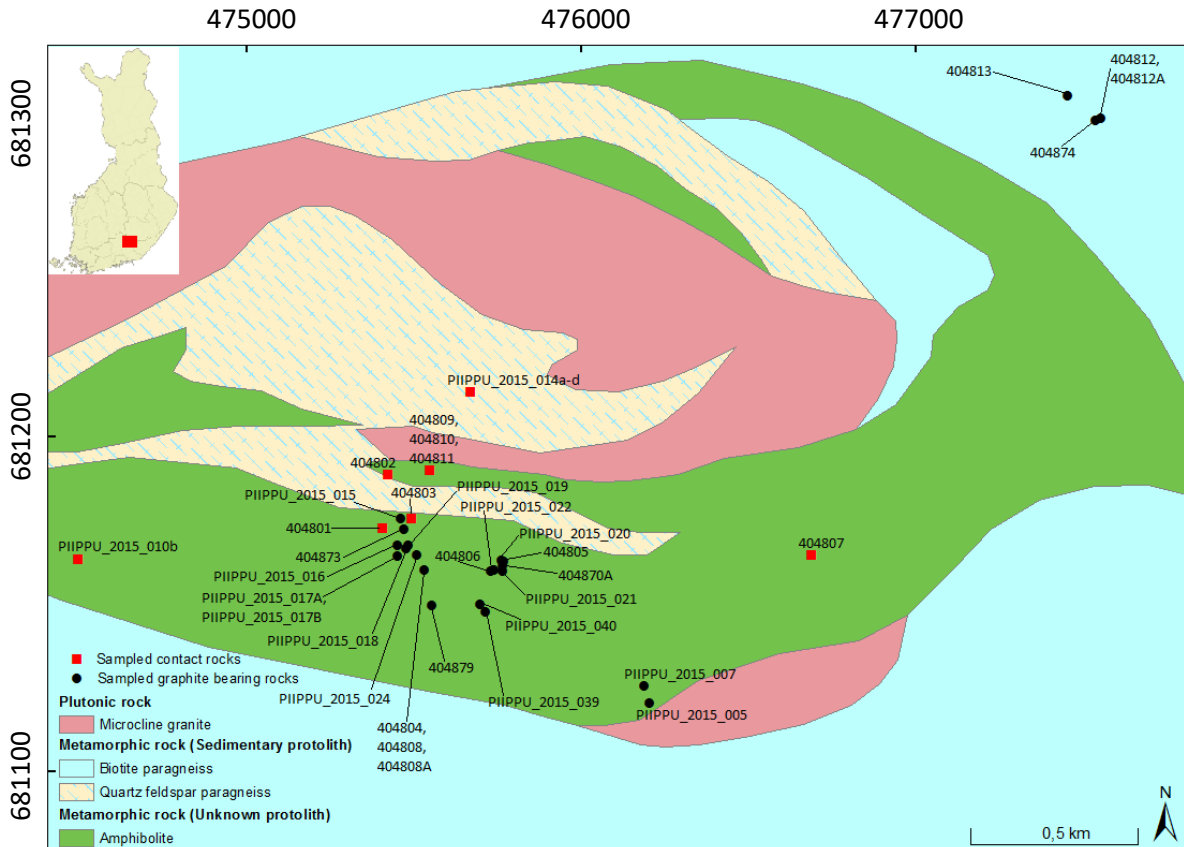
Figure 6. Geological map of the study area Piippumäki. Red squares indicate sampled country rocks, black dots indicate sampled graphite-bearing rocks. The samples in the NE corner of the map are from the abandoned graphite mine in Kärpälä. Modified from the digital geological map database of Finland (DigiKP, Geological Survey of Finland 2017).

3.3 Principal methods used in this survey

The methods used in this work were chosen for their suitability to analyze graphite. Due to the high conductivity of graphite, Slingram was selected for localizing graphite-bearing rocks in the field and for its simple use. For fragmenting the sampled rocks and liberating graphite flakes, selective fragmentation (selFrag) was tested and used. Graphite shows characteristic features in X-ray diffraction and Raman spectroscopy analysis, which are quick and non-destructive analytical methods. Scanning electron microscopy was used for analysis of the character of the liberated graphite flakes and for determining unidentified minerals and possible impurities within the graphite. One pseudosection was constructed to determine the stability field for the observed mineral assemblages in Piippumäki, in comparison with the results of peak metamorphic temperatures obtained from Raman geothermometer calculations and petrographic analysis.

3.3.1 Slingram

Slingram is an electromagnetic instrument that is used to locate conductive layers in the ground. It is highly suitable for locating overburden graphite-bearing rocks due to the high electric conductivity of graphite. It consists of a transmitter and a receiver coil, which are connected by a cable. The transmitter, carried by an operator, produces an oscillating primary magnetic field, which generates electrical currents in the ground (Fig. 7). A secondary magnetic field is generated by the currents and is registered by the operator carrying the receiver (GeoVista, accessed 07.04.2020; Suppala, 2017).

Figure 7. The Slingram equipment disassembled on the ground. The orange transmitter and receiver lie in the back and in the front, respectively. The 60 m cable lies to the right.

The Slingram measurements were performed in Piippumäki perpendicular to the foliation, and the purpose was to cross the boundaries of the conductive graphite-bearing layers. 47 lines (200 m long) were measured with a measurement frequency of 3600 Hz. The coil separation was 60 m, and the line separation was 50 m where the conductor was the strongest and 100 m where it was weaker (see Palosaari et al., 2020).

3.3.2 Selective fragmentation

Selective fragmentation (selFrag) is a quick fragmentation method developed to separate minerals from the host rock by the mineral borders. The minerals are separated by a high-voltage electrical pulse which passes through the rock in liquid (Gnos et al., 2006, Strong et al., 2015). The selFrag lab machine (2 x 2 x 0.8 m) includes a high voltage power supply and a high voltage pulse generator. Up to 1 kg of sample material is placed in portable process vessels that are mounted in an isolated process chamber for fragmentation (Wang et al., 2011).

Selective fragmentation was used on graphite-bearing rocks from Sortland to see if it is a suitable method for separating graphite flakes from the host rock without mechanical defects. The tests were performed at the research laboratory of the Geological Survey of Finland in Espoo.

3.3.3 Scanning electron microscopy

Scanning electron microscopy (SEM) was used for examining the extracted graphite flakes in detail for flake size, impurities, and possible effects of the selective fragmentation process on the flakes. The instrument used is a LEO Gemini 1530 FEG-SEM with a ThermoNoran X-ray detector. Energy dispersive X-ray analysis (EDXA, UltraDry) was used for elemental analysis. The instrument is located at the Laboratory of Molecular Science and Engineering at Åbo Akademi University.

The SEM instrument at Geology and Mineralogy, Åbo Akademi University, was also used for determining unknown minerals in thin sections. The instrument used was a Phenom XL with an energy dispersive detector and acceleration voltage of 15 kV.

3.3.4 X-ray diffraction

X-ray diffraction (XRD) was used for identifying the crystalline nature of graphite, possible impurities, and the distance between the graphene layers in graphite (d_{002}). The measurements were performed with a Bruker D8 Discover instrument with a HI-STAR 2-D detector, located at the Laboratory of Molecular Science and Engineering at Åbo Akademi University. The wavelengths used were Cu–Kα (1.5406 Å), and weighted average of Cu-Kα1 and Cu-Kα2 (and Cu-Kβ); 1.5418 Å (Bragg-Brentano). The analyses were performed with a point detector, and the pulverized samples were scanned multiple times at one point from 20° to 80° for a better signal-to-noise ratio. The results are shown in diffractograms where the x-axis shows the scattering angle (2θ), and the y-axis shows the intensity. The intensities are normalized based on the (002) graphite reflection.

3.3.5 Raman spectroscopy

Graphite shows characteristic features in measurements with Raman spectroscopy, which is optimal and a quick, non-destructive analytical method for graphite characterization. The obtained spectra include first- and second order regions, 1100-1800 cm^{-1} and 2500-3100 cm^{-1}, respectively. The characteristic narrow G band (graphite band) appear at ca. 1580 cm^{-1} in the first order region and 2D band (also called G') at ca. 2700 cm^{-1} in the second order region (Beyssac et al., 2002; Ferrari et al., 2006; Eckmann et al., 2012; Wall, 2012). The G band represents sp^2-hybridized carbon atoms that build up the graphene layers in graphite. The position of the G band is also sensitive to the number of graphene layers in the sample and shifts towards higher wavelengths when number of graphene layers decrease (Wall, 2012). Several D bands (defect-activated) also appear in the first order region at 1150, 1350 (D1), 1500 (D3), and 1620 cm^{-1} (D2). D bands are common in poorly ordered graphite but decrease or disappear with increasing metamorphic grade. However, they can be triggered even by slight structural defects or impurities (Beyssac et al., 2002, Beyssac et al., 2003; Beyssac and Lazzeri, 2012). The 2D band at ca. 2700 cm^{-1} in the second order is asymmetric and is not as high in intensity as the G band. For single-layer graphene, the 2D band is symmetrical with higher intensity than the G band (Ferrari, 2007). Sample preparation and polishing of graphite affects the crystallinity and high order of graphite, which is observed in Raman spectra as increasing intensity for D bands and in the application of the Raman geothermometer (Beyssac et al., 2003; Kouketsu et al. 2019). The D2 (also known as D') band at ca. 1620 cm^{-1} appears because the laser hits the edges of the flakes and cuts graphene layers at different angles (Ferrari, 2007; Malard et al., 2009).

The Raman instrument used is located at the Laboratory of Molecular Science and Engineering at Åbo Akademi University, and the spectra were recorded with a Renishaw Ramascope (system 1000) equipped with a Leica DMLM microscope connected to a CCD camera. An Ar-ion laser (LaserPhysics) with the excitation length of 514 nm and a laser power of 20 mW was used on a Ø 2-µm surface for recording the Raman spectra. The spectrometer was calibrated against a Si standard (520.0 cm^{-1}). On liberated graphite flakes, the measurements were made parallel to the C-axis, while perpendicular to the C-axis on graphite flakes in thin sections. The Raman spectra obtained during this study were constructed with OriginLab software.

3.3.5.1 Raman geothermometer

Beyssac et al. (2002) studied the evolution of the Raman spectra for graphite during increasing metamorphic grade and show that the degree of organization in carbonaceous material and graphite is sensitive to the metamorphic grade. The graphitization process records the peak temperature and

is irreversible (Beyssac et al., 2002). Beyssac et al. (2002) presented a function for estimating the peak metamorphic temperature recorded in graphite based on the R2 ratio, i.e. the peak area ratio, $R2 = \left(\frac{D1}{G+D1+D2}\right)$ in graphite spectra. The R2 ratio decreases with increasing temperature and is described by the linear function $T(°C) = -445R2 + 641$, with a correlation coefficient R^2 = 0.96. The temperature estimation can be done within the range of 330-650 °C. Also, the R1 ratio, which is the peak intensity ratio $R1 = \left(\frac{D1}{G}\right)$, decreases with increasing P/T conditions. Beyssac et al. (2002) showed that the R2 ratio correlates well with the peak temperature, while there is no apparent correlation between R2 and pressure.

Rahl et al. (2005) presented a calibration on the function of Beyssac et al. (2002) for widening the temperature range for the Raman geothermometer, since only little variation is displayed for the R2 ratio at lower temperatures than 330 °C. The calibration takes the R1 ratio into account and is suitable for temperatures between 100-700 °C. The calibrated function used is $T(°C) = 737 + 320(R1) - 1067(R2) + 80.638(R1)^2$ and R^2 = 0.94 (Rahl et al., 2005). The peak areas and heights needed for the Raman geothermometer in this study were obtained from the Raman spectra with OriginLab software.

3.3.6 X-ray fluorescence, pseudosection, and Perple_X

Whole-rock chemical composition was measured with X-ray fluorescence (XRF) at Åbo Akademi University and was used for constructing a pseudosection for examining the P/T field in Piippumäki, in comparison with the observed mineral paragenesis and the Raman geothermometer. A pseudosection shows the stability fields of mineral assemblages for one whole-rock chemical composition (Hirsch et al., 2016). The modeling program Perple_X is used for creating pseudosections, which is a quick thermodynamic calculation software. Perple_X software version 6.8.5 was used for constructing a pseudosection (Connolly, 2005; Connolly, 2009) (http://www.perplex.ethz.ch/).

4. Results and discussion

4.1 Vesterålen

The sampled graphite-bearing rocks are pyroxene gneiss and metapelite, and the graphite appears differently in these rocks. In the pyroxene gneiss, graphite is disseminated as flakes along 120° grain boundaries without any signs of foliation, as seen in thin section (Fig. 8A). The main minerals in the pyroxene gneiss are diopside, graphite, spinel, and garnet (sample 300247.1). In the metapelite (sample 300251.1), on the other hand, graphite is also found as disseminated flakes but appears to be deformed together with biotite (Fig. 8B). The main minerals in the foliated metapelite are K-feldspar,
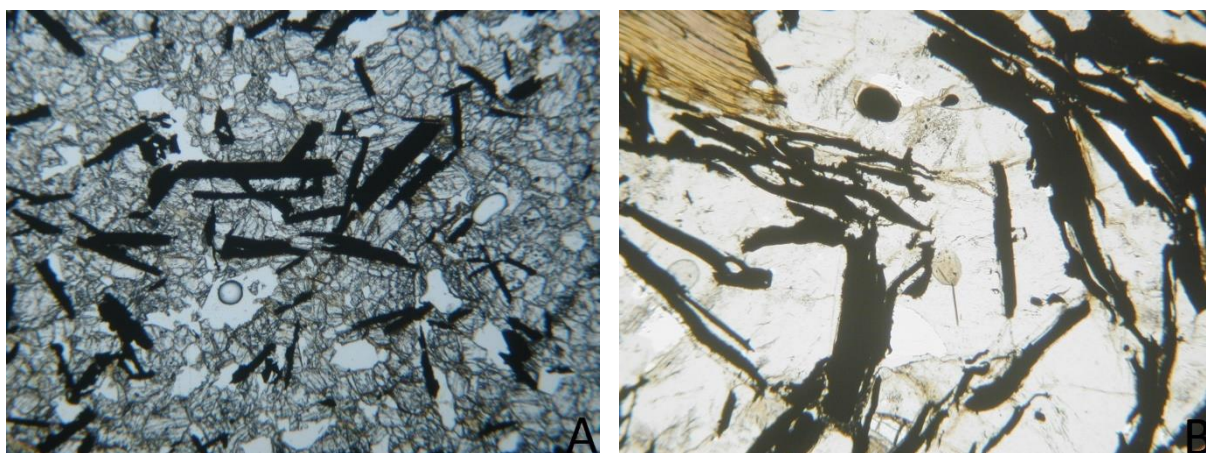

Figure 8. Images of graphite-bearing pyroxene gneiss (A), and metapelite (B) from a polarization microscope. The graphite is seen as black flakes. The images are 1.88 mm across.

quartz, plagioclase, graphite, and biotite, along with minor clinopyroxene, orthopyroxene, apatite, and pyrite. In both host rocks, the graphite appears as flakes of 0.5 up to 1.2 mm in length. The petrographic study of thin sections indicates that the maximum metamorphic grade in Sortland is lower granulite facies, which is shown by the lack of garnet and the observed paragenesis ortho- and clinopyroxene, biotite, hornblende and minor quartz (Best, 2003). No indications of retrograde metamorphism are found in these thin sections.

Graphite flakes were liberated from the host rocks with selective fragmentation (selFrag), which is a quick fragmentation method. However, it is possible that the selFrag deforms the edges of the liberated graphite flakes as seen in Fig. 9A. The liberated graphite flakes were examined in detail with SEM. The images obtained with SEM show clearly that the graphite flakes consist of several layers,
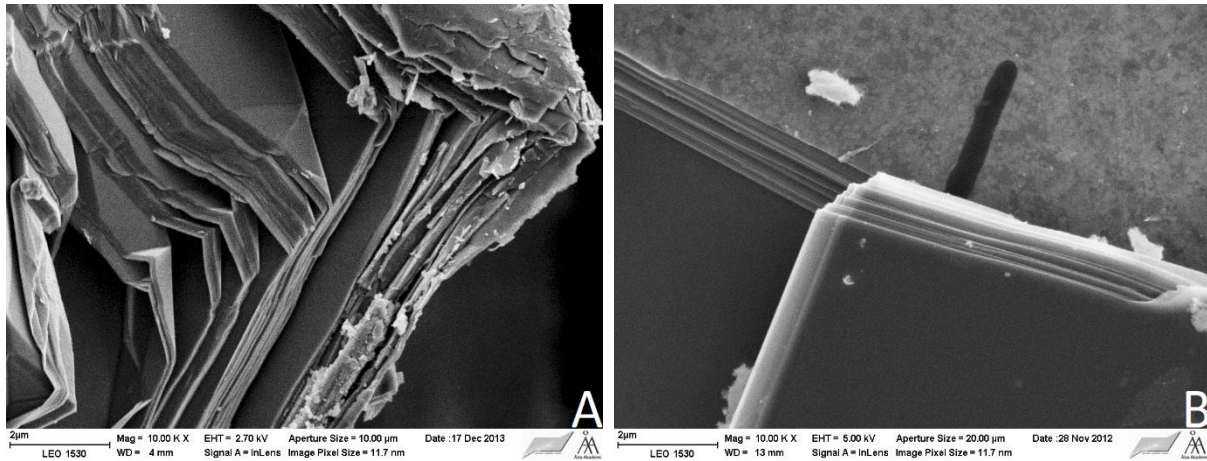
Figure 9. SEM images of graphite flakes obtained by selFrag (A) and manually liberated flakes (B). It is evident that the graphite flakes consist of several, parallel layers. The kink folds in the graphite flake might originate from the selective fragmentation (A).

which build up the flakes (Fig. 9B). Some flakes have clean surfaces and straight edges with no impurities visible. The folds in the graphite flakes in Fig. 9A could originate from the fragmentation by selFrag, but the possible effect of selFrag should be studied further. The XRD measurements were made on both single grain graphite (sample 300247.2) and powder (300289.1 and 300295.1) (Fig. 10). The measurements on single grain show only two sharp reflections: peaks (002) and (004). These
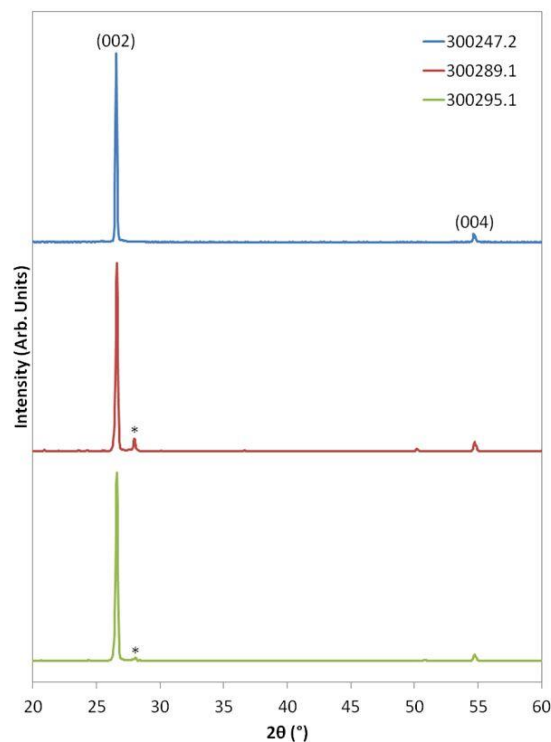

Figure 10. Obtained XRD spectra from three different samples. The samples show characteristic (002) and (004) peaks for graphite. Albite is indicated by an asterisk (*).

peaks are graphite related and indicate a high order in the atomic structure of the graphite grain. For the powdered graphite, the same (002) and (004) reflections are visible along with traces of quartz and albite (albite indicated by an asterisk in Fig. 10). The d_{002}-spacing is 0.335-0.336 nm, which is also the expected distance between the graphene layers in well-developed graphite.

Raman spectroscopy was conducted on graphite samples liberated both manually (sample 300247.2) and selectively (sample 300289.1 and 300295.1). The obtained Raman spectra of the manually liberated sample was measured at two different positions, indicated by the microscope image in Fig. 11A, and the spectra for the selectively liberated samples are shown in Fig. 11B and 11C. The obtained spectra show the characteristic features of graphite: The G band and the 2D band. In the obtained spectra (Fig. 11), the G band is present at ca. 1579 cm^{-1}, which implies that the graphite has formed during metamorphic conditions of high grade (Beyssac et al., 2002). The asymmetrical 2D band is visible at ca. 2730 cm^{-1} and it indicates that the sample consists of several graphene layers stacked onto each other, compared to a symmetrical 2D band in single- and few-layer graphite. A low-intensity D band (defect band) is located at ca. 1350-1360 cm^{-1}. The D band is visible in two of the measured samples (Fig. 11A and 11B) and is absent in one (Fig. 11C). The selFrag appears not have had any damaging effect on the graphitic structure since the D band is absent in sample 300295.1 (Fig. 11C) although the effects of selectively fragmenting graphite samples should be studied further for assurance. There are also other characteristic bands for graphite visible: the 2D' band at ca. 3250 cm^{-1} and the G* band at ca. 2450 cm^{-1}. The obtained Raman spectra imply that quality of the Sortland flake graphite is high.
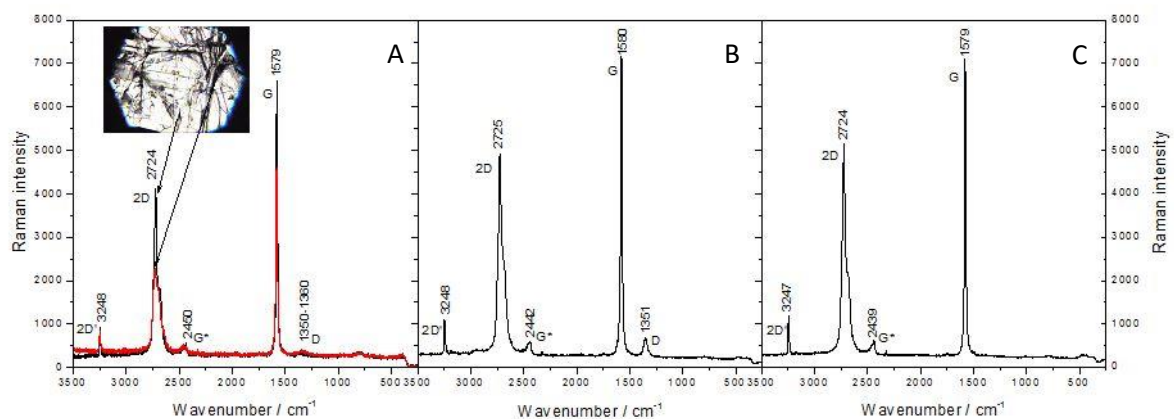

Figure 11. Raman spectra for three graphite samples, both manually (sample 300247.2, A) and selectively fragmented (sample 300289.1, B; 300295.1, C). The measuring points are marked in spectra (A). The spectra show distinct G and 2D bands for graphite, with only weak or absent D bands.

For the graphite samples from Sortland, the function by Beyssac et al. (2002) was used for peak metamorphic temperature estimation from the obtained Raman spectra. The R2 ratios obtained by integrating peak areas are 0.05-0.13, which indicates temperatures between 575 and 620 °C which correlate well with the observed mineral paragenesis in the area. Peak metamorphic temperatures were subsequently calculated for better accuracy and consistency (Table 1.) The samples lacking the D band result in the maximum temperature for the function, i.e. 641 °C (Beyssac et al., 2002) and 737 °C (Rahl et al., 2005). The mean temperature based on Beyssac et al. (2002) is 620 °C and Rahl et al. (2005) is 702 °C, which still correlates with the observed mineral paragenesis and metamorphic grade of lower granulite facies.

Table 1.The calculated peak metamorphic temperatures for the samples from Sortland. The temperatures are based on one measurement per sample.

Sample no.	R1	R2	T/°C ±50 °C (Beyssac et al, 2002)	T/°C ±50 °C (Rahl et al, 2005)
300247.2	0.000	0.000	641	737
300247.2_2	0.096	0.052	618	713
300289.1	0.097	0.138	580	622
300295.1	0.000	0.000	641	737

4.2 Piippumäki

Both graphite-bearing rocks and contact rocks were examined in more detail in thin section. The gneiss in Piippumäki has the main minerals quartz, plagioclase, microcline, biotite, and graphite (Fig. 12A). Pyrite is also found as an accessory mineral, along with indicator minerals garnet, assumably cordierite (see Appendix II), and slightly fibrous sillimanite. Graphite is evenly disseminated in the rock and is aligned in the foliation direction. In some places the graphite is mixed with chloritized biotite where it appears as irregular and deformed, which indicates retrograde metamorphism (Fig. 12B). The garnet
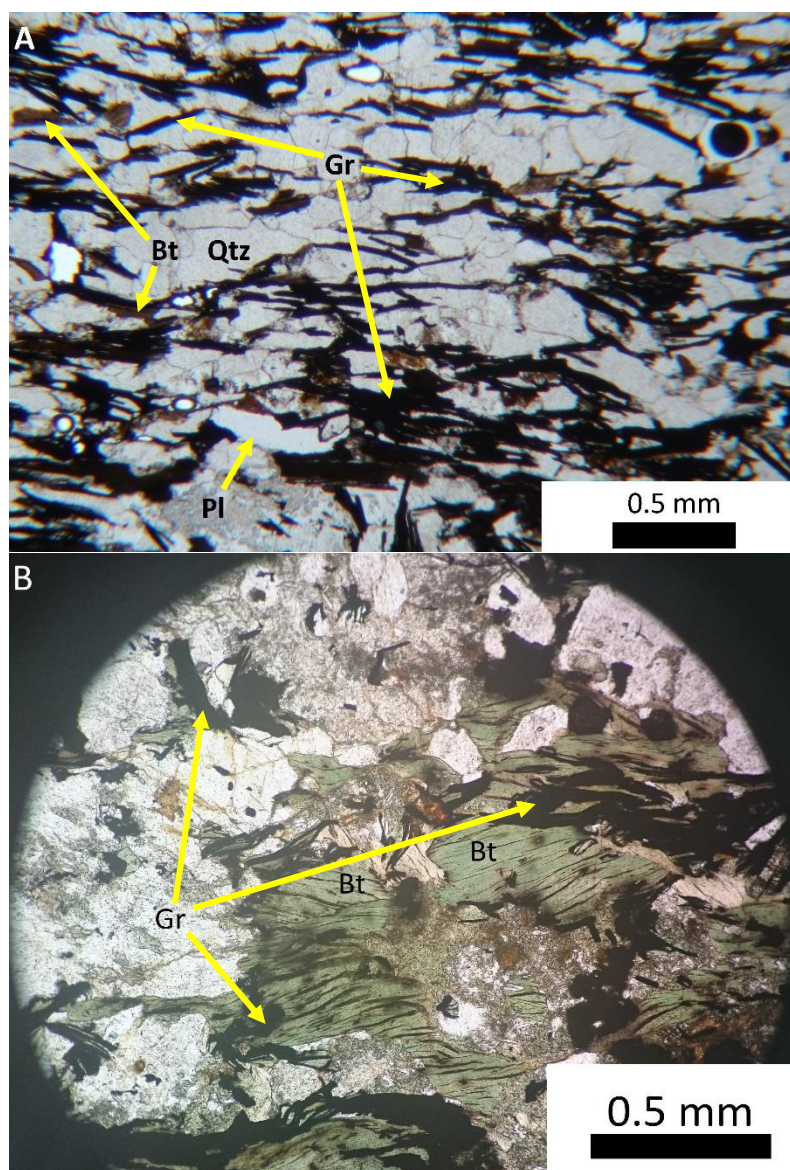

Figure 12. Photomicrographs of typical graphite-bearing quartz-feldspar gneisses in plane-polarized view. (A) Sample PIIPPU_2015_020 and (B) sample PIIPPU_2015_016. Disseminated graphite flakes (Gr) are indicated by yellow arrows in both images and in (B) irregular graphite flakes (Gr) are shown mixed with chloritized biotite (Bt).

is affected by retrograde metamorphism and is found altered to cordierite, which is seen as garnet not being fully isotropic (Fig. 13).
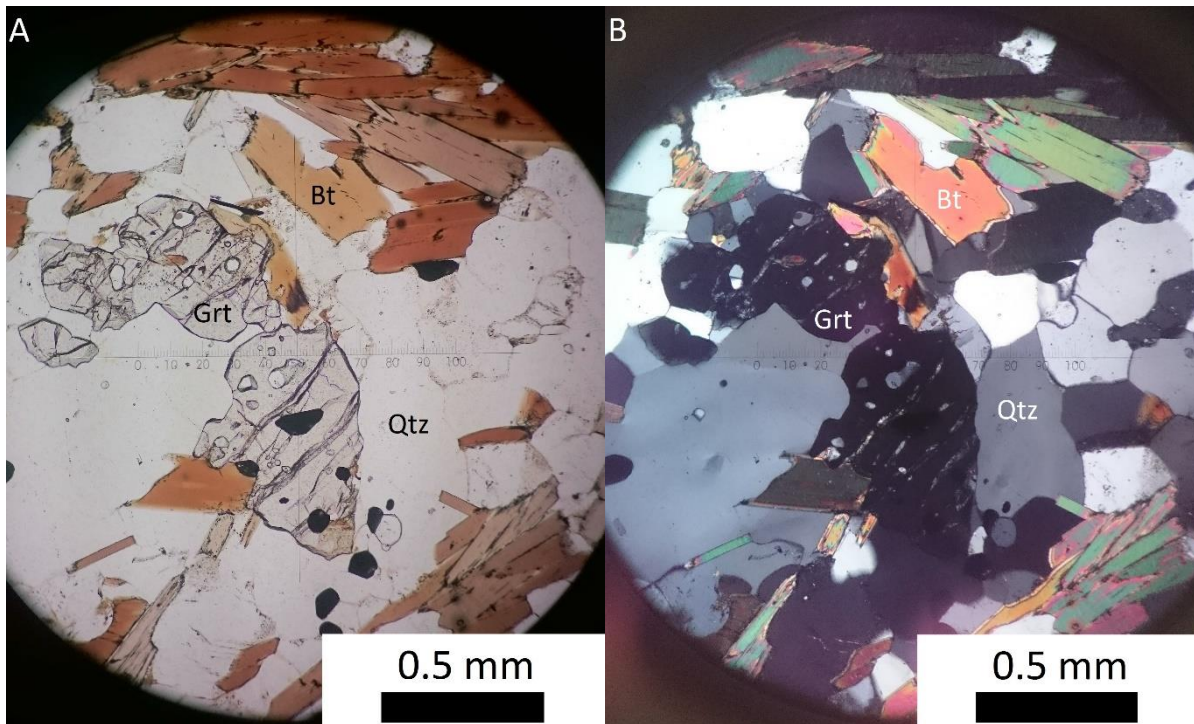

Figure 13. Retrograde garnet in sample 404811, which is seen as the garnet (Grt) not being fully isotropic due to the alteration to cordierite. Plane-polarized image to the left, cross-polarized to the right.

The contact rock to the graphite-bearing gneisses is amphibolite, with the main minerals hornblende, diopside, quartz and plagioclase, and accessory minerals biotite, sulfide and sericite. The amphibolite shows banded and foliated characteristics. Sample 404801 shows pleochroic brown amphibole (Fig. 14A). Sample 404809 consists of diopside and pleochroic green hornblende, is green and banded in appearance (Fig. 14C).
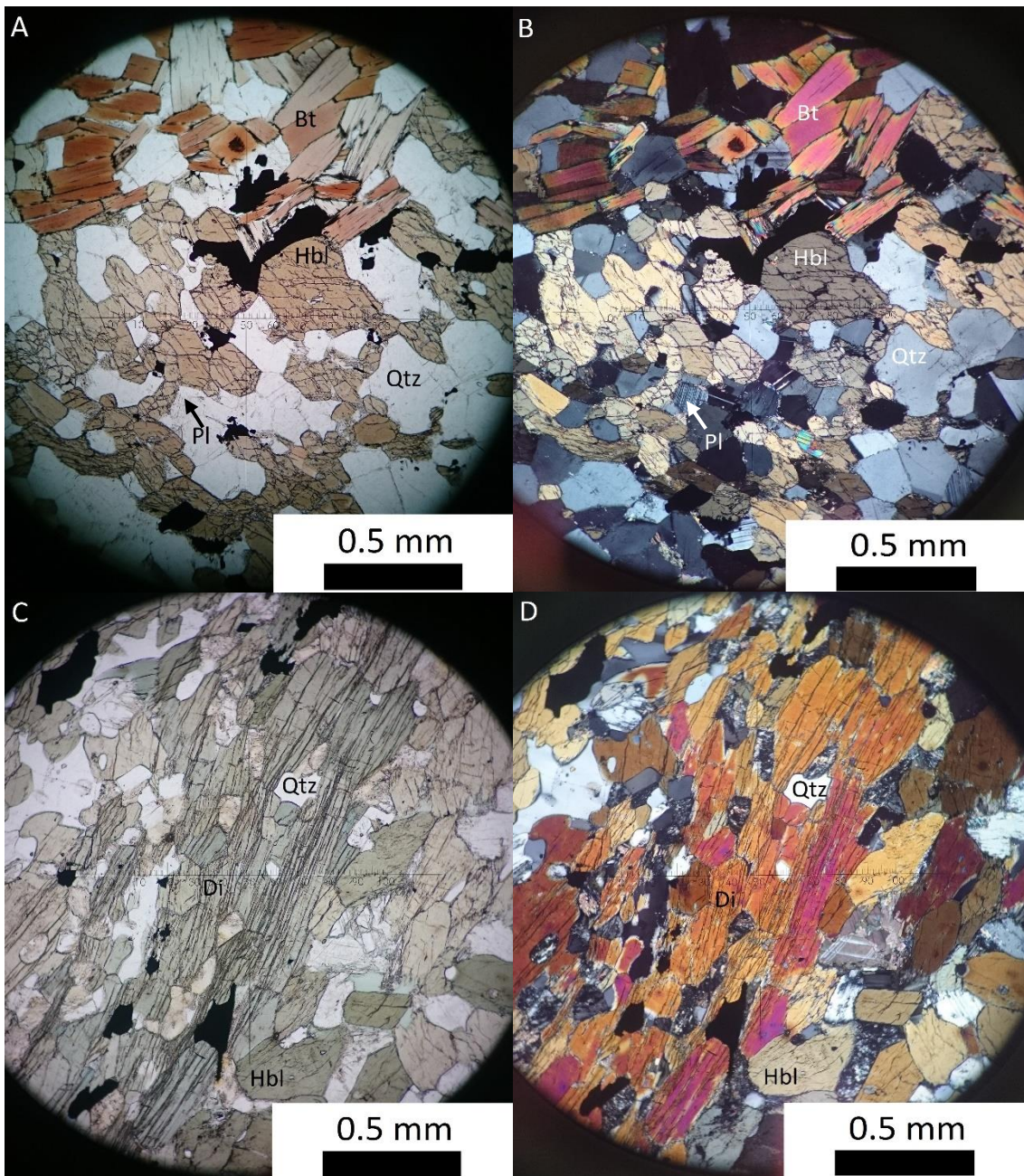
Figure 14. Photomicrographs of samples 404801 (A and B), and 404809 (C and C). Both are amphibolites and shown in both plane- and cross-polarized light. Sample 404801 contains brownish hornblende (Hbl), while sample 404809 contains greenish hornblende (Hbl) together with diopside (Di).

Slingram was used for locating the graphite-bearing layers in the ground more precisely. The obtained results from the Slingram measurements correlate well with airborne electromagnetic data and the graphite findings in the area (Fig. 15). A few graphite observations were made from boulders and therefore does not fit the anomaly. Graphite-bearing rocks were primarily accessed and sampled in old, excavated pits and surrounding rocks were sampled in outcrops. The Slingram measurements combined with the field observations of graphite confirm that the graphite is the conductor causing the anomalies in Piippumäki.
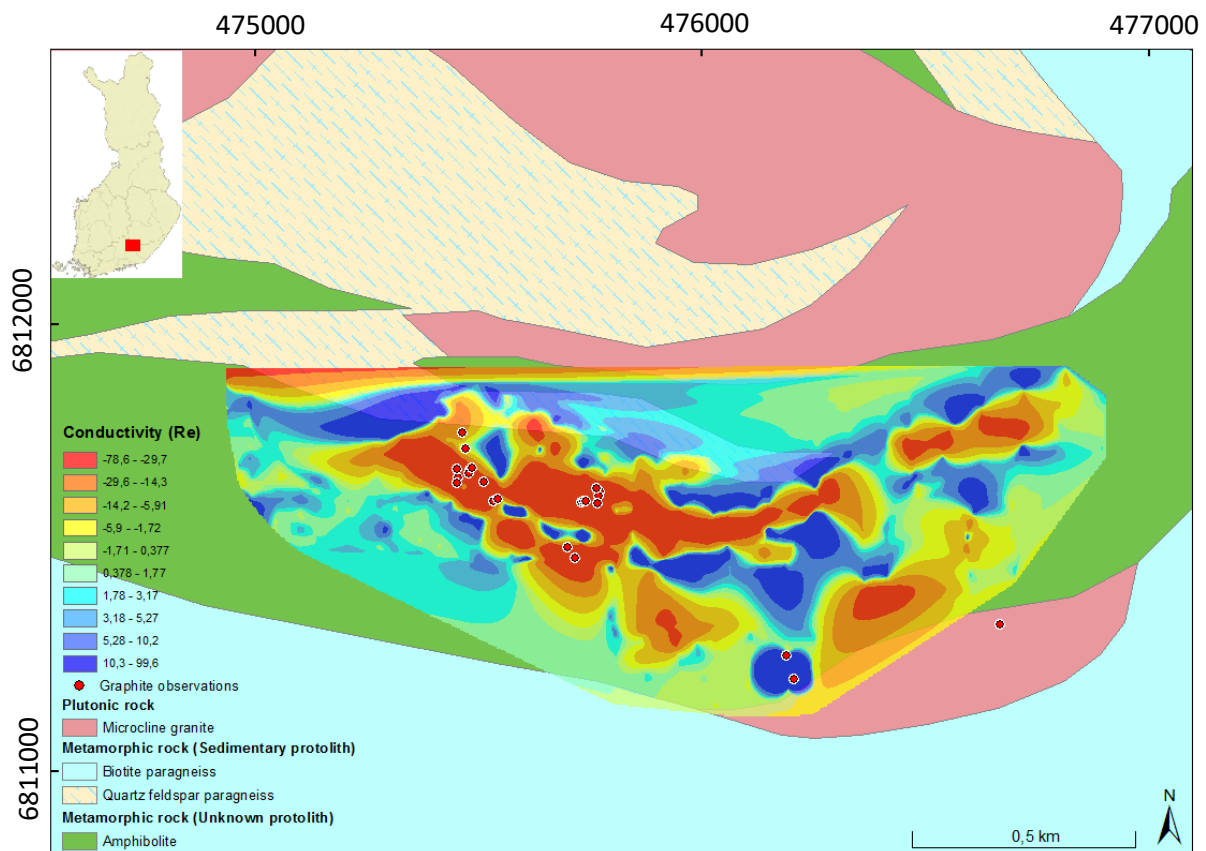

Figure 15. Results from the Slingram measurements from Piippumäki shown on a geological map. Red color indicates high conductivity and blue low conductivity. Graphite observations are indicated by red dots on the map. Modified from the digital geological map database of Finland (DigiKP, Geological Survey of Finland 2017).

SEM was used to examine the liberated graphite flakes and to determine unidentified minerals. The SEM images show that the graphite is flaky in appearance (Fig. 16A) and the flakes are up to 1 mm in size. The surfaces on some graphite flakes are spotty, which can be due to oxidization of the surface or some other factor decreasing the conductivity of the flake (Fig. 16B), but no impurities were observed in the graphite. Cordierite was observed in thin section in sample PIIPPU_2015_014d but was determined as bytownite by SEM analysis (see Appendix II).
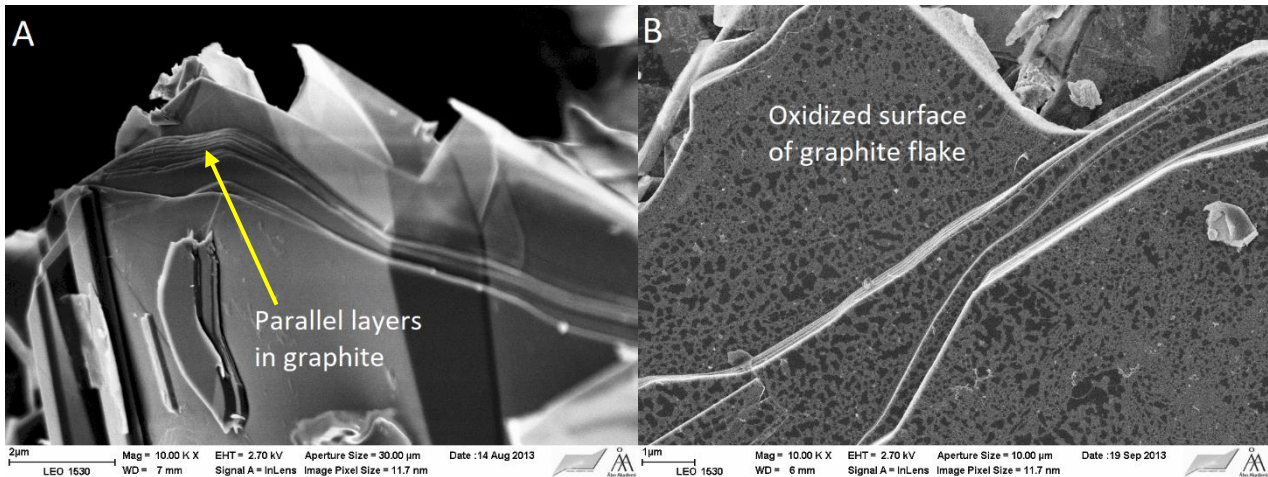
Figure 16. SEM images showing graphite flakes. In sample 404804 (A) the parallel layers in the graphite flake are indicated by the arrow. In sample 404809A (B) oxidized surfaces of graphite flakes are visible.

Total carbon, sulfur, and graphitic carbon were analyzed for 8 samples from Piippumäki (see Appendix III). The majority of the measured carbon is graphitic carbon, with an average of 6.41 % C-graph. The measured sulfur is low, 0.33 % S on average, which is generally lower than black schists in Finland (Loukola-Ruskeeniemi, 1992).

Results from XRD indicate graphite flakes of high quality. All samples show peaks (002) and (004) at 26.6° 2θ and 54.8° 2θ respectively (Fig. 17), which are graphite reflections. The lack of additional graphite reflections shows that the graphite in the samples involves large flakes of graphite. In two samples (404804 and 404805) minor impurities are detectable as some additional peaks, which can originate from mica, quartz, and/or feldspar. Sample 404812 is from Kärpälä, and the obtained spectra shows only the graphite reflections (002) and (004). The d_{002}-spacing is 0.334–0.335 nm, which correlates with graphite of high quality (Pierson, 1993).
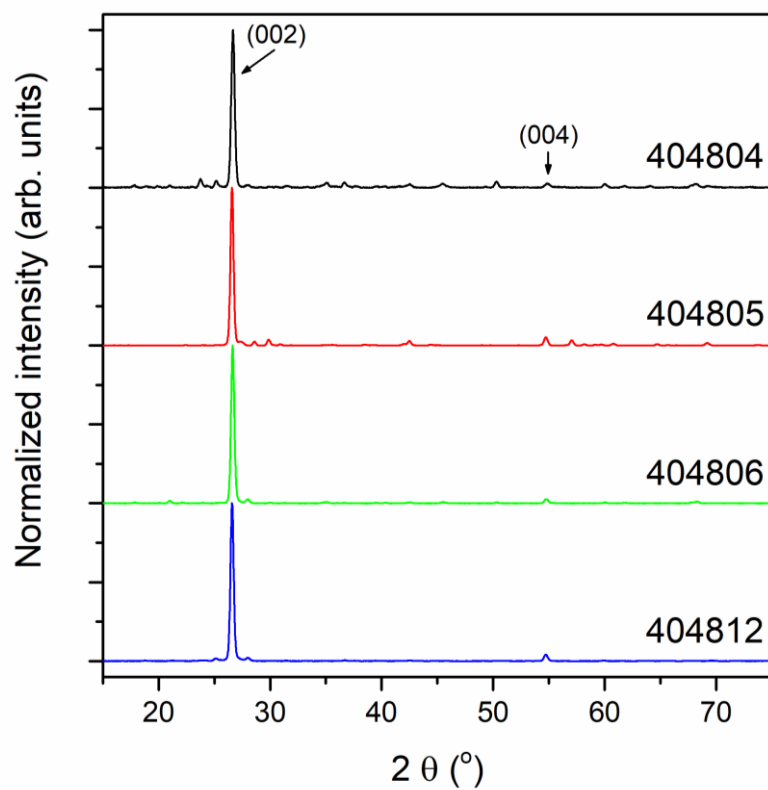

Figure 17. Diffractograms obtained from XRD measurements on four different samples, sample 404812 being from Kärpälä. All diffractograms show characteristic (002) and (004) reflections of graphite.

Raman spectroscopy measurements were applied on liberated graphite grains as well as graphite in thin sections from 11 different samples. Each sample was measured five times. The spectra obtained from liberated grains are very similar to each other and show the distinct G (at ca. 1579 cm^{-1}) and 2D (at ca. 2723 cm^{-1}) bands for graphite (Fig. 18A). The position and intensity of the G band indicate that the sample contains several layers of graphene (Wall, 2012). The 2D band is asymmetrical and has a shoulder towards lower wavenumbers, which indicates that the sample consists of several graphene layers and that the graphite has formed during high metamorphic conditions (Beyssac et al., 2002). Some measurements of samples 404873, 404874, 404879, PIIPPU_2015_020, and PIIPPU_2015_039 lack the D band (Fig. 19). Some D bands of low intensity (D1, D2 and D3) are visible in some of the measured spectra, which imply structural defects or heteroatoms (e.g. O, H, and N) in the graphite.
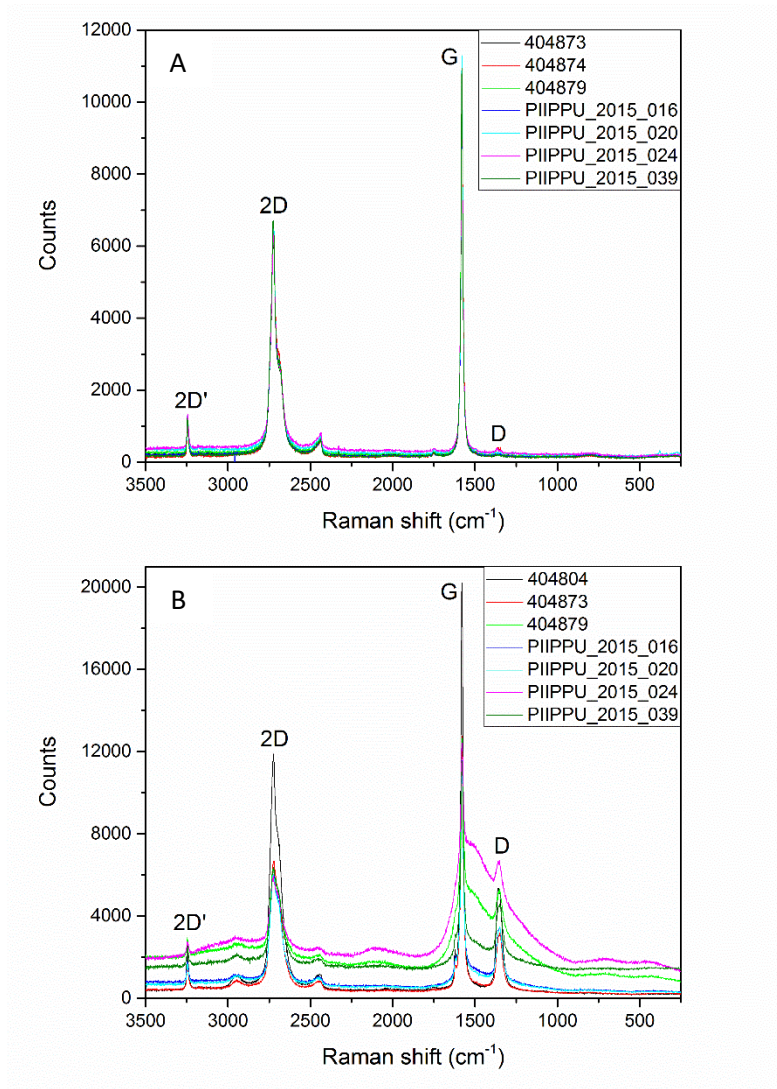

Figure 18. Obtained Raman spectra showing results for graphite grains (A), and for graphite in thin sections (B). Measurements on graphite grains indicate that the material consist of several graphene sheets that are stacked onto each other (A), while measurements on graphite in thin sections show several defect (D) bands (B).

The amount and intensity of the D bands decrease with increasing metamorphic grade. At 2400, 2700, 2900 and 3300 cm^{-1} some peaks of overtone and combination scattering are visible. All samples show the 2D' band at ca. 3247 cm^{-1}, which is a second order of the D2 band (Ferrari, 2007), and a small G* band at ca. 2440 cm^{-1}, of unclear origin (Ferrari and Basko, 2013).
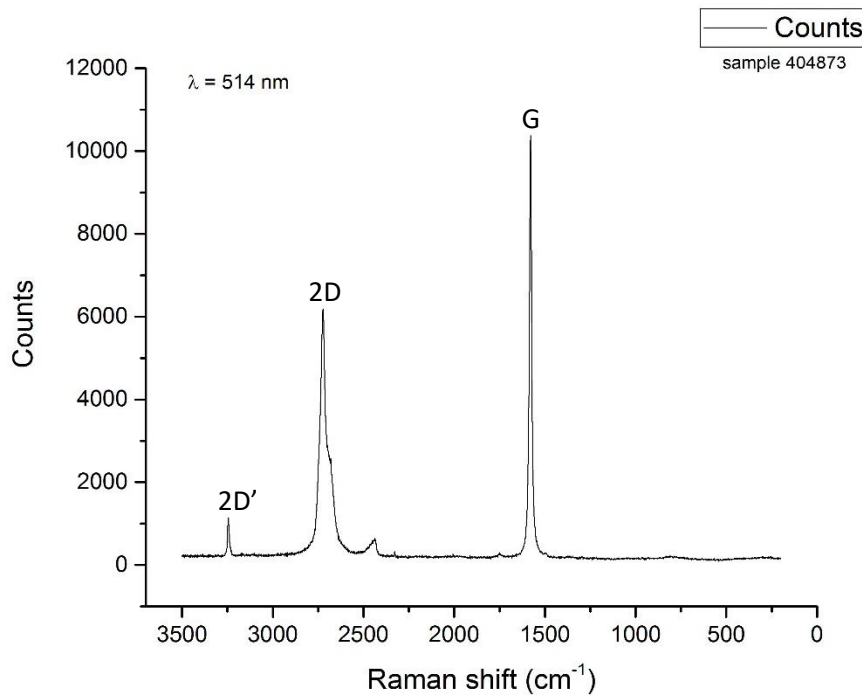

Figure 19. Raman spectrum for sample 404873. The D band is absent.

Graphite present in thin sections was measured for comparison (Fig. 18B) and the results are different from the grains, as expected. This difference is caused by the laser hitting the graphite grains perpendicular to the C-axis, whereas the exposed graphite flakes are damaged by the thin section preparation process (Wopenka and Pasteris, 1993; Kouketsu et al., 2019). The obtained spectra show the characteristic G and 2D bands for graphite, but also several D bands (D, D2, and D3). The D2 band can appear in otherwise defect-free graphite if the laser hits edges on the graphite flakes (Ferrari, 2007). The D3 band originates from defects such as tetrahedral carbons and from graphite of small crystalline size (Beyssac et al., 2002; Nemanich and Solin, 1979). The low intensity band at 2900 cm^{-1} is only visible in the spectra for thin sections and represents a combination mode of the D and 2D bands (Eckmann et al., 2012).

Peak temperature calculations based on the Raman spectra were made on both liberated graphite grains and graphite in thin sections. These temperature estimations were calculated according to the calibration by Rahl et al. (2005) and are presented in Table 2. The obtained temperatures for liberated

grains are between 659 and 719 °C based on the mean values of five parallel measurements. The maximum temperature for the calibration, i.e. 737 °C, is obtained from spectra that lack the D band. These temperatures indicate the minimum temperatures for the peak metamorphism. The retrograde metamorphism observed in thin sections (e.g. chloritization of biotite in PIIPPU_2015_016 in Fig. 12B) is not observed in these Raman temperatures, which indicates that the graphitization process is irreversible (Beyssac and Rumble, 2014) and that the graphitic structure remains unaffected. This observation indicates that graphite of high quality can also be found in retrograde metamorphic areas. The temperatures obtained from spectra from graphite in thin sections were considerably lower than for liberated graphite grains. This difference can be explained by the thin section preparation causing defects in the graphite and the laser hitting the graphite perpendicular to the C-axis.

Table 2. Table showing the calculated peak temperature estimations, based on the mean parameters from the Raman measurements on graphite grains and graphite in thin sections. Five different spots were measured for each sample, and the calculations are based on the mean values for each sample.

Sample no. (grains)	Mean R1	Mean R2	T/°C ±50 °C (Rahl et al, 2005)	Sample no. (thin sections)	Mean R1	Mean R2	T/°C ±50 °C (Rahl et al, 2005)
404873	0.018	0.060	679	404804	0.263	0.383	418
404874	0.014	0.043	696	404873	0.262	0.355	448
404879	0.023	0.080	659	404879	0.307	0.560	245
PIIPPU_2015_016	0.025	0.075	665	PIIPPU_2015_016	0.265	0.365	438
PIIPPU_2015_020	0.006	0.075	719	PIIPPU_2015_020	0.296	0.389	424
PIIPPU_2015_024	0.026	0.067	674	PIIPPU_2015_024	0.350	0.623	194
PIIPPU_2015_039	0.007	0.021	717	PIIPPU_2015_039	0.321	0.525	288

The pseudosection was constructed in the software Perple_X version 6.8.5 based on the whole-rock chemical composition (Appendix III) for sample 404811, which is a quartz-feldspar gneiss (Fig. 20). The phases involved in the construction were biotite (bt), sanidine (sa), white mica (mica), melt, garnet (grt), orthopyroxene (opx), staurolite (st), cordierite (crd), chloritoid (cld), spinel (spl), ilmenite (ilm), and plagioclase (pl). The activity model used for biotite is from Tajcmanová et al. (2009); for sanidine from Waldbaum and Thompson (1968); for white mica from Auzanneau et al. (2010) and Coggon and Holland (2002); for melt from Holland and Powell (2001) and White et al. (2001); for garnet from Holland and Powell (1998); for orthopyroxene from Holland and Powell (1996); for chloritoid from White et al. (2000); and for plagioclase from Newton et al. (1980). Assuming all water in the rock was in biotite, the 1.54 wt% of H_2O was calculated from the mineral mode. Together with the minerals observed during field work and in other thin sections, the indicated stability field of biotite + melt + cordierite + plagioclase + ilmenite + garnet is at ca. 5 kbar and 740 °C.

The pseudosection is uncertain due to cordierite not being found in the thin section of sample 404811. However, cordierite is observed in Piippumäki (Simonen, 1982). The observed mineral assemblages together with the obtained temperatures from the Raman geothermometer (737 °C for the spectra lacking the D band) correlate with Piippumäki being metamorphosed in lower granulite facies during the Svecofennian orogeny as stated by Kähkönen (2005).

The rocks in Piippumäki have also been exposed to retrograde metamorphism, which is observed in thin sections as chlorite – muscovite – epidote overprinting the original garnet – cordierite – sillimanite + melt. Corderite has also been replaced by bytownite during the retrograde process by the reaction $10\ Mg_2Al_4Si_5O_{18}$ (cordierite) $+ 9\ CaO + Na_2O + 20\ H_2O \rightarrow 9\ CaAl_2Si_2O_8$ (bytownite) $+ 10\ Mg_2Al_2SiO_5(OH)_4$
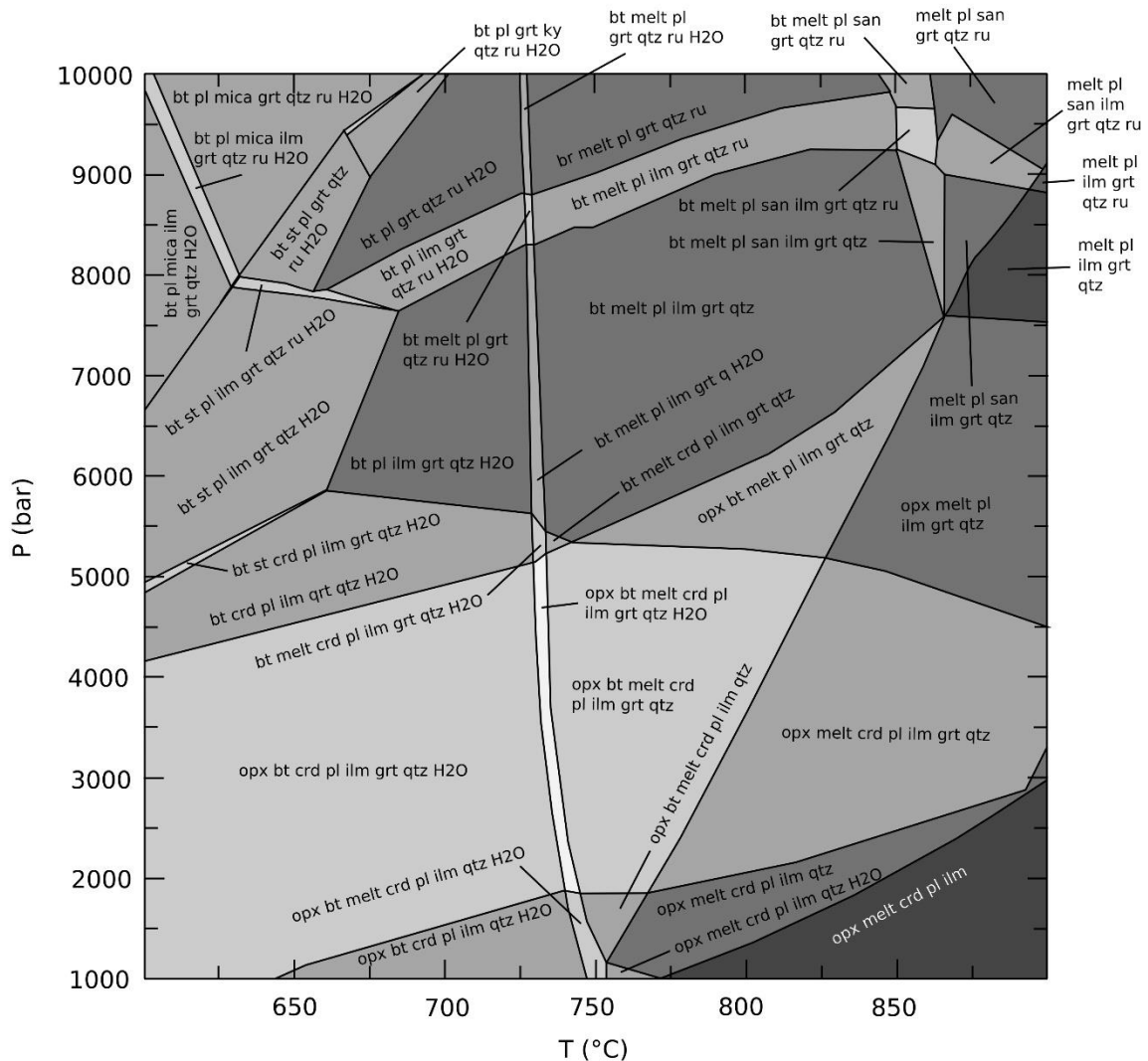

Figure 20. Pseudosection for sample 404811. The mineral assemblage observed in Piippumäki indicate ca 5 kbar and 740 °C with the stability field of biotite (bt), melt, coriderite (crd), plagioclase (pl), ilmenite (ilm), and garnet (grt).

(septochlorite) + 16 SiO$_2$ (quartz) (Ansilewski, 1973), where the CaO probably originates from Ca-rich rocks or from Ca-rich fluids during the retrograde metamorphism. Further work to determine the stability fields for mineral assemblages in specific samples is needed, which includes detailed study of whole-rock geochemistry and pseudosections.

4.3 Comparison to other graphite occurrences

Graphite occurrences in Fennoscandia have been studied to some extent, e.g. in Finland to map graphite occurrences suitable for energy production during the 1980s (Sarapää and Kukkonen, 1983), and more recently in exploration projects due to the interest of battery minerals (Vasara, 2018). Extensive studies on graphite occurrences in northern Norway have also been performed during recent years (Gautneb et al., 2020).

Al-Ani et al. (2020) has studied graphite-bearing rocks and the beneficiation of graphite from a metamorphic schist belt in Rautalampi and Käpysuo in Central Finland where the graphite occurrences are hosted by quartz-mica schist and feldspatic biotite gneiss, which are associated with garnet-sillimanite gneiss and garnet ± cordierite ± orthoamphibole/orthopyroxene rocks and gneissic tonalite. The graphite-bearing rocks are dated to ca. 1.92 Ga. Al-Ani et al. (2020) report graphite flakes up to 1600 μm in size and XRD patterns indicating highly crystalline graphite. The obtained Raman spectra measured on graphite flakes in thin sections show D bands of varying intensities. They also performed beneficiation tests by conventional flotation tests, graphite flake size reduction, and graphite purification with promising results for battery industry qualified graphite concentrate. However, it is shown that thin section preparation and polishing affect the graphitic structure and further affect the Raman spectra and geothermometer calculations. This could be avoided by scanning graphite flakes beneath other minerals (Kouketsu et al., 2019), and could explain the poor results Al-Ani et al. (2020) obtained with Raman. Regarding the high grade rocks the graphite occurrences are associated with, the Raman spectra should indicate less defect bands.

Talga Group Ltd is the owner of the Vittangi graphite project that lies in northern Sweden, consisting of the Nunasvaara and Niska deposits. The Swedish Geological Survey has announced Nunasvaara as a mineral deposit of national interest (Talga, 2020). The Nunasvaara graphite deposit is known as the largest graphite deposit in Sweden consisting of massive and disseminated graphite <0.1 mm in size (Lynch et al., 2016). The deposit is hosted by a horizon of graphite schist in the lower sedimentary formation of the Vittangi greenstone group and was deposited at ca. 2.14 Ga and metamorphosed during the Svecokarelian orogeny (Lynch et al., 2016; Lynch et al., 2018). Pearce et al. (2015) report microcrystalline flake graphite both disseminated in the rocks and as veins in Nunasvaara. Raman

geothermometry is applied on both disseminated graphite and graphite veins, which indicates peak metamorphic temperatures of 400-500 °C (Pearce et al., 2015), which is in line with the regional burial path (Lynch et al., 2018) and is the main difference to the occurrences in Sortland and Piippumäki. Recently, Talga Group, Mitsui, and LKAB announced a Letter of Intent for joint development of the Vittangi graphite mine and lithium-ion battery anode production (LKAB, 2020).

The Woxna graphite mine is located in the county of Gävleborg in central Sweden and owned by Leading Edge Materials Corp. The mine was briefly in production during 2015 but was paused due to low graphite prices. The facilities are now maintained and ready for production (Leading Edge Materials, 2020). The graphite deposit is hosted by Svecokarelian metasedimentary and metavolcanic rocks where the graphite is found as medium- to coarse grained, fine-grained, and very fine-grained (Reed, 2015). Reed (2015) reports that the graphite in Woxna is dominantly related to contact metamorphism induced by pegmatite intrusions, in contrast with the other occurrences in Fennoscandia.

Gautneb et al. (2020) review graphite occurrences of economic potential from Senja, Vesterålen, and Holandsfjord in northern Norway. Mining activities have ceased in these areas, except the Skaland graphite mine on Senja that has been in production since 1922. The current location of the mine in Trælen has a total carbon content of 30 %. The mining company is investing in producing anode material and has conducted pre-feasibility studies for an anode material plant in Norway (Skaland Graphite, n.d.; Mineral Commodities, 2020). Rantitsch et al. (2016) report an R2 value of 0.17 and that the graphite in Skaland is fully ordered flake graphite. Accumulation and enrichment of graphite is seen in F_2 folds in eastern Senja. The occurrences studied by Gautneb et al. (2020) resemble each other regarding, e.g. age, mineralogy, and their metamorphic history. The protoliths of the graphite-bearing rocks are 2.2–1.7 Ga in age and metamorphosed in upper amphibolite and granulite facies during the Svecofennian orogeny, which corresponds to several other occurrences in Fennoscandia. Gautneb et al. (2020) have made inferred resource estimations for the graphite occurrences based on length, width, average dip, and contained graphite. These inferred resources have a low confidence level but could be applied to other occurrences in Fennoscandia for indicative resource estimations together with flake size distribution and purity of the graphite concentrate prior to drilling campaigns.

Within the FennoFlakes project, several other studies have been done by M.Sc. and B.Sc. students, among them Kujanpää (2017) and Nygård (2017). Kujanpää (2017) studied the graphite occurrence in the northern Viistola–Hyypiä area in eastern Finland, which was initiated by previous studies during 1970s and 1980s by the Geological survey of Finland (GTK) and motivated by the strong
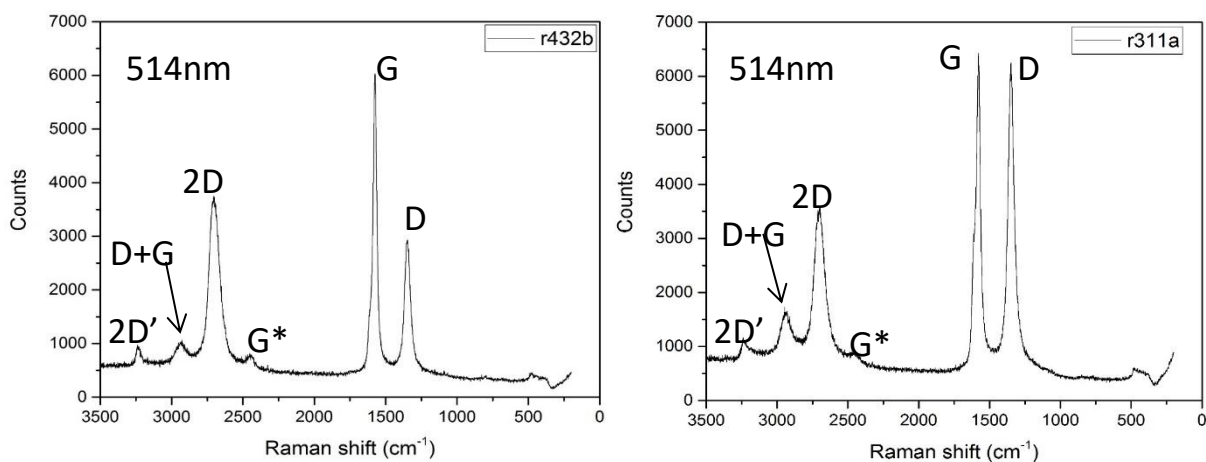
Figure 21. Raman spectra of two samples from the Viistola–Hyypiä area. The spectra show intense D bands with additional bands around the 2D band, which indicates graphite of lower quality (Kujanpää, 2017).

electromagnetic anomalies observed in the area. The Viistola–Hyypiä area belongs to the Karelian Schist Belt, which consists of 2.5–1.9 Ga sedimentary and volcanic rocks that were metamorphosed during 1.95–1.8 Ga in greenschist-lower amphibolite facies. The graphite schist in Viistola–Hyypiä is ca. 2 km in length and 2–25 m wide, but the graphite is very fine grained (< 0.01 mm in size). Collected samples were analyzed with Raman spectroscopy, XRD, and SEM, and the results imply that the graphite in Viistola–Hyypiä is of low quality due to the low metamorphic degree. The obtained Raman spectra show the characteristic G and 2D bands for graphite, and very intense D bands (Fig. 21). The additional bands close to the 2D band are quite distinct and are situated at ca. 2450, 2850, and 3200 cm^{-1}. These additional bands, along with the D band, should diminish during increasing metamorphic conditions. This is an important observation and supports previous studies as it indicates that the retrograde metamorphism in Piippumäki has not affected the graphitic structure and the quality of the graphite. Nygård (2017) studied the graphite occurrence in Haapamäki, northern Savo. The graphite is observed in migmatites, metamorphosed black shale horizons, and shear zones, and was localized by field work and Slingram measurements. The highest concentrations of graphite, up to 50 % C, are found in shear zones that are located in the fold hinge in Haapamäki. SEM, XRD, and Raman spectroscopy were applied for characterization. The results indicate flake graphite of high quality and varying flake sizes up to 2 mm, some reaching up to 10 mm in size. The Raman geothermometer indicates a minimum metamorphic temperature of 670 °C ± 50 °C, which corresponds to the petrographic observations and constructed KFMASH-diagrams. The main difference to the graphite occurrences in Sortland and Piippumäki is the enrichment of graphite in shear zones in Haapamäki. Nygård (2017) observed passive enrichment of graphite, where the graphite is enriched during

shearing. Beowulf Mining has conducted exploration activities and drilling campaigns in the fold limb further to the east of Haapamäki in Aitolampi, where the graphite schist is associated with quartz-feldspar-biotite gneiss. The resource is estimated to 26.7 Mt with 1,275 kt graphite and an average graphitic carbon content of 4.8 %. The concentrates are being tested for battery anodes (Beowulf Mining, 2020).

5 Conclusions

The aim of this study has been to identify and characterize occurrences with flake graphite of high quality in the Fennoscandian shield through field work, analytical work, and comparison to occurrences studied by others. Previous studies have shown that graphite occurrences of interest are present in the Fennoscandian Shield and that especially Raman spectroscopy is a useful method to characterize graphite and to determine the peak metamorphic temperatures. The electromagnetic instrument Slingram is also a suitable tool to quickly locate conductive graphite-bearing rocks in the ground.

45 samples (7 from Sortland and 38 from Piippumäki) were collected for this study. The analytical methods that have been used to characterize flake graphite in Sortland and Piippumäki are SEM, XRD and Raman spectroscopy together with petrographic examination of thin sections. Based on the Raman and XRD measurements the graphite is of high quality with a highly symmetric structure and very little defects in both of the study areas. Raman spectroscopy has shown great capability for not only characterizing graphite, but also as a tool to determine the peak temperature recorded in graphite during metamorphism, as shown by previous studies (Beyssac et al., 2002; Rahl et al., 2005). However, the sample preparation should be done carefully to avoid affecting the graphitic structure and it should be considered during Raman measurements. The recorded Raman spectra show no indications of retrograde metamorphism, which is observed in thin sections from Piippumäki by chloritization of biotite, and cordierite being replaced by bytownite. The lower granulite facies metamorphism in Piippumäki is supported by the presence of biotite, garnet, quartz, sillimanite, and reported cordierite, and temperatures above 700 °C indicated by the Raman geothermometer. Further studies among pseudosections are still needed for precision. Selective fragmentation was tested for liberation of graphite flakes from the host rock and was found to be a quick and simple fragmentation method. However, some deformation of the graphite flakes is observable in the SEM images, but the effects are not seen in the Raman spectra. The use of selFrag for liberating graphite flakes should therefore be studied further to be able to conclude if the graphite flakes are damaged or not, since big flakes have the highest price on the market. Further studies for Sortland and

Piippumäki should include drilling campaigns and enrichment tests for resource and feasibility estimations.

This study shows that there are occurrences of high-quality flake graphite in Fennoscandia and that flake graphite of high quality also can be found at locations where retrograde metamorphism has taken place. Further studies and research could also focus on black shales and metamorphosed black shales in high metamorphic areas, e.g. within the Svecofennian Schist Belt in Finland, by comparing the metamorphic map of Finland with the map of black shales (Arkimaa et al., 2000; Hyvönen et al., 2013; Hölttä and Heilimo, 2017). The outlook for graphite production, especially within the battery anode industry, is promising in the European Union and the rest of Europe due to the current activities in Norway, Sweden, and Finland.

Acknowledgements

References

Al-Ani, T., Leinonen, S., Ahtola, T. and Salvador, D. (**2020**) *High-Grade Flake Graphite Deposits in Metamorphic Schist Belt, Central Finland – Mineralogy, and Beneficiation of Graphite for Lithium-Ion Battery Applications.* Minerals, 10, 680.

Ansilewski, J. (**1973**) *Replacement of cordierite by basic plagioclase.* Acta Geologica Polonica, 23, 509-518.

Arkimaa, H., Hyvönen, E., Lerssi, J., Loukola-Ruskeeniemi, K., and Vanne, J. (**2000**) *Suomen Mustaliuskeet aeromagneettisella kartalla – Proterozoic black shale formations and aeromagnetic anomalies in Finland 1:1 000 000.* Geological Survey of Finland.

Auzanneau, E., Schmidt, M.W., Vielzeuf, D. and Connolly J.A.D. (**2010**) *Titanium in phengite: a geobarometer for high temperature eclogites*. Contributions to Mineral Petrology, 159, 1–24.

Beowulf Mining (**2020**) *Aitolampi – Graphite*. https://beowulfmining.com/projects/fennoscandian-finland-graphite/aitolampi/ (Accessed 24.11.2020).

Best, M.G. (**2003**) *Igneous and Metamorphic Petrology.* 2nd edition, Wiley-Blackwell, San Fransisco, 752 pp.

Beyssac, O., Goffé, B., Chopin, C. and Rouzaud, J.N. (**2002**) *Raman spectra of carbonaceous material in metasediments: a new geothermometer*. Journal of Metamorphic Geology, 20, 859-871.

Beyssac, O., Goffé, B., Petitet, J-P., Froigneux, E., Moreau, M. and Rouzand, J-N. (**2003**) *On the characterization of disordered and heterogeneous carbonaceous materials by Raman spectroscopy.* Spectrochimica Acta Part A, 59, 2267-2276.

Beyssac, O. and Lazzeri, M. (**2012**) *Application of Raman spectroscopy to the study of graphitic carbons in the Earth Sciences*. European Mineralogical Union Notes in Mineralogy, 12, 12:415-454.

Beyssac, O., and Rumble, D. (**2014**) *Graphitic Carbon: A Ubiquitous, Diverse and Useful Geomaterial*. Elements, 10, 415-420.

Buseck, P.R. and Beyssac, O. (**2014**) *From Organic Matter to Graphite: Graphitization.* Elements, 10, 421-426.

Chelgani, S.C., Rudolph, M., Kratzsch, R., Sandmann, D. and Gutzmer, J. (**2016**) *A Review of Graphite Beneficiation Techniques*. Mineral Processing and Extractive Metallurgy Review, 37:1, 58-68.

Coggon, R., and Holland, T.J.B. (**2002**) *Mixing properties of phengitic micas and revised garnet-phengite thermobarometers*. Journal of Metamorphic Geology, 20, 683–696.

DigiKP, Geological Survey of Finland (**2017**) Digital map database of the bedrock of Finland. https://gtkdatagtkfi/Kalliopera/indexhtml (accessed 25.10.2019).

Eckmann, A., Felten, A., Mishchenko, A., Britnell, L., Krupke, R., Novoselov, K.S. and Casiraghi, C. (**2012**) *Probing the Nature of Defects in Graphene by Raman Spectroscopy*. Nano Letters, 12, 3925-3930

Ekholm, E. (**2015**) *Bestämning av metamorfosgraden i Sortland, nordvästra Norge.* MSc thesis, Åbo Akademi University, 56 pp.

European Commission (**2020**) *Critical Raw Materials Resilience: Charting a Path towards greater Security and Sustainability*. 24pp. https://eur-lex.europa.eu/legal-content/EN/TXT/?uri=CELEX:52020DC0474 (Accessed 09.11.2020).

Ferrari, A.C. (**2007**) *Raman spectroscopy of graphene and graphite: Disorder, electron-phonon coupling, doping and nonadiabatic effects.* Solid State Communications, 143, 47-57.

Ferrari, A.C. and Basko, D.M. (**2013**) *Raman spectroscopy as a versatile tool for studying properties of graphene.* Nature Nanotechnology, 8, 235-246.

Ferrari, A.C., Meyer, J.C., Scardaci, V., Casiraghi, C., Lazzeri, M., Mauri, F., Piscanec S., Jiang, D., Novoselov, K.S., Roth, S. & Geim, A.K. (**2006**) *Raman Spectrum of Graphene and Graphene Layers*. Physical Review Letters, 97, 187401–1–187401-4.

Gautneb, H. and Tveten, E. (**1992**) *Grafittundersøkelser og geologisk kartlegging på Langøya, Sortland kommune, Nordland*. Norges geologiske undersøkelse Report 92.155, 86 pp.

Gautneb H. and Tveten, E. (**2000**) *The geology, exploration and characterisation of graphite deposits in the Jennestad area, Vesterålen, northern Norway*. Norges geologiske undersøkelse Bulletin, 436, 67-74.

Gautneb, H., Rønning, J.S., Engvik, A.K., Henderson, I.H.C., Larsen, B.E., Knežević Solberg, J., Ofstad, F., Gellein, J., Elvebakk, H., and Davidsen, B. (**2020**) *The Graphite Occurrences of Northern Norway, a Review of Geology, Geophysics, and Resources.* Minerals, 10, 24pp.

Geovista. *Slingram/HLEM & VLF*. https://www.geovista.se/en/methods/slingramhlem/ (Accessed 07.04.2020).

Gnos, E., Kurz, D. & Eggenberger U. (**2006**) *Electrodynamic disaggregation of geological material.* 4th Swiss Geoscience Meeting, Bern.Hirsch, D., Baldwin, J. and Perkins, D. (**2016**) *Pseudosections.* https://serc.carleton.edu/19591 (Accessed 17.11.2020).

Griffin, W.L., Taylor, P.N., Hakkinen, J.W., Heier, K.S., Iden, I.K., Krogh, E.J., Malm, O., Olsen, K.I., Ormaasen, D.E., and Tveten, E. (**1978**) *Archaean and Proterozoic crustal evolution in Lofoten-Vesterålen, N Norway.* Journal of the Geological Society, 135, 629-647.

Holland, T. and Powell, R. (**1996**) *Thermodynamics of order-disorder in minerals. 2. Symmetric formalism applied to solid solutions.* American Mineralogist, 81, 1425–1437.

Holland, T.J.B. and Powell, R. (**1998**) *An internally consistent thermodynamic data set for phases of petrological interest*. Journal of Metamorphic Geology 16, 309–343.

Holland, T. and Powell, R. (**2001**) *Calculation of phase relations involving haplogranitic melts using an internally consistent thermodynamic dataset*. Journal of Petrology, 42, 673–683.

Hyvönen, E., Airo, M-L., Arkimaa, H., Lerssi, J., Loukola-Ruskeeniemi, K., Vanne, J., and Vuoriainen, S. (**2013**) *Airborne geophysical, petrophysical and geochemical characteristics of palaeoproterozoic black shale units in Finland: Applications for exploration and environmental studies.* In: Hölttä, P. (ed.) Geologian Tutkimusraportti 198 – Geological Survey of Finland, Report of Investigation, 198, 59-61.

Hölttä, P. and Heilimo, E. (**2017**) *Metamorphic Map of Finland.* Special Paper – Geological Survey of Finland, 60, 75-126.

Kouketsu, Y., Miyake, A., Igami, Y., Taguchi, T., Kagi, H. and Enami, M. (**2019**) *Drastic effect of shearing on graphite microtexture: attention and application to Earth science*. Progress in Earth and Planetary Science, 6:23.

Kujanpää, P. (**2017**) *Kvalitetsbestämning av flakgrafit i norra Viistola-Hyypiäområdet, östra Finland.* Master's thesis, Åbo Akademi University, 60 pp.

Kähkönen, Y. (**2005**) *Svecofennian Supracrustal Rocks,* in: Lehtinen, M., Nurmi, P.A., Rämö, O.T. (eds) Precambrian Geology of Finland. Developments in Precambrian Geology, Elsevier, 14, 343-405.

Landis, C.A. (**1971**) *Graphitization of Dispersed Carbonaceous Material in Metamorphic Rocks.* Contributions to Mineralogy and Petrology, 30, 34-45.

Leading Edge Materials (**2020**) *Woxna graphite*. https://leadingedgematerials.com/woxna-graphite/ (Accessed 23.11.2020).

LKAB (**2020**) *Talga, Mitsui and LKAB confirm intent for joint development of the Vittangi graphite mine and battery anode production.* https://www.lkab.com/en/news-room/press-releases/talga-mitsui-and-lkab-confirm-intent-for-joint-development-of-the-vittangi-graphite-mine-and-battery-anode-production/ (Accessed 23.11.2020).

Loukola-Ruskeeniemi, K. (**1992**) *Geochemistry of Proterozoic metamorphosed black shales in eastern Finland, with implications for exploration and environmental studies.* Academic dissertation, University of Helsinki, Geological Survey of Finland, 101pp.

Lund, S., Kauppila, J., Sirkiä, S., Palosaari, J., Eklund, O., Latonen, R-M., Smått, J-H., Peltonen, J. and Lindfors, T. (**2021**) *Fast high-shear exfoliation of natural flake graphite with temperature control and high yield*. Carbon, 174, 123-131.

Luque, F.J., Huizenga, J-M., Crespo-Feo, E., Wada, H., Ortega, L. & Barrenechea, J.F. (**2014**) *Vein graphite deposits: geological settings, origin, and economic significance.* Mineralium Deposita, 49, 261-277.

Lynch, E.P., Hellström, F.A. and Huhma, H. (**2016**) *The Nunasvaara graphite deposit, northern Sweden: New geochemical and U-Pb zircon age results from the host greenstones*. Conference abstract, Nordic Geological Winter Meeting 13–15 January 2016, Helsinki http://www.geologinenseura.fi/winter_meeting/abstracts_newnum_pdf/S2_1_365.pdf (Accessed 23.11.2020).

Lynch, E.P., Hellström, F.A., Huhma, H., Jönberger, J., Persson, P-O. and Morris, G.A. (**2018**) *Geology, lithostratigraphy and petrogenesis of c. 2.14 Ga greenstones in the Nunasvaara and Masugnsbyn*

areas, northernmost Sweden. In: Bergman S (ed) Geology of the Northern Norrbotten ore province, northern Sweden, Rapporter och meddelanden, Sveriges geologiska undersökning, vol 141, 19–77.

Malard, L.M., Pimenta, M.A., Dresselhaus, G. & Dresselhaus, M.S. (**2009**) *Raman spectroscopy in graphene*. Physics Reports, 473, 51-87.

Mineral Commodities (**2020**) *MRC completes pre-feasibility study for active anode material plant in Norway, addressing the fast growing battery market.* https://www.mineralcommodities.com/wp-content/uploads/2020/09/PFS-for-Active-Anode-Plant-in-Norway.pdf (Accessed 1.12.2020).

Mineral Deposits and Exploration (**n.d.**) Geological Survey of Finland. https://gtkdata.gtk.fi/mdae/index.html (Accessed 27.11.2020).

Nemanich, R.J. and Solin, S.A. (**1979**) F*irst- and second-order Raman scattering from finite-size crystals of graphite*. Physical Review B, 20, 392-401.

Newton, R.C., Charlu, T.V. and Kleppa, O.J. (**1980**) *Thermochemistry of the high structural state plagioclases.* Geochimica et Cosmochimica Acta, 44, 933-941.

Nironen, M., Kousa, J., Luukas, J. and Lahtinen, R. (**2016**) *Geological map of Finland – Bedrock 1:1 000 000.* Geological Survey of Finland.

Nurmela, P. (**1989**) *Katsaus Suomen grafiittiesiintymiin.* Geological survey of Finland, report M 81/1989/1.

Nygård, H. (**2017**) *Kvalitetsbestämning av flakgrafit i Haapamäki, Leppävirta, Norra Savolax.* Master's thesis, Åbo Akademi University, 69 pp.

Palosaari, J., Latonen, R-M., Smått, J-H., Blomqvist, R. and Eklund, O. (**2016**) *High-quality flake graphite in a high-grade metamorphic region in Sortland, Vesterålen, northern Norway.* Norwegian Journal of Geology, vol 96, 19-26.

Palosaari, J., Latonen, R-M., Smått, J-H., Raunio, S. and Eklund, O. (**2020**) *Graphite prospect of Piippumäki – an example of a high-quality graphite occurrence in eastern Finland.* Mineralium Deposita, 55, 1647–1660**.**

Pearce, M.A., Godel, B.M. and Thompson, M. (**2015**) *Microstructures and Mineralogy of a World-Class Graphite Deposit*. Society of Economic Geologists, Annual Conference 2015 Hobart, Australia. Program and abstracts.

Pierson, H.O. (**1993**) *Handbook of carbon, graphite and fullerenes.* Noyes Publications, New Jersey, 399 pp.

Rahl, J.M., Anderson, K.M., Brandon, M.T. and Fassoulas, C. (**2005**) *Raman spectroscopic carbonaceous material thermometry of low-grade metamorphic rocks: Calibration and application to tectonic exhumation in Crete, Greece.* Earth and Planetary Science Letters, 240, 339-354.

Rantitsch, G., Lämmerer, W., Fisslthaler, E., Mitsche, S. and Kaltenböck, H. (**2016**) *On the discrimination of semi-graphite and graphite by Raman spectroscopy.* International Journal of Coal Geology, 159, 48-56.

Reed, G.C. (**2015**) *Technical report for the Woxna graphite project, central Sweden.* https://leadingedgematerials.com/wp-content/uploads/2015/05/2015-05-11_Woxna_NI43-101.pdf (Accessed 23.11.2020).

Robinson, G.R., Jr., Hammarstrom, J.M., and Olson, D.W., (**2017**) *Graphite, chap. J*. In: Schulz, K.J., DeYoung, J.H., Jr., Seal, R.R., II, and Bradley, D.C., (Eds.), Critical mineral resources of the United States—Economic and environmental geology and prospects for future supply. U.S. Geological Survey Professional Paper 1802, J1– J24.

Sarapää, O. and Kukkonen, I. (**1983**) *Raportti vuoden 1982 grafiittitutkimuksista*. Geological Survey of Finland. Arkistoraportti M81/1983/2, 23 pp.

Simandl, G.J., Paradis, S., and Akam, C. (**2015**) *Graphite deposit types, their origin, and economic significance*. In: Simandl, G.J. and Neetz, M., (Eds.), Symposium on Strategic and Critical Materials Proceedings, November 13-14, 2015, Victoria, British Columbia, British Columbia Ministry of Energy and Mines, British Columbia Geological Survey Paper 2015-3, 163-171.

Simonen, A. (**1982**) Mäntyharjun ja Mikkelin kartta-alueiden kallioperä. Summary: pre-quaternary rocks of the Mäntyharju and Mikkeli map-sheet areas. Geological map of Finland 1:100 000, explanation to the maps of pre-quaternary rocks, sheets 3123 and 3142. Geological Survey of Finland.

Skaland Graphite (**n.d.**) https://graphite.no/ (Accessed 1.12.2020).

Strong, T., Bala, S.A., Holm-Denoma, C.S., Romeijn, E., Parvaz, D., & Roberts, J.E. (**2015**) *Mechanical and Chemical Dissolution Methods Versus Selective Fragmentation for Mineral and Fossil Separation and Concentrates from Select Geologic Materials.* Poster at Geological Society of America Annual Meeting 2015.

Suppala, I. (**2017**) *Sähkömagneettiset menetelmät*. p. 38-39. In: Huotari, T. and Wennerström, M. (Eds.), Integroitujen geofysikaalisten ja kallioperägeologisten tutkimusmenetelmien kehittäminen yhdyskuntarakentamisen tarpeisiin. Report of Investigation 231, Geological Survey of Finland. 142 pp.

Tajcmanová L, Connolly JAD, Cesare B (**2009**) *A thermodynamic model for titanium and ferric iron solution in biotite*. Journal of Metamorphic Geology 27: 153–164.

Talga (**2020**) *Vittangi*. https://www.talgagroup.com/irm/content/vittangi1.aspx?RID=285 (Accessed 23.11.2020).

Vasara, H. (**2018**) *Sector reports – Mining industry*. Publications of the Ministry of Economic Affairs and Employment, Sector reports 40/2018. 89 pp.

Waldbaum DR, Thompson JB (**1968**) Mixing properties of sanidine crystalline solutions: 2. Calculations based on volume data. American Mineralogist, 53: 2000–2017.

Wall, M. (**2012**) *Raman spectroscopy optimizes graphene characterization.* Advanced Material & Processes, 170, 35-38.

Wang, E., Shi, F. & Manlapig, E. (**2011**) *Pre-weakening of mineral ores by high voltage pulses.* Minerals Engineering, 24, pp. 455-462.

White, R.W., Powell, R., Holland, T.J.B. and Worley, B.A. (**2000**) *The effect of TiO_2 and Fe_2O_3 on metapelitic assemblages at greenschist and amphibolite facies conditions: mineral equilibria calculations in the system K_2O-FeO-MgO-Al_2O_3-SiO_2-H_2O-TiO_2-Fe_2O_3*. Journal of Metamorphic Geology, 18, 497–511.

White, R.W., Powell, R. and Holland, T.J.B. (**2001**) *Calculation of partial melting equilibria in the system Na_2O-CaO-K_2O-FeO-MgO-Al_2O_3-SiO_2-H_2O (NCKFMASH).* Journal of Metamorphic Geology, 19, 139–153.

Wopenka B. and Pasteris, J.D. (**1993**) *Structural characterization of kerogens to granulite-facies graphite: Applicability of Raman microprobe spectroscopy*. American Mineralogist, 78, pp. 533-557.

World Bank (**2020**) *Minerals for Climate Action: The Mineral Intensity of the Clean Energy Transition* by Hund, K., La Porta, D., Fabregas, T.P., Laing, T. & Drexhage, J., Climate-smart Mining Facility. World Bank Group. 112 pp. (Accessed 09.11.2020).

APPENDIX I

Table including the collected samples and which analytical methods were applied. The sample IDs starting with 300xxx are from Sortland and the rest are from Piippumäki. The sample IDs followed by an asterisk (*) are analyzed by ActLabs for total carbon and total sulfur.

Sample ID	SelFrag	SEM	XRD	Raman spectroscopy	Thin section	Raman geothermometer	Whole-rock geochemistry	Graphite bearing rock	Country rock
300220.1	X	X						X	
300247.1		X			X	X		X	
300247.2		X	X	X				X	
300251.1	X	X			X			X	
300266.3	X	X						X	
300289.1	X	X	X	X		X		X	
300295.1	X	X	X	X		X		X	
404801					X				X
404802					X				X
404803					X				X
404804		X	X	X	X	X		X	
404805		X	X	X				X	
404806		X	X	X				X	
404807		X			X				X
404808		X						X	
404808A		X						X	
404809					X				X
404810					X				X
404811					X		X		X
404812 (Kärpälä)		X	X	X				X	
404812A (Kärpälä)		X						X	
404813		X						X	
404870A*							X		
404873		X		X	X	X		X	
404874 (Kärpälä)				X		X		X	
404879		X		X	X	X		X	
PIIPPU_2015_005		X						X	
PIIPPU_2015_007		X						X	
PIIPPU_2015_010b					X				X
PIIPPU_2015_014a					X				X
PIIPPU_2015_014b					X				X
PIIPPU_2015_014c					X				X
PIIPPU_2015_014d		X			X				X
PIIPPU_2015_015		X						X	
PIIPPU_2015_016*		X		X	X	X	X	X	
PIIPPU_2015_017A*							X	X	
PIIPPU_2015_017B*							X	X	
PIIPPU_2015_018		X						X	
PIIPPU_2015_019*		X					X	X	
PIIPPU_2015_020*				X	X	X	X	X	
PIIPPU_2015_021		X						X	
PIIPPU_2015_022*							X	X	
PIIPPU_2015_024*				X	X	X	X	X	
PIIPPU_2015_039		X		X	X	X		X	
PIIPPU_2015_040		X						X	

APPENDIX II

Photomicrographs of sample PIIPPU_2015_014d showing the supposed cordierite, which actually is bytownite as seen in SEM analysis (below).
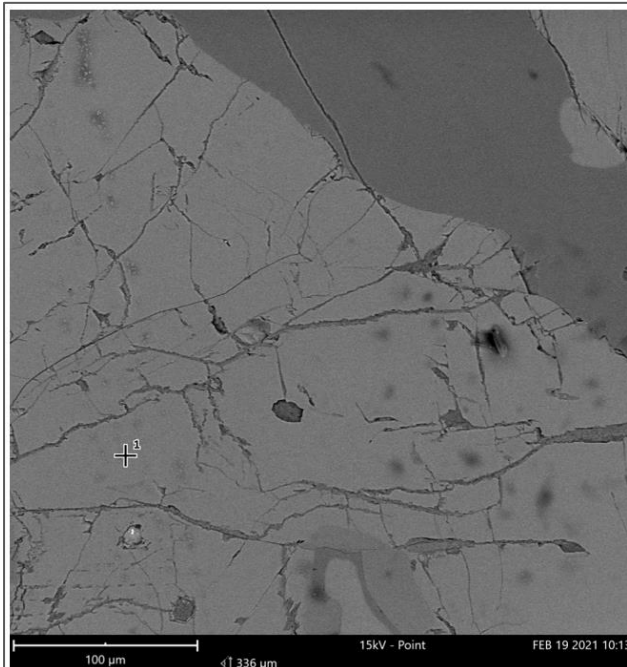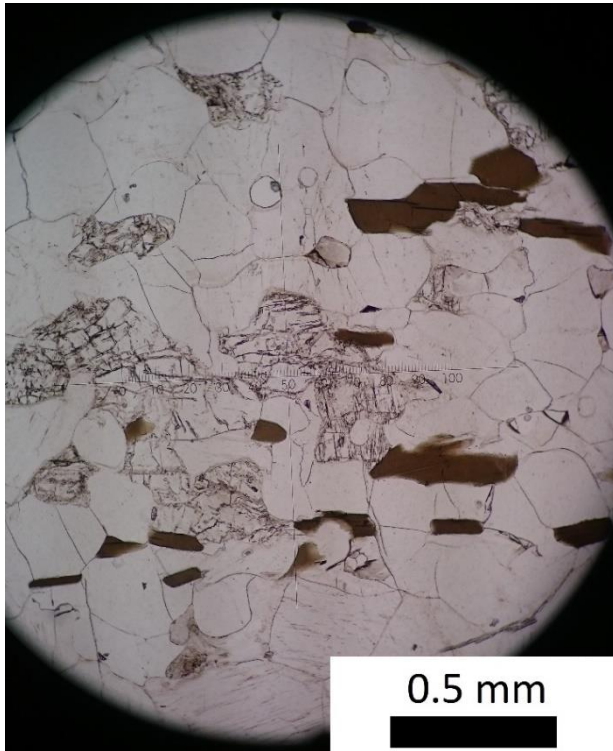
Element Symbol	Atomic Conc.	Weight Conc.	Oxide Symbol	Stoich. wt Conc.
O	64.54	50.03		
Si	16.09	21.90	SiO_2	49.54
Al	13.44	17.57	Al_2O_3	35.11
Ca	4.44	8.63	CaO	12.76
Na	1.22	1.36	Na_2O	1.93
K	0.27	0.51	K_2O	0.65

End member   mole %
An   74.94
Ab   20.51
Or   4.54
Based on Ca,Na.K ratios only

Si+Ti+Al+Fe3= 4.164
ideal =   4.000

Ca+Na+K=   0.836
ideal =   1.000

FOV: 336 µm, Mode: 15kV - Point, Detector: BSD Full, Time: FEB 19 2021 10:13

APPENDIX III

Whole-rock chemical composition for sample 404811 (analyzed at Åbo Akademi University) and the total carbon and sulfur for graphite-bearing rocks from Piippumäki (analyzed at ActLabs Ltd).

Sample no.	SiO_2	TiO_2	Al_2O_3	FeO	MnO	MgO	CaO	Na_2O	K_2O	H_2O	Total
404811	59.74	1.48	15.32	12.31	0.17	3.57	1.78	2.16	1.89	1.54	99.96
	Total C (%)			Total S (%)			C-graph (%)				
404870A	14.8			0.09			14.7				
PIIPPU_2015_016	5.32			0.09			5.13				
PIIPPU_2015_017A	2.96			0.06			2.91				
PIIPPU_2015_017B	3.02			0.07			2.91				
PIIPPU_2015_019	4.56			1.66			4.66				
PIIPPU_2015_020	9.67			0.3			9.5				
PIIPPU_2015_022	9.12			0.23			9.05				
PIIPPU_2015_024	2.43			0.15			2.39				

APPENDIX IV

Author's contribution

Jenny Palosaari has contributed to the majority of this work with the help from co-authors. Palosaari has planned and conducted field work, sampled the rocks, prepared the samples for analysis, and studied thin sections in microscope. Jennifer Juslenius, Erik Leino, Henrik Nygård, Sauli Raunio, Robert Rundqvist, Isa Witick, and Christoffer Österholm were assisting during field work for Palosaari et al. (2020). Palosaari also performed Raman spectroscopy measurements, analyzed the data, and calculated the peak temperature estimations. Palosaari got help from Pentti Hölttä concerning the construction of the pseudosection for Palosaari et al. (2020), and from Jukka Marmo, Seppo Töllikkö and Ahti Nissinen regarding the selFrag at the Geological Survey of Finland for Palosaari et al. (2016).

Rose-Marie Latonen contributed with the Raman spectroscopy measurements, analyzing the data, and producing the spectra in Palosaari et al. (2016). Latonen also contributed with the peak temperature estimations. In Palosaari et al. (2020) Latonen helped with analyzing the data from the Raman spectroscopy measurements. Latonen is also the second supervisor for the author.

Jan-Henrik Smått contributed to this work by performing the XRD measurements and helped with analyzing the results for Palosaari et al. (2016 and 2020).

Linus Silvander contributed to this work by operating the SEM for Palosaari et al. (2016 and 2020).

Rasmus Blomqvist contributed to Palosaari et al. (2016) with supervising the field work performed in Sortland, northern Norway.

Sauli Raunio contributed to Palosaari et al. (2020) by being an active part in the field work, contributing with valuable discussions regarding the analysis results, and helping with constructing the maps in ArcGIS. Raunio also took part in the electromagnetic measurements for Palosaari et al. (2020).

Olav Eklund is the supervisor for the author and has contributed with valuable discussions and opinions regarding this work. Eklund also contributed with in-house SEM analysis on some of the thin sections.

GEOLOGICAL
SOCIETY OF NORWAY

High-quality flake graphite occurrences in a high-grade metamorphic region in Sortland, Vesterålen, northern Norway

Jenny Palosaari[1], Rose-Marie Latonen[2], Jan-Henrik Smått[3], Rasmus Blomqvist[4] & Olav Eklund[1]

[1]Department of Geology and Mineralogy, Åbo Akademi University, Tuomiokirkkotori 1, 20500 Turku.
[2]Johan Gadolin Process Chemistry Centre, Laboratory of Analytical Chemistry, Åbo Akademi University, Piispankatu 8, 20500 Turku.
[3]Center for Functional Materials, Laboratory of Physical Chemistry, Åbo Akademi University, Porthaninkatu 3, 20500 Turku.
[4]Norwegian Graphite AS, Laivurintie 11, 21100 Naantali.

E-mail corresponding author (Jenny Palosaari): jenny.palosaari@abo.fi

The aim of this study has been to determine the quality of flake graphite in high-grade metamorphic rocks in Sortland, Vesterålen, northern Norway. Flake graphite is present in graphite schist and samples were collected at three different locations, Hornvatnet, Lamarkvatnet and Vikeid. The host rocks of the graphite schist are dolomite or calcite marble, pyroxene gneiss and amphibolite. Granulite-facies metamorphism on sedimentary material led to the formation of the graphite schist. According to previous studies, the graphite content of the schists in the area varies between 5 and 30%. Sampled graphite schists were fragmented by selective fragmentation (selFrag) and analysed using scanning electron microscopy, Raman spectroscopy and X-ray diffraction. The grain size and texture of the sampled graphite schists vary macroscopically. Some contain abundant, visible, big (up to 5 mm in size) and ordered graphite flakes with layered structure whereas other schists contain smaller graphite flakes and a lower graphite content. Pictures from the SEM indicate that the graphite flakes consist of several, parallel, graphene layers with clean surfaces. The results from both Raman spectroscopy and XRD support the SEM analyses that the flake graphite consists of several layers and also imply that the flake graphite is almost free from defects.

Introduction

Graphite is formed in metamorphic rocks under reducing conditions and increasing temperature and pressure. The typical source of graphite in metamorphic rocks is sedimentary organic matter which, when subjected to increasing metamorphic grade, forms a flaky variant of graphite. In the industry, the biggest consumer of flake graphite is the refractories industry, because flake graphite improves the refractory products' resistance to heat and erosion.

Flake graphite is also used in the steel industry, in brakes, and as lubricants (Mitchell, 1993). Additionally, flake graphite can be used to produce graphene, as demonstrated in 2004 by Konstantin Novoselov and Andre Geim (Novoselov et al., 2004). Graphene is a one atom thick, two-dimensional, hexagonal lattice layer of carbon atoms with many properties desirable in developing better electronics, e.g., in batteries, conductors, transparent electrodes and supercapacitors (Singh et al., 2011). The high electrical conductivity of graphene is prominent (Geim & Kim, 2008) and could be utilised in many different electronic devices such as in smartphone displays.

In this paper we describe flake graphite occurrences in Sortland, Vesterålen, northern Norway. They are located in a high-grade metamorphic domain on the island of Langøy. This work builds upon previous mapping, exploration and characterisation of graphite occurrences in Norway performed, e.g., by the Geological Survey of Norway in the 1990s (Gautneb & Tveten, 2000). The aim of this study has been to determine the abundance of high-grade flaky graphite showing a well-ordered crystal lattice free from contaminants, thus suitable for industrial and technological use.

Graphite

Graphite consists of multiple layers of graphene, which is a two-dimensional network of one-atom thick layers of carbon. The carbon atoms in graphene are connected by strong covalent bonds and the layers are connected by weak van der Waals bonds (Hazen et al., 2013). In oxidising environments, graphite decomposes at 600°C, whereas in non-oxidising environments it melts at 3550°C (Mitchell, 1993). Graphite occurs most commonly in metamorphic rocks, but also in magmatic rocks as an accessory mineral (Hazen et al., 2013). Graphite is a common mineral in Norwegian rocks; however, it is rarely found at levels of economic interest regarding grade and carbon content. Graphite in metamorphic rocks is formed from sediments rich in organic matter as a result of metamorphism. Initially, the organic matter goes through a process of

carbonisation during diagenesis, which results in the solid residue getting enriched in carbon while impurities escape. The remaining carbon can be subjected to further burial and metamorphism and thus become completely graphitised (Buseck & Beyssac, 2014).

Flake graphite is most commonly present in mica schist and quartzite, or schist rich in both mica and feldspar. Impurities in graphite ore are generally quartz, feldspar, mica and amphibole. Since carbon creates a reducing environment, any metals present are bound to sulphur as sulphides. A good graphite ore should contain as few sulphide minerals as possible. Flake graphite ores are usually stratabound, and the ore bodies commonly occur as lenses in the surrounding bedrock (Mitchell, 1993).

Geological setting

The graphite schists investigated in this study are located on the island of Langøya close to Jennestad in Sortland, Lofoten–Vesterålen, northern Norway, at three different locations: Hornvatnet, Lamarkvatnet and Vikeid (Fig. 1). The graphite-bearing rocks belong to a suite of high-grade metasupracrustal rocks of Palaeoproterozoic age, probably deposited at around 1.95–1.87 Ga – the same time as the major depositional stage in arc environments in the Svecofennian domain (Lahtinen et al., 2002). Calcite and dolomite marbles, amphibolites and
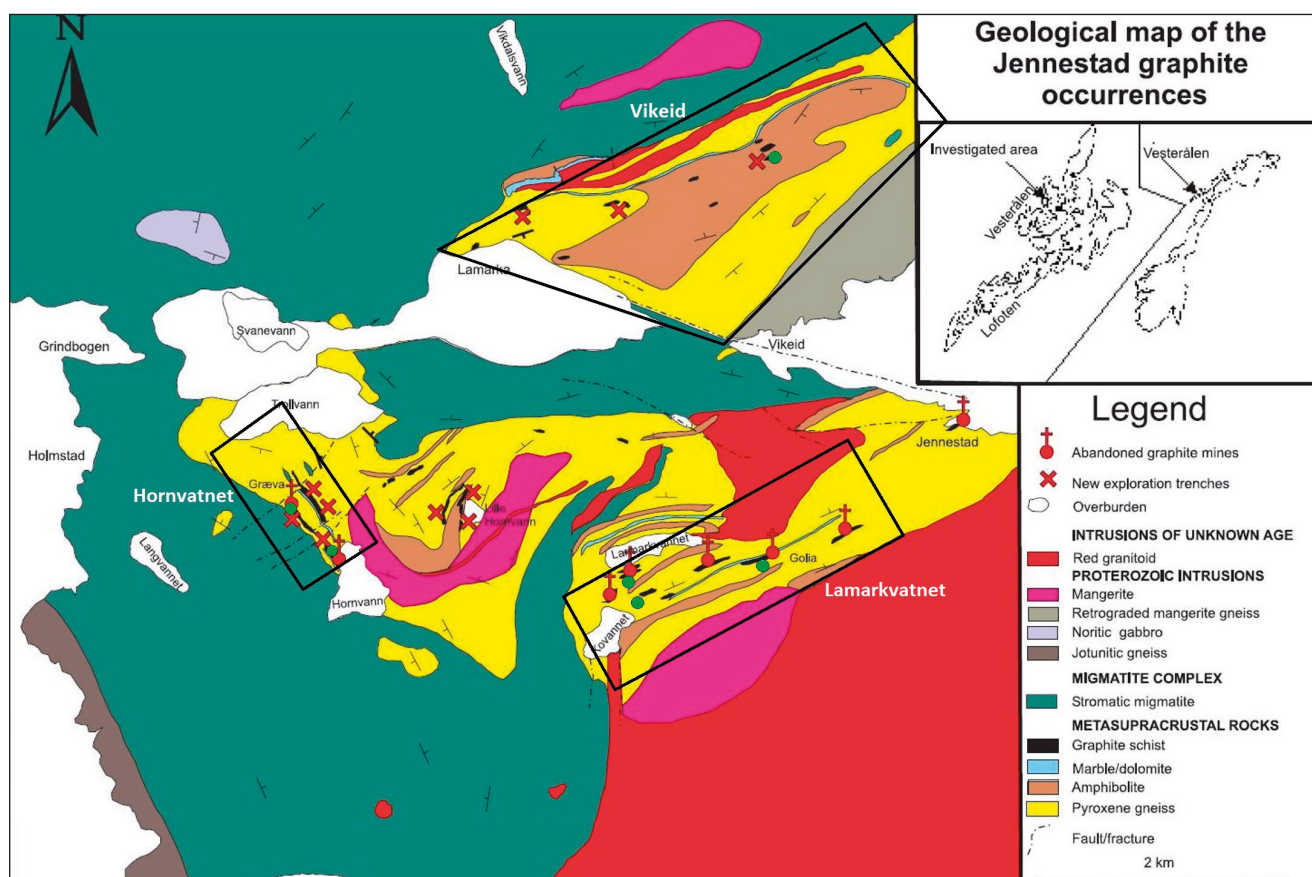

Figure 1. Geological map of the graphite occurrences (black veins) in Jennestad, Sortland (modified from Gautneb & Tveten, 2000). The investigated areas for this study are marked with black lines and the sample collection sites with green dots.

pyroxene gneisses are part of this suite. Based on their chemical composition, the protoliths of the metasupracrustal rocks are of sedimentary and volcanic origin, probably from a shallow-marine environment (Griffin et al., 1978). The islands of Lofoten–Vesterålen can be divided into western and eastern segments. The western segment consists of gneisses in granulite facies and an intrusive anorthosite-mangerite-charnockite-granite (AMCG) complex, principally 1.8 Ga in age (Corfu, 2004), while the eastern part consists of rocks in amphibolite facies and felsic intrusive rocks which lack orthopyroxene. The transition zone also coincides with the eastern border of a high-magnetic anomaly (Corfu, 2007). All locations in this study lie in the transition zone between amphibolite and granulite facies. According to Ekholm (2015), there is some difference in metamorphic grade in the bedrock surrounding the graphite; orthopyroxene is found only in the Hornvatnet area, which is the westernmost of the investigated areas. This implies that the metamorphic grade in the area is increasing to the west. The bedrock in contact with the graphite schists consists of calcite and dolomite marble (hanging wall) and amphibolite (footwall), but pyroxene gneisses are also found close to the graphite schists. The rocks of the Lofoten–Vesterålen area have been subjected to granulite-facies metamorphism at several occasions during Archaean and Proterozoic time. Since evidence for all these metamorphisms is found on both sides of the transition zone between granulite and amphibolite facies, the zone could represent a tectonic boundary instead of a transition due to just one metamorphic event (Corfu, 2007).

In the area, the graphite schists and the other associated metasupracrustal rocks are mostly covered by superficial deposits. The best locality to study the setting of the graphite schists is at the entrance of the abandoned graphite mine Golia, south of Lamarkvatnet (Fig. 1). There, the graphite-bearing bodies are commonly 2–4 m thick (Gautneb & Tveten, 2000). The graphite schist strikes NW–SE at Hornvatnet, N–S and NE/E–SW/W at Lamarkvatnet and NE–SW at Vikeid. The graphite schists at Hornvatnet are steeply dipping, nearly vertical, towards southwest. At Lamarkvatnet and the Golia mine, the graphite schist strikes from west to east and dips *c.* 60° towards north (Gautneb & Tveten, 1992). The amount of graphite in the graphite schists in the area varies a lot between *c.* 10% and 30%, but the average graphite content is approximately 19 wt.% (Gautneb & Tveten, 1992).

Materials and methods

Of the samples collected, 7 samples of graphite schists were prepared for further study (Table 1). Macroscopically, the graphite schists differ slightly from each other concerning grain size and graphite content. The grain sizes in the schists vary from fine to medium, but some of the schists are even coarse grained. To determine the quality of the flake graphite, flakes extracted by selective fragmentation (selFrag) were subjected to study by scanning electron microscopy (SEM), X-ray diffraction (XRD) and Raman spectroscopy.

Petrography

The petrography of the material was documented from thin-sections and SEM. With SEM, the principal composition of some minerals was measured. No detailed metamorphic study was undertaken, because of the uncertainties in the chemical composition obtained by SEM. However, we present some general data of the mineral chemistry. Depending on the host rock, graphite appears in different ways. Graphite was found in two main rock types in the sampling area: pyroxene gneiss and metapelite. The pyroxene gneiss (Fig. 2A) consists mainly of diopside ($wo_{53.43}$, $en_{42.04}$, $fs_{4.54}$, (Fe/Fe+Mg) = 0.10 and Al_2O_3 around 3 wt.%), graphite and poikiloblasts of spinel ((Fe/Fe+Mg) = 0.331, ZnO = 2.5 wt.%) and some garnet ($pyr_{81.35}$, $alm_{15.20}$, $gross_{3.45}$ and $r_{1.07}$). In the pyroxene gneiss, black veins are identified as graphite and brown veins as iron oxides together with minor amounts of Mg, Si and Al. The graphite grains appear as nails and are located at 120° mineral borders. The foliated metapelite (Fig. 2B) contains K-feldspar, quartz, plagioclase (oligoclase), graphite and biotite, while clinopyroxene ($wo_{49.97}$, $en_{36.74}$, $fs_{3.28}$, Fe/Fe+Mg = 0.27), orthopyroxene, apatite and pyrite are present as minor phases in the sample. The Ti content of the biotite was measured to approximately 6 wt.%. The metapelite samples are mainly evenly grained and medium to fine grained in size. The graphite appears deformed together with the biotite. The majority of the graphite flakes in the samples are stubby, elongated and 0.5–1 mm long, and some flakes reach up to 1.2 mm in length.

Table 1. *Processing and analytical methods applied to the Sortland graphite schist samples.*

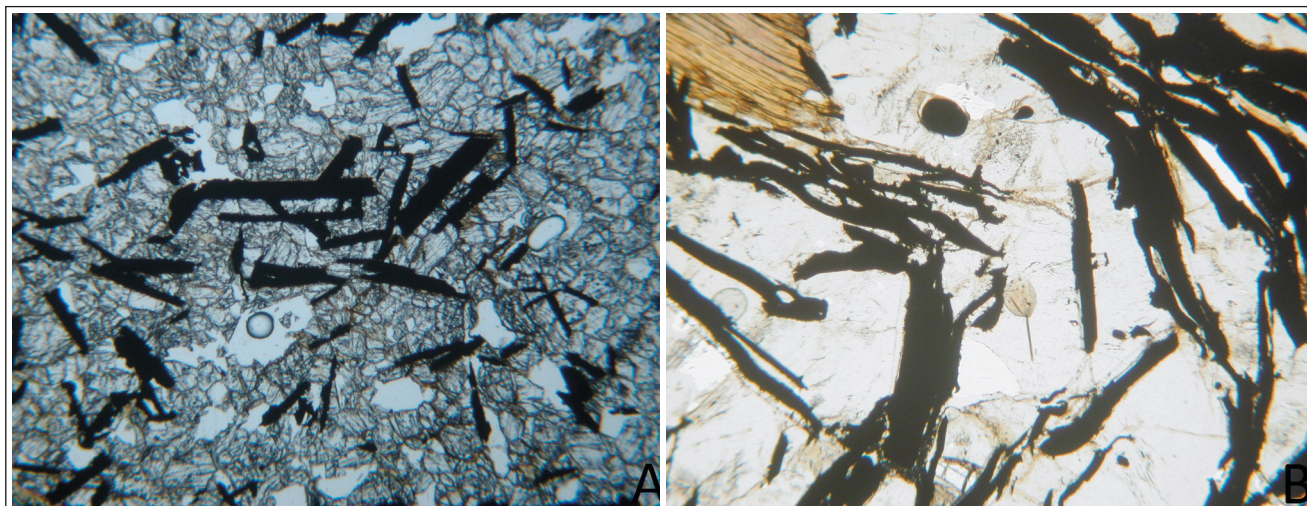| Sample	300220.1	300247.1	300247.2	300251.1	300266.3	300289.1	300295.1
Coordinates (UTM33)	X: 507563 Y: 7625339	X: 509899 Y: 7625179	X: 509899 Y: 7625179	X: 509989 Y: 7625014	X: 510968 Y: 7625359	X: 510983 Y: 7628548	X: 507235 Y: 7625664
Location	Hornvatnet	Lamarkvatnet	Lamarkvatnet	Lamarkvatnet	Lamarkvatnet	Vikeid	Hornvatnet
Selective fragmentation	X			X	X	X	X
SEM	X	X	X	X	X	X	X
XRD			X			X	X
Raman			X			X	X

Figure 2. (A) Graphite-bearing pyroxene gneiss and (B) metapelite as seen in a polarisation microscope. The black nails are graphite flakes. The pictures are 1.88 mm across.

Selective fragmentation

Selective fragmentation (selFrag) was performed at the research laboratory of the Geological Survey of Finland in Espoo. This method was used to test if it is suitable for separating graphite from other minerals and separating the graphite flakes from each other. The method uses short (2–5 Hz), high-voltage pulses (150–200 kV) directed on the sample in a container filled with water and gaseous nitrogen. The goal is to obtain mineral aggregates fragmented at mineral grain boundaries (Wang et al., 2011).

The first round of fragmentation for sample 300289.1 was performed with 25 pulses at 100 kV with a frequency of 3 Hz, which took 2–3 minutes. For the second round of fragmentation the pulses were increased to 50 at 100 kV and for the third round to 100 at 130 kV. The settings were then changed because the material did not fragment as desired. Samples 300220.1, 300251.1, 300266.3 and 300295.1 were fragmented using the same settings for three rounds, i.e., 50 pulses at 130 kV with 3 Hz frequency, except on round two for sample 300251.1 with 30 pulses at 130 kV and 3 Hz frequency. After fragmentation, the samples were left to dry in an oven at 60°C for four days. The material was sieved into different fractions after fragmentation: >2 mm; 1–2 mm; 0.59–1 mm; 0.5–0.59 mm; 0.25–0.5 mm; and <0.25 mm.

Scanning electron microscopy

The scanning electron microscope (SEM), a LEO Gemini 1530 FEG–SEM instrument with a ThermoNoran X-ray detector, at the Laboratory of Inorganic Chemistry, Åbo Akademi University was used to examine two thin-sections and the graphite flakes obtained by selective fragmentation. Sample 300247.2 consisted of graphite flakes that were manually extracted from the graphite schist. As the graphite sample is conductive, no additional conductive layer was needed. The samples from the selective fragmentation were also examined with the SEM. Energy dispersive X-ray analysis (EDXA, Ultradry) was used for elemental analysis. The goal was to deter-

mine if the graphite schists differ from each other in flake size, if there are any impurities in the schists or in the graphite flakes, and how the selective fragmentation might have affected the samples.

X-ray diffraction

X-ray diffractometry (XRD) was used to determine the distance between the graphene layers in the flake graphite and to check for potential impurities. The analysed samples were 300247.2, 300289.1 and 300295.1 (Table 1). The XRD used was a Bruker D8 Discover, located at the Laboratory of Physical Chemistry at Åbo Akademi University, and the wavelength used was Cu–Kα (1.5406 Å). The measurements with the X-ray diffractometer were performed with a point detector. The samples were measured on a single spot and scanned in the range 20° to 80° several times for a better signal-to-noise ratio. Samples 300289.1 and 300295.1 were ground to powder (grinding can contribute to better statistics obtained from the analysis) while 300247.2 was a single Ø 2 mm grain with a thickness of 0.5 mm.

Raman spectroscopy

Raman spectroscopy can reveal defects in the sample and how thick the layers are in, e.g., flake graphite. The peak metamorphic conditions can also be defined from Raman spectroscopy measurements, since the variations in the metamorphic grade affect the degree of organisation of the carbonaceous material (Beyssac et al., 2002). The tested samples were 300247.2, 300289.1 and 300295.1 (Table 1) and the measurements were made with the Raman spectrometer at the Laboratory of Analytical Chemistry, Åbo Akademi University. The Raman spectra were recorded using a Renishaw Ramascope (system 1000) equipped with a Leica DMLM microscope connected to a CCD camera. The measurements were made by using an Ar-ion laser (LaserPhysics) with the excitation wavelength of 514 nm on a *c.* Ø 2 μm surface area with a laser power of 20 mW. The spectrometer was calibrated against a Si standard (520.0 cm^{-1}).

Results

The mineralogy of the pyroxene gneiss and metapelite was identified in thin-sections and with SEM. According to the results from the analyses, the pyroxene gneiss consists mostly of diopside and graphite and the metapelite of K-feldspar, quartz, plagioclase, biotite and graphite. The graphite flakes vary in size (Fig. 2A, B), and are up to 1.2 mm in length. The flakes are both evenly distributed

Figure 3. Distinct graphite flakes after fragmentation in a selFrag device (sample 300266.3), fraction 0.5–1 mm. The big flake is approximately 1 mm in length.

in the rock and concentrated in fractures and along the foliation. Some graphite flakes seem to be folded and broken, which may imply that the rock has been affected by tectonic stresses after the crystallisation of the graphite flakes. The flakes are situated in possible pressure shadows and also associated with metamorphic triple-junction textures (seen in Fig. 2A) throughout the sample.

Selective fragmentation

After three sets of high-voltage pulses the graphite schists were fragmented, but not completely. Many mineral grains were still attached to each other on a microscopic scale. In an optical microscope, graphite, feldspars, quartz and some rusty unidentified minerals were observed in the sample. Some graphite flakes were still attached to other minerals, while others were not (Fig. 3). The results from fragmentation of the samples obtained with selFrag are promising, but the method needs to be optimised and investigated further in order to establish the optimal parameters for fragmentation and for not breaking the graphite flakes.

Scanning electron microscopy on grains

The different size fractions of graphite flakes obtained after fragmentation were examined with a scanning electron microscope (Table 1). Almost all graphite fragmented by selFrag is deformed. This could be an effect of the high voltage electrical pulses passing through the samples in the selFrag, but could also be a result of tectonic deformation. In some places, the layers of the graphite flakes seem to have slipped relative to each other and space has formed between the layers in microscopic folds (Fig. 4A). These structures must have formed during the secondary handling of the sample, i.e., the selFrag treatment. The SEM images also show that all the samples consist of flaky graphite, i.e., that one graphite flake consists of several layers, with regular and irregular flake edges and clean flake surfaces. Sample 300247.2 differs from the other samples in that the graphite flakes do not appear to be as intensely deformed as in the other samples (Fig. 4B).
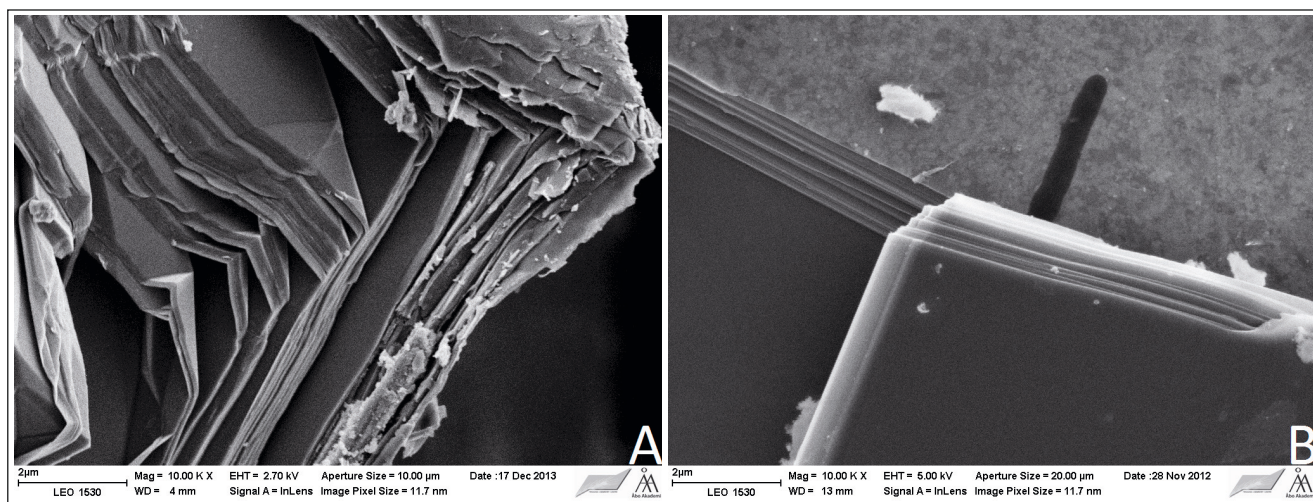

Figure 4. (A) Selectively fragmented graphite flakes (sample 300220.1) as seen in SEM; and (B) manually fragmented flakes from graphite schist (sample 300247.2). The graphite flakes fragmented by selFrag are folded.

X-ray diffraction

The obtained XRD results on graphite, both single grain and powder, are presented in Fig. 5. For the 300247.2 sample (single grain), only two sharp reflections related to graphite are visible, indexed as (002) and (004), and indicate a long-range ordering in the atomic structure of the flake graphite. For the 300289.1 and 300295.1
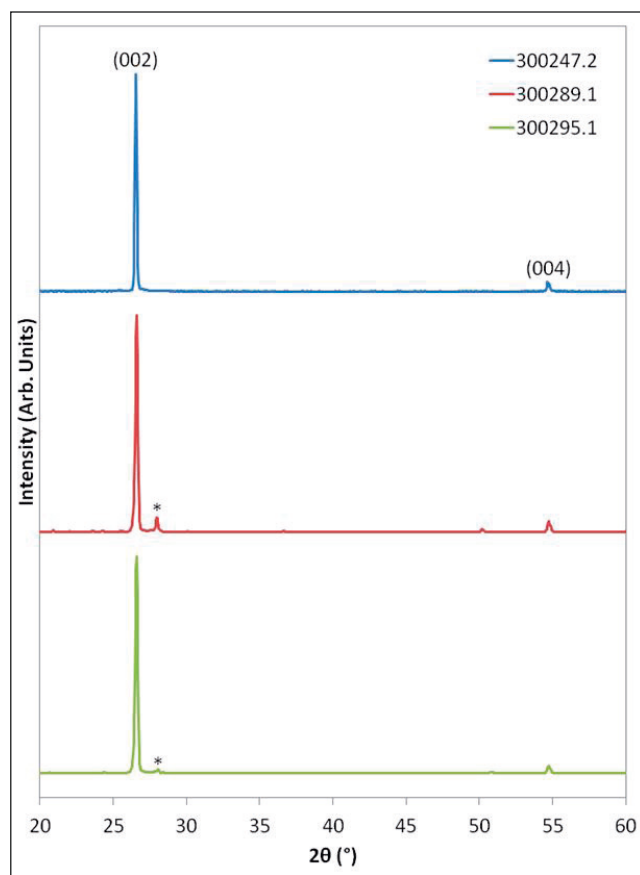
samples (powder), traces of quartz and albite were also observed in addition to the (002) and (004) graphite reflections (e.g., albite is indicated with an asterisk in Fig. 5). The slight peak broadening of the (002) reflection for the latter samples indicates that the graphite crystals are smaller or slightly less ordered. There appear not to be any differences between the (002) position of the samples, which indicates that the distances between the graphene layers are similar. The d spacing between the graphene layers was analysed from the (002) reflection to be 0.335–0.336 nm, which is the expected distance between the graphene layers in graphite (Pierson, 1993).

Raman spectroscopy measurements

Both manually fragmented (300247.2) and selectively fragmented (300289.1 and 300295.1) samples were examined with Raman spectroscopy. The spectrum of the manually fragmented sample is shown in Fig. 6A, measured at two different positions on the crystal shown on the microscope image in the inset. The Raman spectra of the samples fragmented by the selFrag method are shown in Fig. 6B, C. The most intense features of Raman spectra of graphite are the so-called G band and 2D band (also called G' band) (Ferrari et al., 2006; Eckmann et al., 2012; Wall, 2012). The G band is characteristic for the in-plane vibrational mode involving sp^2-hybridised carbon atoms which comprise the graphene sheets in graphite. The position of the G band is highly sensitive to the number of graphene layers and in graphite it is at c. 1580 cm^{-1}. The G band position shifts to a higher energy (higher wavenumbers) location as the layer thickness decreases (Wall, 2012).

The narrow G band in the manually and selectively fragmented samples is present at c. 1579 cm^{-1} (Fig. 6), which implies that the material is graphite formed at high-grade metamorphic conditions (Beyssac et al., 2002). If the G band were to be present at lower wavenumbers, the material would possibly be amorphous graphite (Ferrari et al., 2006). The 2D band is supposedly unrelated to the G band; rather, it is an overtone of the so-called D band. The D

Figure 5. The XRD results for samples 300247.2 (blue), and 300289.1 (red) and 300295.1 (green). The plots have been offset for clarity.
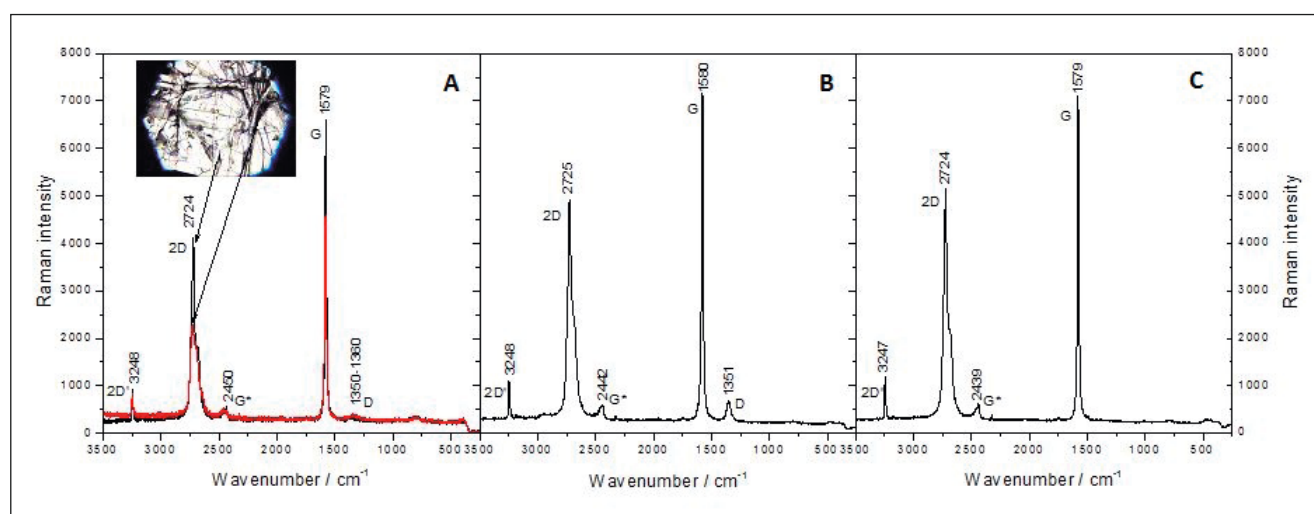

Figure 6. Raman spectra of (A) sample 300247.2, (B) sample 300289.1 and (C) sample 300295.1. The measuring points are marked with arrows in (A). The laser excitation wavelength used is 514 nm.

band, located at *c.* 1350 cm^{-1}, is characteristic for unorganised carbon. It is also known as a disorder or defect band and represents a mode from sp^3-bound carbon (Ferrari, 2007; Wall, 2012). The D band intensity decreases in relation to the G band due to stiffening of aromatic planes. On the other hand, the intensity of the D band increases with a decrease in the graphite crystal size and therefore it can be said that the presence of the D band indicates that the crystallite size is smaller than a few microns. A low-intensity D band is visible at 1350–1360 cm^{-1} in the manually fragmented sample shown in Fig. 6A and at 1351 cm^{-1} in one of the selectively fragmented samples (300289.1) shown in Fig. 6B. The other selectively fragmented sample (sample 300295.1, Fig. 6C) did not show any D band at all.

In contrast to a single-layer graphene having a symmetrical 2D band with a high intensity at *c.* 2700 cm^{-1}, the 2D band in bulk graphite is composed of four components, two of which have higher relative intensities than the other two and shown as a shoulder towards lower intensities (Ferrari, 2007; Malard et al., 2009; Wall, 2012). The maximum of the 2D band in the manually fragmented sample is located at 2749 cm^{-1} and in the selectively fragmented samples at 2725 cm^{-1} and 2724 cm^{-1}, respectively (Fig. 6). The asymmetric 2D band implies that there are many parallel layers of graphene in the samples. The fourth characteristic band visible in the graphite Raman spectra is called the 2D' band at *c.* 3250 cm^{-1}. It is the second order of the intra-valley peak called D' at *c.* 1620 cm^{-1}. The D' band becomes visible when the laser is shot on a boundary edge, formed by cutting the graphene planes at different angles (Malard et al., 2009). The 2D' band is visible in all the graphite spectra shown in Fig. 6. The fifth characteristic band in graphite Raman spectra is visible at *c.* 2450 cm^{-1} and is called as G*. Several assignments exist for this band, but it is believed to originate from an inter-valley process as an overtone of in-plane modes (Nemanich & Solin, 1979; Ferrari & Basko, 2013).

The degree of organisation of carbonaceous material is found to be highly sensitive to variations in the metamorphic grade. It has been shown by comparing Raman spectra from several reference samples from different metamorphic belts that Raman spectroscopy can be used as an indicator of the metamorphic conditions (Wopenka & Pasteris, 1993; Beyssac et al., 2002). The ratio between the peak area of the D band and the sum of the areas of the G, D and D' bands (R) has been used as a reliable parameter to follow the graphitisation process. A linear relationship between R and temperature has shown R values <0.2 at temperatures between 500 and 650°C. In contrast, no clear trend has been shown between R values and pressure. The R values for the manually fragmented sample shown in Fig. 6A are 0.05 and 0.15 for the spectra measured at different locations on the sample surface. The corresponding R value for the selectively fragmented sample (Fig. 6B) is 0.13. According to the geothermometer based on Raman spectroscopy, the flake graphite deposits in Sortland in Vesterålen were formed at temperatures between 575 and 620°C. The metamorphic pressure during the graphitisation process, on the other hand, is more difficult to determine by Raman spectroscopy, but could have been between 5 and 20 kbar.

Discussion

The transformation of carbonaceous material to fully ordered graphite is dependent on the temperatures during diagenesis and metamorphism (Buseck & Beyssac, 2014). At lower grades of metamorphism, organic matter transforms into graphite. With increasing metamorphic conditions, annealing processes purify the graphite layers and initiate growth of the flakes. During these processes, the lattice structure converts to more perfect graphene layers (Buseck & Huang, 1985). The grade of metamorphism is thus essential for the quality of flake graphite. In Sortland, the maximum grade of metamorphism is lower granulite facies, since garnet is not present, while the observed paragenesis (ortho- and clinopyroxene, biotite, hornblende and minor quartz) indicates granulite facies (Best, 2003).

Our petrographical and SEM studies have shown how the graphite flakes are evenly distributed in the graphite schist and are up to >1 mm in size. Selective fragmentation (selFrag) has turned out to be effective for obtaining graphite flakes from the graphite schist. By using SEM, Raman spectroscopy and XRD we could establish that the graphite flakes consist of several layers of graphene, that the crystallographic ordering within the flakes is high, and that there are no remarkable defects in the crystal structure. Raman spectroscopy was the most suitable method for analysis of the quality of the flake graphite. The quality varies between the examined graphite schists: the samples with visible graphite flakes (sample 300247.2) and/or high carbon contents (samples 300219.1, 300230.2 and 300295.1) are of high quality, whereas the samples of lower quality are those with low carbon content (300266.3 and 300251.1), and the sample (300289.1) that indicated the presence of sulphur during fragmentation.

Future studies should focus on exfoliation of flake graphite, i.e., how to separate graphite flakes from the host rock and the flakes from each other. Furthermore, as flake graphite is of substantial economic value, a non-destructive exfoliation process should be developed to obtain as large flakes as possible from the host rock.

Conclusions

Flake graphite from Sortland, northern Norway, has been examined. The bedrock in Sortland consists of pyroxene gneiss, amphibolite, calcite and dolomite marble with serpentinised olivine, and graphite-bearing metapelite metamorphosed to amphibolite and lower granulite facies. Several metamorphic events have been recorded in the rocks in the Lofoten–Vesterålen region, which have led to the formation of flake graphite from sedimentary carbonaceous material. According to our SEM, XRD and Raman spectroscopy results, flake graphite in Sortland is of high quality and does not contain any significant impurities. The Raman spectroscopy measurements show that the flake graphite has formed at temperatures between 575 and 620°C, temperatures indicating amphibolite facies. However, these numbers should be treated with caution, since they are not in accordance with the general petrography of the rocks of the area that indicates lower

granulite facies. There does not appear to be any difference in the quality of the flake graphite between the rocks in the three investigated areas. The results indicate that the Sortland flake graphite is of high quality and excludes the presence of any significant number of defects in the graphite deposits. The selFrag method also seems to be useful for cleaning and fragmentation purposes for extraction of the graphite.

Reference list

Best, M.G. 2003: *Igneous and Metamorphic Petrology*. 2nd edition, Wiley-Blackwell, San Fransisco, 752 pp.

Beyssac, O., Coffé, B., Chopin, C. & Rouzaud, J.N. 2002: Raman spectra of carbonaceous material in metasediments: a new geothermometer. *Journal of Metamorphic Geology 20*, 859–871. doi: 10.1046/j.1525-1314.2002.00408.x.

Buseck, P.R. & Huang, B. 1985: Conversion of carbonaceous material to graphite during metamorphism. *Geochimica et Cosmochimica Acta 49*, 2003–2016. doi: 10.1016/0016-7037(85)90059-6.

Buseck, P.R. & Beyssac, O. 2014: From Organic Matter to Graphite: Graphitization. *Elements 10*, 421–426. doi: 10.2113/gselements.10.6.421.

Corfu, F. 2004: U-Pb Age, Setting and Tectonic significance of the Anorthosite-mangerite-Charnockite-Granite Suite, Lofoten-Vesterålen, Norway. *Journal of Petrology 45*, 1799–1819. doi: 10.1093/petrology/egh034.

Corfu, F. 2007: Multistage metamorphic evolution and nature of the amphibolite-granulite facies transition in Lofoten-Vesterålen, Norway, revealed by U-Pb in accessory minerals. *Chemical Geology 241*, 108–128. doi: 10.1016/j.chemgeo.2007.01.028.

Eckmann, A., Felten, A., Mishchenko, A., Britnell, L., Krupke, R., Novoselov, K.S. & Casiraghi, C. 2012: Probing the Nature of Defects in Graphene by Raman Spectroscopy. *Nano Letters 12*, 3925–3930. doi: 10.1021/nl300901a.

Ekholm, E. 2015: *Bestämning av metamorfosgraden i Sortland, nordvästra Norge*. MSc thesis, Åbo Akademi University, 56 pp.

Ferrari, A.C. 2007: Raman spectroscopy of graphene and graphite: Disorder, electron-phonon coupling, doping and nondiabatic effects. *Solid State Communications 143*, 47–57. doi: doi:10.1016/j.ssc.2007.03.052.

Ferrari, A.C. & Basko, D.M. 2013: Raman spectroscopy as a versatile tool for studying the properties of graphene. *Nature Nanotechnology 8*, 235–246. doi: 10.1038/nnano.2013.46.

Ferrari, A.C., Meyer, J.C., Scardaci, V., Casiraghi, C., Lazzeri, M., Mauri, F., Piscanec S., Jiang, D., Novoselov, K.S., Roth, S. & Geim, A.K. 2006: Raman Spectrum of Graphene and Graphene Layers. *Physical Review Letters 97*, 187401–1–187401-4. doi: 10.1103/PhysRevLett.97.187401.

Gautneb, H. & Tveten, E. 1992: Grafittundersøkelser og geologisk kartlegging på Langøya, Sortland kommune, Nordland. *Norges geologiske undersøkelse Report 92.155*, 86 pp.

Gautneb H. & Tveten, E. 2000: The geology, exploration and characterisation of graphite deposits in the Jennestad area, Vesterålen, northern Norway. *Norges geologiske undersøkelse Bulletin 436*, 67–74.

Geim, A.K. & Kim, P. 2008: Carbon Wonderland. *Scientific American 298*, 90–97. doi: 10.1038/scientificamerican0408-90.

Griffin, W.L., Taylor, P.N., Hakkinen, J.W., Heier, K.S., Iden, I.K. Krogh, E.J., Malm, O., Olsen, K.I., Ormaasen, D.E. & Tveten, E. 1978: Archean and Proterozoic crustal evolution in Lofoten-Vesterålen, N Norway. *Journal of the Geological Society 135*, 629–647. doi: 10.1144/gsjgs.135.6.0629.

Hazen, R.M., Downs, R.T., Jones, A.P. & Kah, L. 2013: Carbon Mineralogy and Crystal Chemistry. *Reviews in Mineralogy & Geochemistry 75*, 7–46. doi: 10.2138/rmg.2013.75.2.

Lahtinen, R., Huhma, H. & Kousa, J. 2002: Contrasting source components of the Paleoproterozoic Svecofennian metasediments: Detrital zircon U–Pb, Sm–Nd and geochemical data. *Precambrian Research 116*, 81–109. doi: 10.1016/S0301-9268(02)00018-9.

Malard, L.M., Pimenta, M.A., Dresselhaus, G. & Dresselhaus, M.S. 2009: Raman spectroscopy in graphene. *Physics Reports 473*, 51–87. doi: 10.1016/j.physrep.2009.02.003.

Mitchell, C.J. 1993: Industrial Minerals Laboratory Manual: Flake Graphite. *British Geological Survey Technical Report WG/92/30*, 31 pp.

Nemanich, R.J. & Solin, S.A. 1979: First- and second-order Raman scattering from finite-size crystals of graphite. *Physical Review B 20*, 392–401. doi: 10.1103/PhysRevB.20.392.

Novoselov, K.S., Geim, A.K., Morozov, S.V., Jiang, D., Zhang, Y., Dubonos, S.V., Grigorieva, I.V. & Firsov, A.A. 2004: Electric Field Effect in Atomically Thin Carbon Films. *Science 306*, 666–669. doi: 10.1126/science.1102896.

Pierson, H.O. 1993: *Handbook of carbon, graphite and fullerenes*. Noyes Publications, New Jersey, 399 pp.

Singh, V., Joung, D., Zhai, L., Das, S., Khondaker, S.I. & Seal, S. 2011: Graphene based materials: Past, present and future. *Progress in Materials Science 56*, 1178–1271. doi: 10.1016/j.pmatsci.2011.03.003.

Wall, M. 2012: Raman spectroscopy optimizes graphene characterization. *Advanced Material & Processes 170*, 35–38.

Wang, E., Shi, F. & Manlapig, E. 2011: Pre-weakening of mineral ores by high voltage pulses. *Minerals Engineering 24*, 455–462. doi: 10.1016/j.mineng.2010.12.011.

Wopenka, B. & Pasteris, J.D. 1993: Structural characterization of kerogens and granulite-facies graphite: Application of Raman microprobe spectroscopy. *American Mineralogist 78*, 533–557.

ARTICLE

The flake graphite prospect of Piippumäki—an example of a high-quality graphite occurrence in a retrograde metamorphic terrain in Finland

J Palosaari[1] · R-M Latonen[2] · J-H Smått[3] · S Raunio[4] · O Eklund[1]

Abstract

The flake graphite occurrence in Piippumäki, Eastern Finland, as indicated by an airborne electromagnetic anomaly, was located during fieldwork by electromagnetic measurements with Slingram. The anomaly is approximately 0.1×1 km in size. The flake graphite is hosted by quartz-feldspar gneiss and amphibolite that have been subjected to retrograde metamorphism. This is observed in thin sections as granulite facies (garnet + cordierite + sillimanite + melt) regressing to greenschist facies (epidote, chlorite, albite, and white mica). The graphite (up to 1 mm large flakes) is found in graphite-bearing layers in the gneiss, and to a minor extent disseminated in the amphibolite. The average total sulfur (TS) is 0.33%, total carbon (TC) is 6.49%, and the average content of graphitic carbon (Cg) is 6.41% for the analyzed graphite-bearing rocks. SEM, XRD, and Raman spectroscopy were used for analyzing the flake graphite, indicating that the graphite is almost defect-free, of high quality, and has not been affected by the retrograde metamorphism. The peak metamorphic temperature of 737 °C was determined by a Raman thermometer, and no temperatures of greenschist facies were observed. A pseudosection was constructed from whole-rock chemical composition and indicated equilibration at ca 5 kbar and 740 °C, which corresponds to the observed mineral assemblages.

Keywords Flake graphite · Raman spectroscopy · Retrograde metamorphism · Fennoscandian shield

Introduction

Natural graphite has been listed as a critical raw material by the European Union since 2011 (European Commission 2017a). As the demand of natural graphite is increasing in the EU, it is important to identify high-quality graphite

✉ J Palosaari
  jenny.palosaari@gmail.com

1 Geology and Mineralogy, Åbo Akademi University, FI-20500 Turku, Finland

2 Laboratory of Analytical Chemistry, Åbo Akademi University, FI-20500 Turku, Finland

3 Laboratory of Physical Chemistry, Åbo Akademi University, FI-20500 Turku, Finland

4 Oy Fennoscandian Resources Ab, Turku, Finland

occurrences. In 2010–2014, China was the biggest producer of natural graphite in the world producing 69% while Europe produced only 1% (European Commission 2017b). Graphite is a versatile material and is used, e.g., in batteries and refractories due to its high electrical conductivity and heat resistance (Beyssac and Rumble 2014). Graphite is composed of sheets of graphene, which are one carbon atom thick, and is a very soft mineral due to the weak van der Waals forces between the graphene sheets. The graphene sheets themselves are durable, owing to the covalent bonds between the carbon atoms in their hexagonal structure. Graphitic carbon appears in different geological settings and forms either through graphitization of organic matter or by deposition from carbon-saturated fluids (Beyssac and Rumble 2014).

An extensive part of the Fennoscandian shield consists of the Svecofennian domain characterized by amphibolite to granulite facies metamorphic bedrock. Since high quality of graphite can be related to high grade metamorphism, supracrustal rocks of the Svecofennian domain are a promising target for high-quality flake graphite deposits. Graphite occurrences in Fennoscandia have been studied quite extensively, e.g., by Gautneb and Tveten (2000), Pearce et al.

(2015), Palosaari et al. (2016a), and Rønning et al. (2018). Several projects regarding graphite exploration were active in 2016 in Norway, Sweden, and Finland (Gautneb 2016). For the time being, the only active graphite mine in Fennoscandia is Skaland Graphite AS in Norway. The mining activity at Woxna graphite mine in Sweden ceased in 2015 (Leading Edge Materials 2018). Although graphite is a common mineral in metamorphosed supracrustal sequences and in the Finnish bedrock, graphite deposits of economic interest are uncommon. Graphite occurrences in Finland have been extensively explored and mapped by the Geological survey of Finland for use in energy production during the 1980s (e.g., Sarapää and Kukkonen 1984a; Sarapää and Kukkonen 1984b; Ahtola and Kuusela 2015), and were later explored for flake graphite ores and for flake graphite production (Palosaari et al. 2016b; Beowulf Mining plc 2019). In addition, a few mining companies have investigated the flake graphite finding in Piippumäki (Nurmela 1989). Kärpälä is another graphite deposit near Piippumäki where the ore was exploited during the late nineteenth century (Puustinen 2003). Piippumäki is ideal for studying graphite because the graphite is found in outcrop and thus easy to access. We chose to study Piippumäki based on previous studies in the area and comparison of the metamorphic map (Hölttä and Heilimo 2017) with the map of black shales in Finland (Arkimaa et al. 2000).

In order to characterize the graphite in Piippumäki and to understand its behavior in metamorphic processes, we used thin sections, SEM, XRD, and Raman spectroscopy. At the research site, we conducted fieldwork and electromagnetic measurements with Slingram, which is an electromagnetic instrument used for detecting conductive layers in the ground. In this study, we define the geological environment for the flake graphite finding and the suitability of the graphite present for technical applications. We use Piippumäki as an example but argue that our findings are applicable for any other area with graphite in high grade metamorphic rocks.

Geological setting

The study area of Piippumäki is situated in the northern part of the Southern Finland Subprovince (SFS) of the Svecofennian province (Nironen et al. 2016), 50 km southwest of the town of Mikkeli (Fig. 1). The area is approximately 0.5 × 1 km in size. The largest graphite deposit in Finland (Kärpälä) is situated 5 km northeast of Piippumäki. It was exploited until 1947 for industrial purposes.

The rocks in Piippumäki are Paleoproterozoic in age and were formed during the Svecofennian orogeny when the arc complexes Western Finland, and Southern Finland docked to the Archean continent (Nironen 2017). The sediments were deposited off the coast of the Archean continent and were subsequently metamorphosed during the orogeny

(Kähkönen 2005). The metamorphism took place at 1.88–1.79 Ga and reached upper amphibolite and granulite facies at 4–6 kbar. The rocks close to the northern border of the SFS comprise andalusite schists and sillimanite gneisses (Hölttä and Heilimo 2017).

The dominating rocks in the study area are migmatitic garnet-, cordierite-, and sillimanite-mica schists and gneisses. Amphibolite and quartz-feldspar gneiss appear as layers. Graphite- and sulfide-rich layers are also present. The graphite-rich layers can be up to a few meters thick (Simonen 1982). Diopside-bearing quartz-feldspar gneiss and diopside-amphibolite are also found here. The gneisses and schists strike E-W and predate plutonic rocks in the area (microcline granite), based on the contact relations observed. A cross section by Simonen (1982) shows that quartz-feldspar gneisses and the associated amphibolites lie in the middle of anticlines and therefore stratigraphically lie beneath the mica gneisses. This also indicates that Piippumäki is part of an anticline (Simonen 1982). A strong electromagnetic (EM) anomaly, interpreted as black shale, is observed across the study area in Piippumäki (Mineral Deposits and Exploration, n.d., Geological Survey of Finland, Hyvönen et al. 2013). The conductor continues towards Kärpälä graphite deposit.

In order to determine the origin of the graphite, Rankama (1948) analyzed the $^{12}C/^{13}C$ ratio in graphite from Kärpälä and suggested that the graphite is organic in origin, based on the average $^{12}C/^{13}C$ ratio of 91.7 (corresponds to $\delta^{13}C$ of − 29.6). Rankama (1948) also suggested that the graphite in Kärpälä has originally been a layer of bituminous sediment that was deformed into a lenticular graphite deposit. According to Simonen (1982), the graphite formed during metamorphism from organic matter in sediments.

Materials and methods

For this work, we collected 48 samples and analyzed the graphite quality, metamorphic grade, and petrography in 34 of them (Fig. 2). We also sampled the waste rock pile in the vicinity of Kärpälä. We analyzed both thin sections and individual graphite flakes of the samples by SEM, XRD, and Raman spectroscopy (Online Resource 1). Carbon and sulfur content in the samples was analyzed by TD-MS, CS, and IR by Actlabs Ltd. (Table 1). Whole-rock chemical composition analyzed with XRF at Åbo Akademi University was used for constructing the pseudosection (Table 1). Besides geological mapping, we performed electromagnetic ground measurements with Slingram. The study area is mostly covered by sandy till, but some of the graphite-bearing rocks are accessed in old excavated pits.
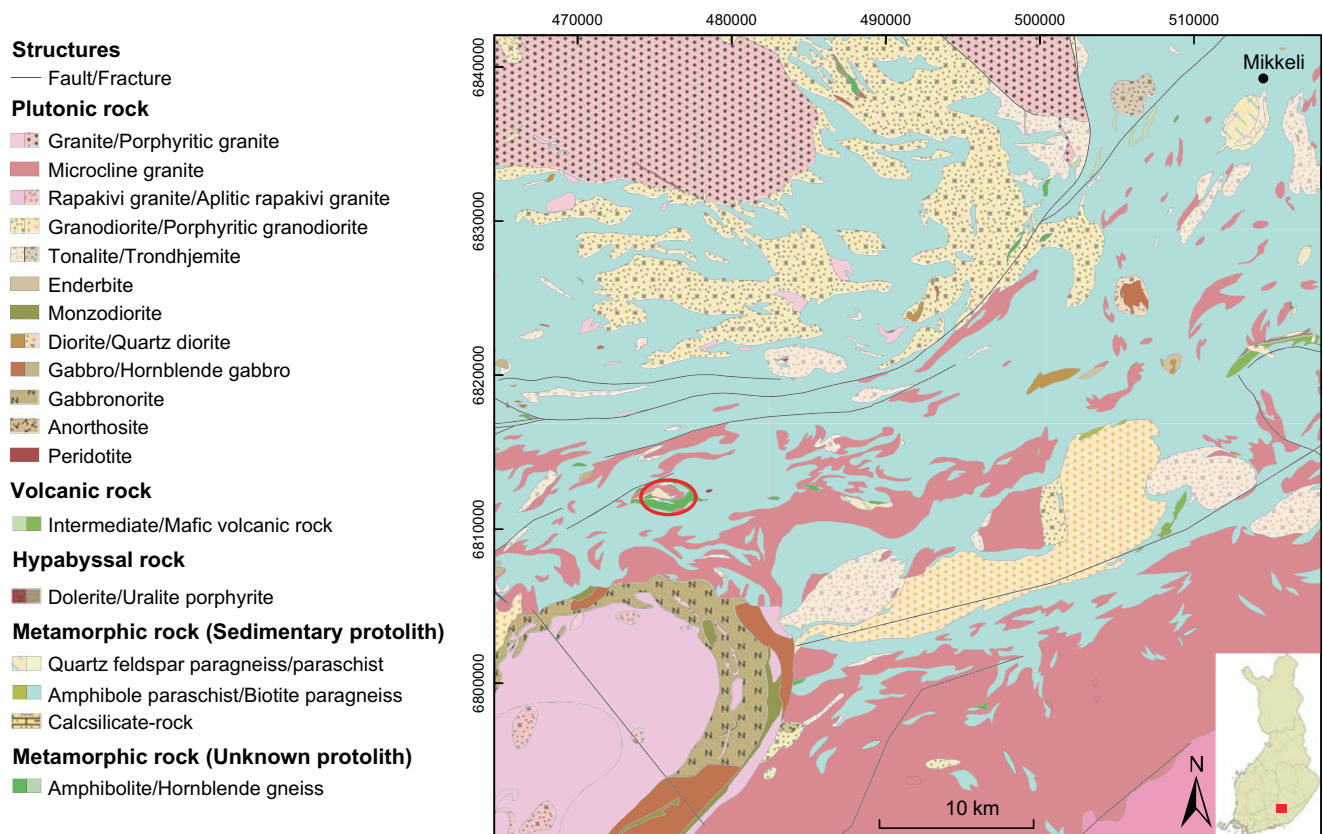
Fig. 1 Overview of the bedrock surrounding the study area of Piippumäki, which is indicated by the circle, ca 50 km from Mikkeli. Modified from the digital geological map database of Finland (DigiKP, Geological Survey of Finland 2017)

Slingram

Slingram was used for locating the conductive graphite layers accurately, and we performed the measurements perpendicular to the foliation with a measurement frequency of 3600 Hz and coil separation of 60 m. We measured a total of 47 parallel lines with Slingram with a 50-m line separation where the conducting layer is strongest, and a 100-m line separation at the easternmost lines where the conductor is weaker (Fig. 3). The lines are ca 200 m in length, aiming to cross the boundaries of the conductor.

Scanning electron microscopy

We examined the appearance of graphite flakes and possible impurities with SEM at the Laboratory of Inorganic Chemistry at Åbo Akademi University both in thin sections and individual graphite flakes (20 samples in total, see Online Resource 1). A LEO Gemini 1530 FEG–SEM instrument equipped with a ThermoNoran X-ray detector was used. Energy dispersive X-ray analysis (EDXA, Ultradry) was used for elemental analysis. We picked out individual graphite flakes directly from samples and washed them. No additional conductive layer was needed when examining the graphite flakes.

X-ray diffraction

To characterize the crystalline nature of the flake graphite samples and to identify potential impurities, we used XRD. We performed the measurements with a Bruker D8 Discover instrument, located at the Laboratory of Physical Chemistry at Åbo Akademi University, on four different samples (404804, 404805, 404806, 404812) using a HI-STAR 2-D detector. The wavelength used was a weighted average of Cu-Kα1 and Cu-Kα2 (and Cu-Kβ): 1.5418 Å (Bragg-Brentano). The results are presented in diffractograms with the scattering angle (2θ) on the x-axis and the intensity on the y-axis. The intensities of the diffractograms have been normalized based on the (002) graphite reflection.

Raman spectroscopy

We investigated the quality of graphite, as well as possible lattice defects, using Raman spectroscopy. Using the calibration of Rahl et al. (2005), we estimated peak metamorphic temperatures in graphite from the Raman results. The Raman spectra were recorded at the Laboratory of Analytical Chemistry at Åbo Akademi University using a Renishaw Ramascope (system 1000) equipped with a Leica DMLM microscope connected to a CCD camera. The measurements were made by using an
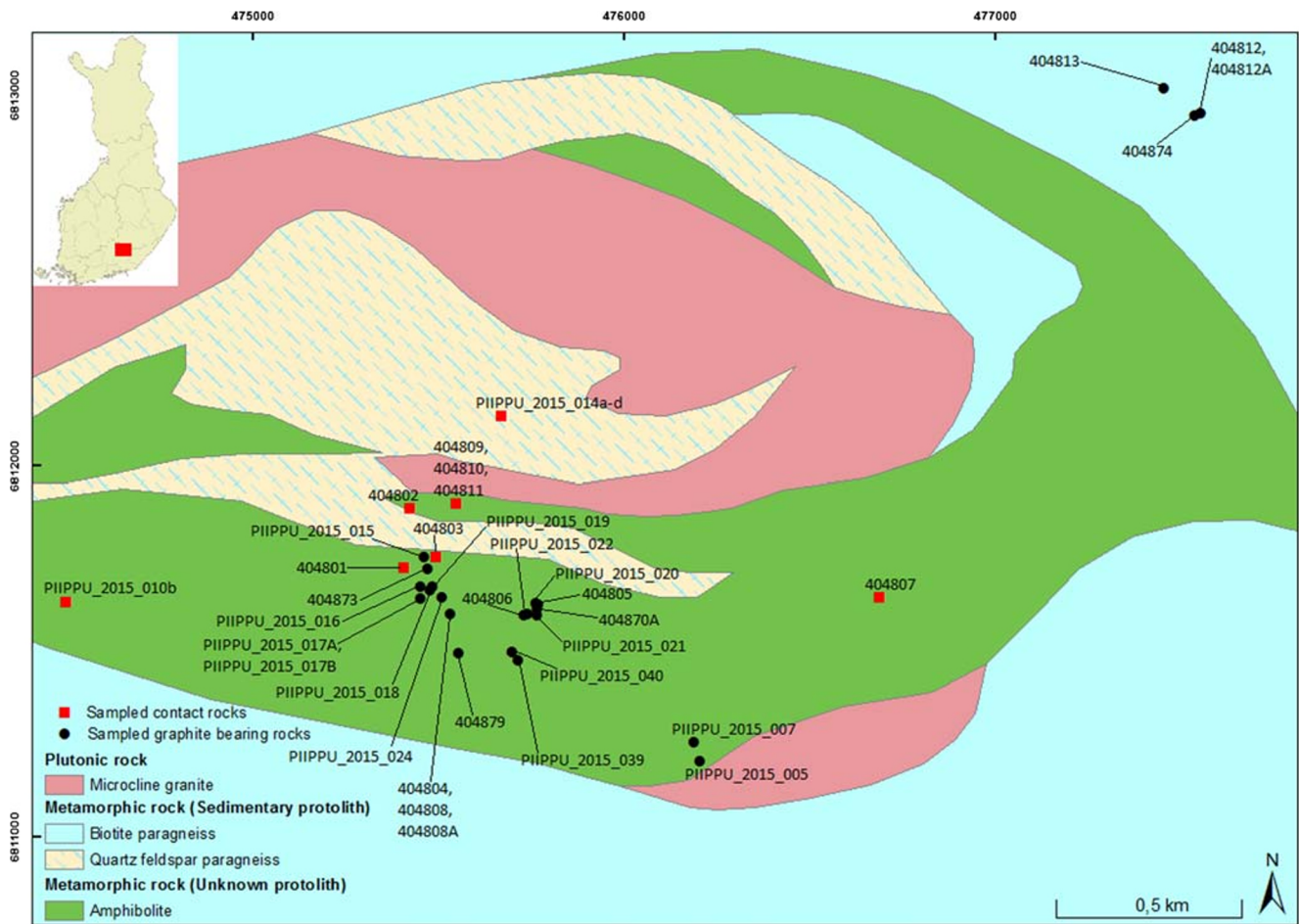
Miner Deposita (2020) 55:1647–1660

Fig. 2 Bedrock map of the study area with the sample locations. Red squares indicate contact rocks (amphibolite and quartz-feldspar gneiss) and black circles indicate graphite-bearing rocks. The graphite is hosted by metasedimentary layers within the amphibolite. The samples in the NE part of the map are sampled near the old graphite mine Kärpälä. Modified from the digital geological map database of Finland (DigiKP, Geological Survey of Finland 2017)

Ar-ion laser (LaserPhysics) with the excitation wavelength of 514 nm on a ca Ø 2-μm surface area with a laser power of 20 mW. The spectrometer was calibrated against a Si standard (520.0 cm^{-1}). We performed measurements on 11 different graphite flake samples, which were either in thin sections or individual hand-picked grains (see Online Resource 1). The measurements were made parallel to the C-axis on the graphite grains (perpendicular to the graphene sheets in graphite) and

Table 1 Whole-rock chemical composition for a quartz-feldspar gneiss and total C and S for graphite-bearing rocks from Piippumäki. Sample 404811 was analyzed with XRF at Åbo Akademi University, and the rest were analyzed by Actlabs Ltd

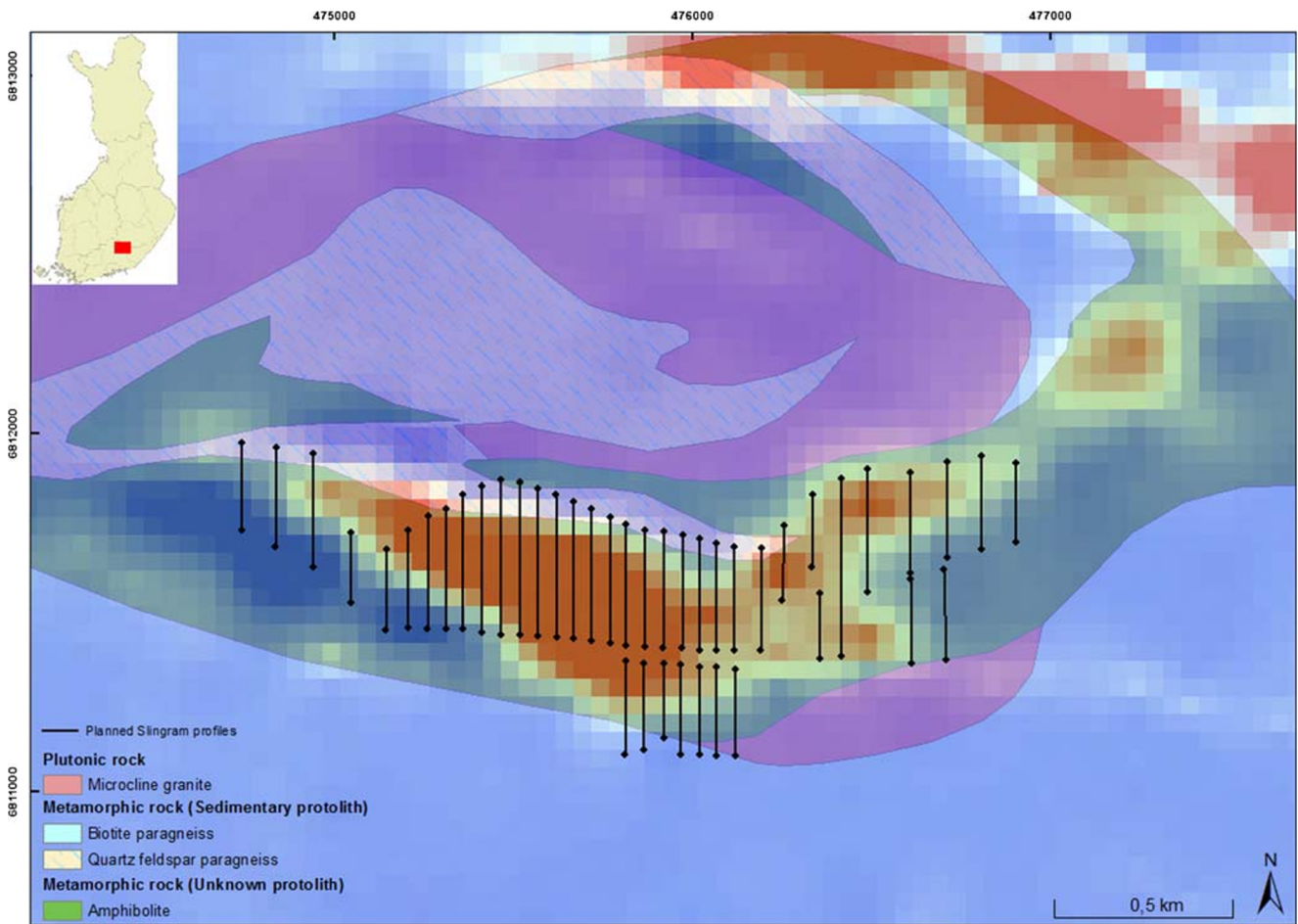| Sample no.	SiO$_2$	TiO$_2$	Al$_2$O$_3$	FeO	MnO	MgO	CaO	Na$_2$O	K$_2$O	H$_2$O	Total
404811	59.74	1.48	15.32	12.31	0.17	3.57	1.78	2.16	1.89	1.54	99.96
	Total C (%)				Total S (%)			C-graph (%)			
PIIPPU_2015_019	4.56				1.66			4.66			
PIIPPU_2015_016	5.32				0.09			5.13			
PIIPPU_2015_017A	2.96				0.06			2.91			
PIIPPU_2015_017B	3.02				0.07			2.91			
PIIPPU_2015_020	9.67				0.3			9.5			
PIIPPU_2015_022	9.12				0.23			9.05			
PIIPPU_2015_024	2.43				0.15			2.39			
404870A	14.8				0.09			14.7			

Fig. 3 Map showing the planned Slingram lines in Piippumäki in reference to the airborne geophysical measurements. Red indicates high conductivity, blue indicates low conductivity. Modified from the digital geological map database of Finland (DigiKP, Geological Survey of Finland 2017)

perpendicular to the *C*-axis on graphite in thin sections. The results from Raman spectroscopy measurements are presented by spectra with the wavenumber (Raman shift) on the *x*-axis and the intensity on the *y*-axis. The obtained spectra consist of first- and second-order regions, 1100–1800 cm^{-1} and 2500–3100 cm^{-1}, respectively (Beyssac et al. 2002).

In total, 8 samples (see Online Resource 1) were measured for the temperature estimates, which are based on a mean value of five measurements on each sample. The peak temperature estimates are based on peak areas and peak heights. The areas of the peaks were determined by using the Lorentzian function in Origin 2015 by OriginLab Co. We chose the calibration of Rahl et al. (2005), which is based on the equation of Beyssac et al. (2002), for the temperature estimations in this study because it is suitable for a broader temperature range of 100–700 °C compared with 330–650 °C ± 50 °C of Beyssac et al. (2002). We used T(°C) = 737 + 320(*R*1) − 1067(*R*2) + 80.638(*R*1)^2 to calculate the metamorphic temperatures. In this equation, $R1 = \left(\frac{D1}{G}\right)_H$, where the subscript H refers to the height of the bands D1 and G, and

$R2 = \left(\frac{D1}{G+D1+D2}\right)_A$, where the subscript A refers to the area of the bands D1, D2, and G. The maximum temperature that can be calculated with this method is 737 °C.

Results

Fieldwork

We made field observations on graphite-bearing rocks, primarily in test trenches dug by the Rautaruukki company in 1985. The trenches lie perpendicular to the foliation. When examining the trenches, we found some new outcrops with graphite. The main rocks in the research area are quartz-feldspar gneiss and amphibolite. The geological map in Fig. 2 shows the locations of the sampled material, and the samples are divided into graphite-bearing rocks and contact rocks. The quartz-feldspar gneiss is of sedimentary origin and is the host rock of the graphite-bearing layers, with layers of amphibolite

also being present. The gneiss consists mainly of medium-grained quartz and feldspar with abundant biotite. The gneiss shows distinct foliation, and at some places it is affected by partial melting. Sillimanite is present in the leucosome. Sulfides are present in the mica- and graphite-rich layers, which appears as a rusty surface in outcrop. The protolith of the Piippumäki amphibolite is unknown. It is diopside-bearing and has hornblende, quartz, and plagioclase as main minerals. The rock is gray to dark gray in color, fine-grained, and banded, and at some places boudins are present. Minor graphite dissemination is observed in some places.

The graphite is present in the quartz-feldspar gneiss as layers and is also disseminated to a minor extent in the host rock and the amphibolite. At contacts between the graphite-bearing rock and the host rock, graphite is usually found concentrated along the contacts. Graphite is present as large flakes, mainly < 1 mm. Graphite flakes > 180 μm are considered large (Northern Graphite 2019). Observations from the test trenches indicate that the electromagnetic anomaly is caused by the graphite-rich layers in the quartz-feldspar gneisses.

In general, the lithological units in Piippumäki dip 75–85° and strike W-E. In the eastern parts of Piippumäki, the foliation changes slightly towards NE. The measured fold axis in Piippumäki dips ca 60° towards NW, NE, and SW. This indicates that the area is the top of an anticline, as suggested by Simonen (1982).

The observed structures correspond well to the electromagnetic anomalies in the area. The airborne electromagnetic map correlates with our results from the ground measurements with Slingram. The graphite observations conform to the electromagnetic map produced from the data of the Slingram measurements (showing the conductivity anomaly) (Fig. 4). The anomaly is ca 1-km long and 100-m wide, and curves across the area towards NW and NE.

Petrography

The Piippumäki gneisses are composed of quartz, plagioclase, biotite, and graphite (Fig. 5). Pyrite is also present in small amounts (1–2%). The biotite and graphite are parallel to the foliation of the gneiss. The gneiss is fine-grained and equigranular, but medium-grained at migmatitic parts. The quartz grains show undulose extinction, which indicates that the mineral has undergone deformation. Graphite is disseminated in the rock as flakes and irregular grains (Fig. 5a). In places, the graphite is present as mixed grains together with chloritized biotite (Fig. 5b). In these mixed grains, the graphite is more irregular and deformed.

The metamorphic indicator minerals garnet, cordierite, and sillimanite are present in the quartz-feldspar gneisses. Garnet is found in sample 404811, sillimanite and cordierite in sample PIIPPU_2015_014d. Sample 404811 is a quartz-feldspar

gneiss with quartz and feldspar as the main minerals. Biotite (partly chloritized) is also abundant. The garnets are not fully isotropic (Fig. 6), indicating that alteration from garnet to cordierite has started. The matrix in sample PIIPPU_2015_014d consists primarily of microcline and quartz with veins of sillimanite, and minor cordierite and biotite (Fig. 7a, b, c, d). Cordierite appears with distinct patchy twinning and at some places with cracks filled with pinite. The alteration from garnet to cordierite is also visible in the thin section (Fig. 7c, d).

Amphibolite is the immediate host rock of the graphite-bearing metasedimentary layers, and is composed of hornblende, diopside, quartz, and plagioclase, with accessory minerals biotite, sulfide, and sericite. The amphibolite is banded and foliated, and the grain size is fine to medium. Samples 404801 and 404809 represent the amphibolites in Piippumäki. In sample 404801, the amphibole is pleochroic brown, while in 404809, it is pleochroic green (Fig. 8). Sample 404809 is diopside-bearing (Fig. 8c, d), green, and banded.

Whole-rock chemical composition

One sample was analyzed for whole-rock chemical composition and eight samples for graphitic carbon and sulfur content. The results show that the carbon in the samples is graphitic carbon. The amounts of total carbon range from 2.43 to 14.8% C, graphitic carbon from 2.39 to 14.7 wt% Cg (average 6.4 wt% C), and total sulfur from 0.06 to 1.66 wt% S (average 0.33 wt% S) (Table 1).

High-T/low-P metamorphism in the rocks of the Piippumäki area is indicated by the paragenesis garnet – cordierite – sillimanite + melt, and no orthopyroxene is observed in the samples. This indicates temperatures around 750 °C and pressures around 5 kbar. This granulite facies assemblage is overprinted by epidote, chlorite, and white mica (pyrophyllite, as determined by SEM and EDX) indicating greenschist metamorphism with temperatures not higher than 400 °C. To examine the P/T field for the investigated area, a pseudosection based on whole-rock chemical composition of sample 404811 (Table 1) was constructed with the Perple_X version 6.8.5. Calculations involved the phases biotite (bt), sanidine (sa), white mica (mica), melt, garnet (grt), orthopyroxene (opx), staurolite (st), cordierite (crd), chloritoid (cld), spinel (spl), ilmenite (ilm), and plagioclase (pl). The activity model used for biotite is from Tajcmanová et al. (2009); for sanidine from Waldbaum and Thompson (1968); for white mica from Auzanneau et al. (2010) and Coggon and Holland (2002); for melt from Holland and Powell (2001) and White et al. (2001); for garnet from Holland and Powell (1998); for orthopyroxene from Holland and Powell (1996); for chloritoid from White et al. (2000); and for plagioclase from Newton et al. (1980). The H$_2$O content of 1.54 wt% was calculated from the mineral mode, assuming that all water in the rock was in biotite. The paragenesis garnet – cordierite – biotite –
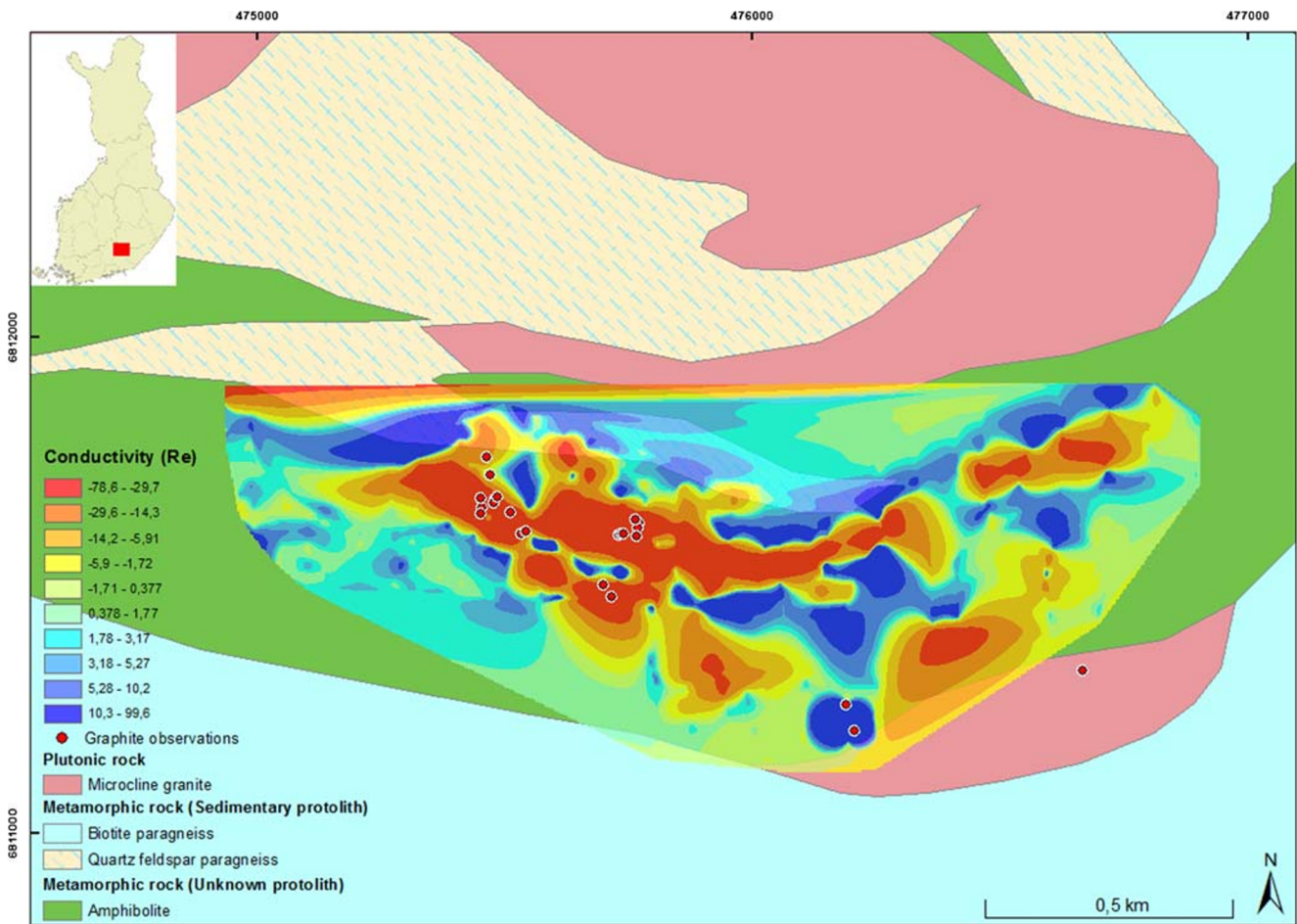
Fig. 4 Map showing results from the Slingram measurements. Very negative values indicate high conductivity (low resistivity), and positive values indicate low conductivity (high resistivity). The dots show graphite observations and coincide with the conductive area. Modified from the digital geological map database of Finland (DigiKP, Geological Survey of Finland 2017)

plagioclase + melt was found in the pseudosection at roughly 5 kbar and 740 °C (Fig. 9).

Scanning electron microscopy

SEM images show that the graphite grains appear as regular and stacked parallel flakes (Fig. 10a). Some samples are oxidized on the surfaces (Fig. 10b). No impurities in the graphite are visible in the SEM images.

X-ray diffraction

Diffraction patterns of four of the investigated samples are presented in Online Resource 2. Only small differences between the samples can be observed. All samples display a strong and narrow peak at 26.6° 2θ and a weaker peak a 54.8° 2θ, which are related to the (002) and (004) reflections of graphite, respectively. The lack of any other graphite reflections indicates that the graphite consists of large crystalline flakes oriented in parallel with the sample holder. In addition to these peaks originating from graphite, samples 404804 and

404805 show additional peaks coming from some impurity phases. In comparison, the graphite material in sample 404806 is relatively clean, while the material from Kärpälä (sample 404812) only shows the (002) and (004) reflections from graphite.

The spacing between the graphene layers in the samples can be calculated based on Bragg's law using the diffraction angles of the (002) peak. The calculations for d(002) of the four samples indicate that the spacing between the layers is 0.334–0.335 nm.

Raman spectroscopy

Raman spectroscopy results measured from liberated graphite grains show little variance (Online Resource 3a). The G band, which is a result of in-plane vibrations of aromatic carbon in the structure of graphite (Ferrari et al. 2006; Eckmann et al. 2012), is positioned at ca 1579 cm^{-1} in the first-order region in all spectra. This indicates that the samples consist of sp^2-hybridized carbon atoms (i.e., graphene layers). The high intensity and the position of the G band indicate that there are

Fig. 5 Plane-polarized image of thin section PIIPPU_2015_020 (**a**) and PIIPPU_2015_016 (**b**). **a** Is a typical graphite-bearing quartz-feldspar gneiss, with graphite (grf) as the black nails and some irregular grains disseminated throughout the sample. **b** The irregular graphite grains are visible and are also mixed with chloritized biotites
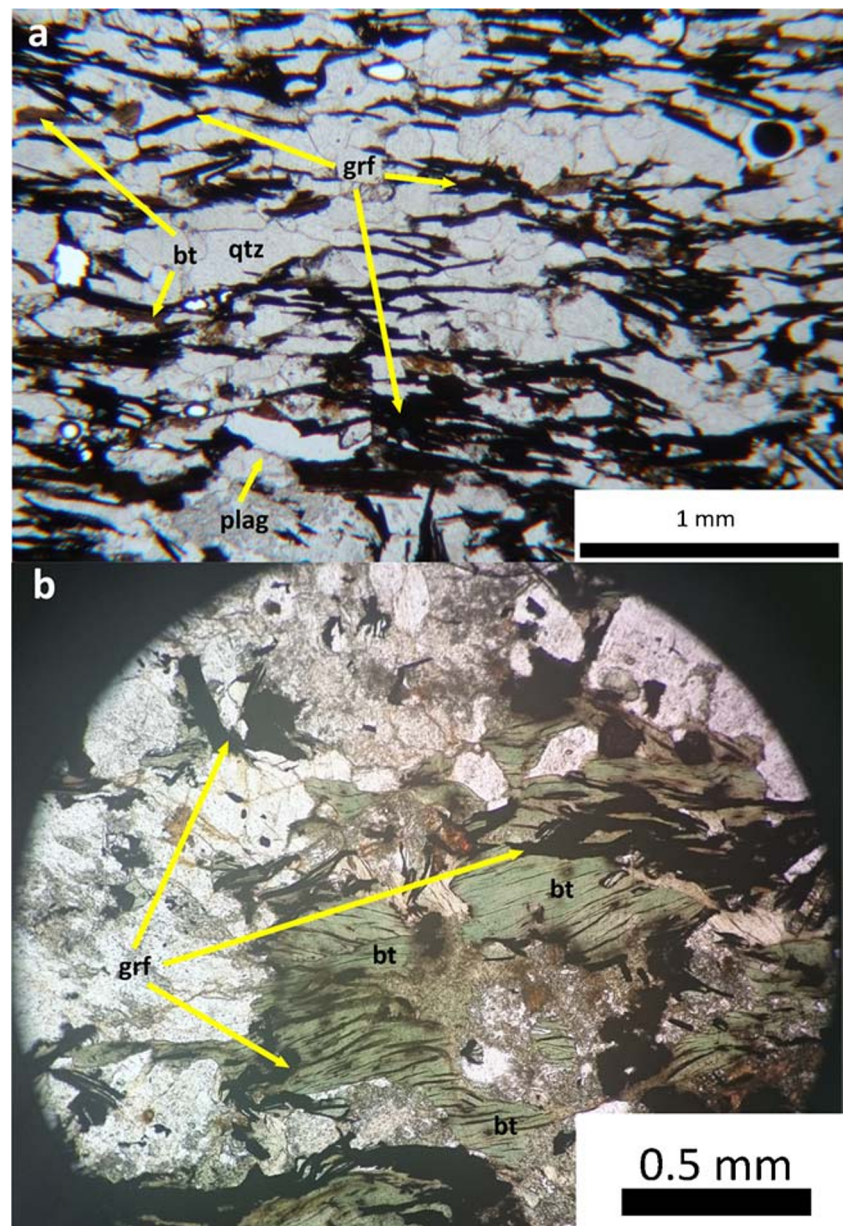
several graphene layers present in the sample (Wall 2012). In the first-order region, a number of D bands (D1, D' (D2), and D3) characterize defects in graphite, such as heteroatoms (e.g., O, H, and N) or structural defects. Samples 404804 and 404812 (sampled in Kärpälä) have weak D bands at 1360 cm^{-1} and 1354 cm^{-1}, respectively (Online Resource 4). With increasing metamorphism and order in the graphite, the number and intensity of the D bands decrease. The second-order region in the spectra comprises peaks of overtone and combination scattering at 2400, 2700, 2900, and 3300 cm^{-1}. In the studied samples, an asymmetric 2D (also called G' or S1) band with a shoulder facing towards lower wavenumbers is visible at ca 2723 cm^{-1} in all spectra which indicates that the graphite has been formed at high metamorphic grades and has

many parallel stacked graphene layers in the graphite structure (Beyssac et al. 2002). All samples show a 2D' peak at ca 3247 cm^{-1} which is a second order of the D' (D2) band and is activated by a single-phonon intravalley scattering process (Ferrari 2007). All samples also show a small peak at ca 2440 cm^{-1} (called G* and sometimes D + D"), the origin of which has been debated (Ferrari and Basko 2013). It is present both in defected and defect-free samples and is believed to originate from an intervalley process as an overtone of in-plane modes (Nemanich and Solin 1979).

We measured thin sections to compare the effect of laser orientation with respect to the graphene layers in graphite sheets. The measurements made on thin sections gave different results compared with the measurements on handpicked

Fig. 6 Garnet in sample 4048011. The alteration process from garnet to cordierite has started, which is shown as garnet not being fully isotropic. To the left in plane-polarized light, and cross-polarized to the right
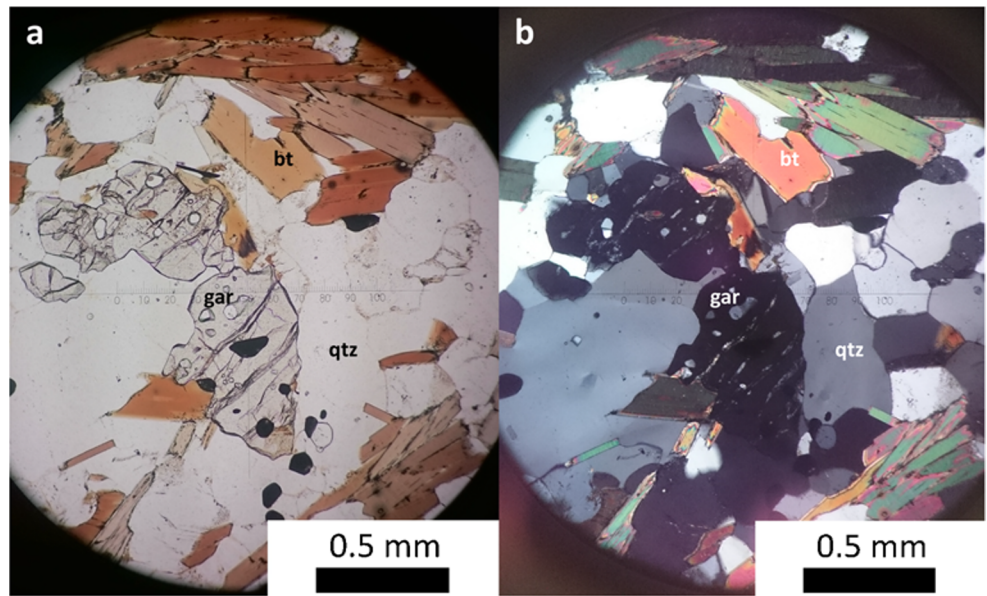

Fig. 7 Microscope images of thin section PIIPPU_2015_014d, to the right in cross-polarized light. Images **a** & **b** show quartz banded with veins of sillimanite fibers, and **c** & **d** show cordierite (altered from garnet), which are the colorless grains with high relief in the center
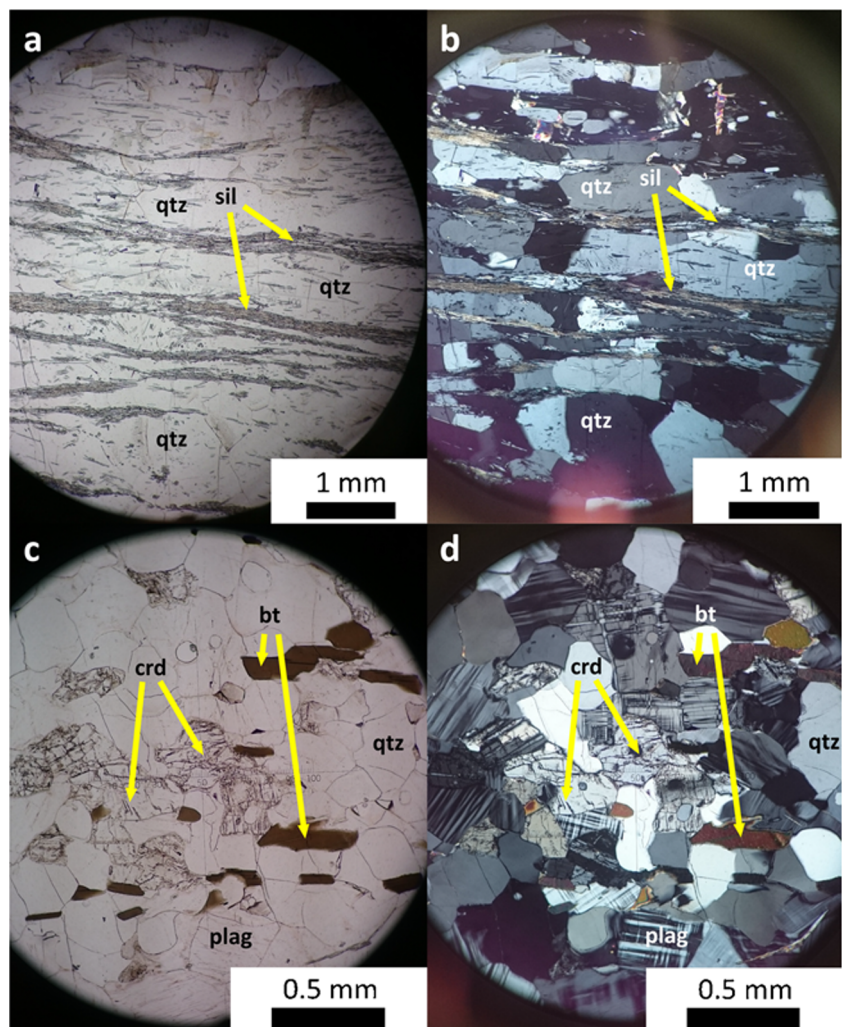
Fig. 8 Microscope images of samples 404801 (**a** & **b**) and 404809 (**c** & **d**), which both are amphibolites, in plane- and cross-polarized light. Upper images show brownish hornblende, and lower images show greenish hornblende together with diopside
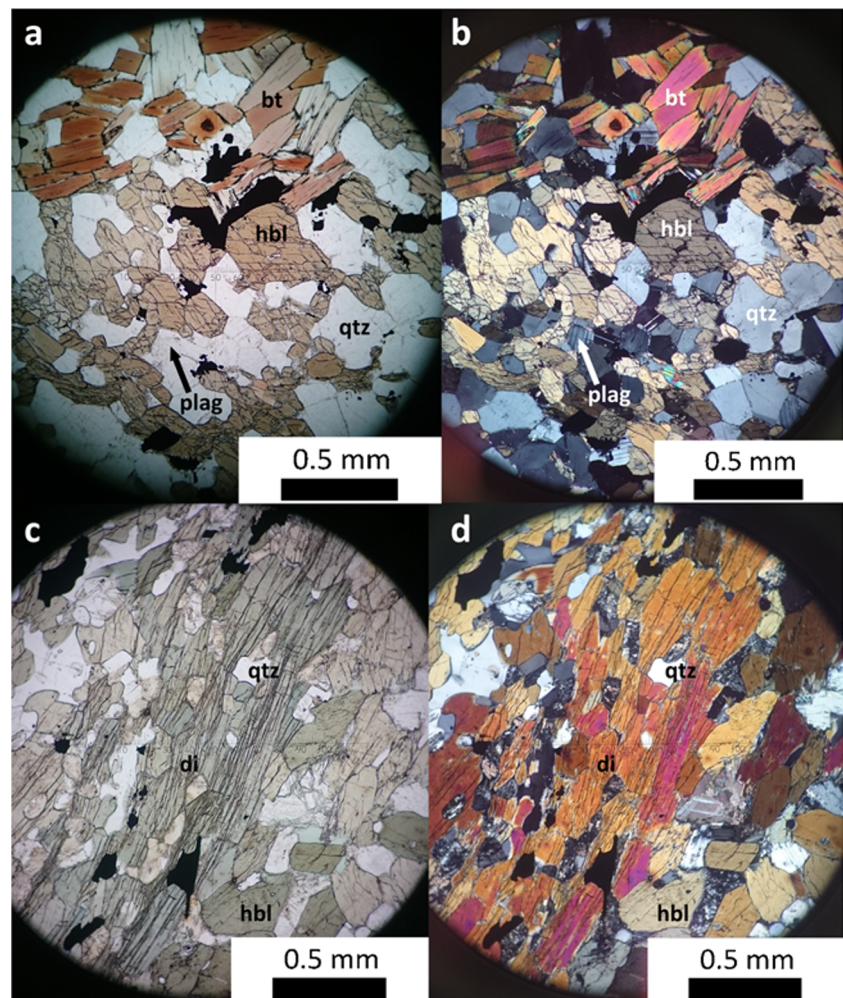
graphite grains due to the fact that the laser was directed parallel to the graphite sheets (perpendicular to the C-axis on graphite) and not perpendicular as during measurement of the grains. Besides the G and 2D bands, these spectra show several D bands, usually three (D1, before referred to as D, D2, and D3) (Online Resource 3b). The D' band can be visible in the spectra if the laser is shot at edges of the flakes, even if the rest of the sample lacks defects (Ferrari, 2007). In this way, defects from the grain boundaries become visible. The origin of the wide D3 band is out-of-plane defects such as tetrahedral carbons in the otherwise 2-dimensional graphene structure (Beyssac et al. 2002) and small crystalline size (Nemanich and Solin 1979). A new peak at 2900 cm^{-1} is also visible in the spectra measured from the thin sections. It originates from a combination mode of the D and 2D (D') bands (Eckmann et al. 2012).

The results from peak temperature calculations are presented in Online Resource 5. The estimates made according to Rahl et al. (2005) give temperatures between 659 and 719 °C based on the mean values obtained from the five parallel measurements on the graphite grains from Piippumäki and Kärpälä regions. Some measurements lack the D band

and give maximum temperatures for the calibration, i.e., 737 °C. Temperatures measured from thin sections were considerably lower than measurements from handpicked grains. This can be explained by the defects generated during the thin section preparation procedure and the different measurement angle in comparison with the C-axis on graphite.

Discussion

Discovery of strong electromagnetic anomalies and previously made studies in the Piippumäki area were the motivation for this study. These conductors appear to be caused by graphite in the bedrock, and Slingram was used to locate the graphite-bearing layers more precisely (Fig. 4). The graphite appears mainly as dissemination in the quartz-feldspar gneiss and flakes up to 1 mm in size are visible.

The supracrustal rocks in Piippumäki were metamorphosed during the Svecofennian orogeny in low pressure granulite facies (Kähkönen 2005). A P/T determination, where whole-rock chemical composition was used to construct a

Fig. 9 Pseudosection for sample 404811 constructed in Perple_X based on the whole-rock chemical composition of the rock. The sample coincides with the stability field of biotite (bt), melt, cordierite (crd), plagioclase (pl), ilmenite (ilm), and garnet (grt) at ca 5 kbar and 740 °C. No orthopyroxene (opx) was observed in this sample. The program Krita was used for drawing the pseudosection
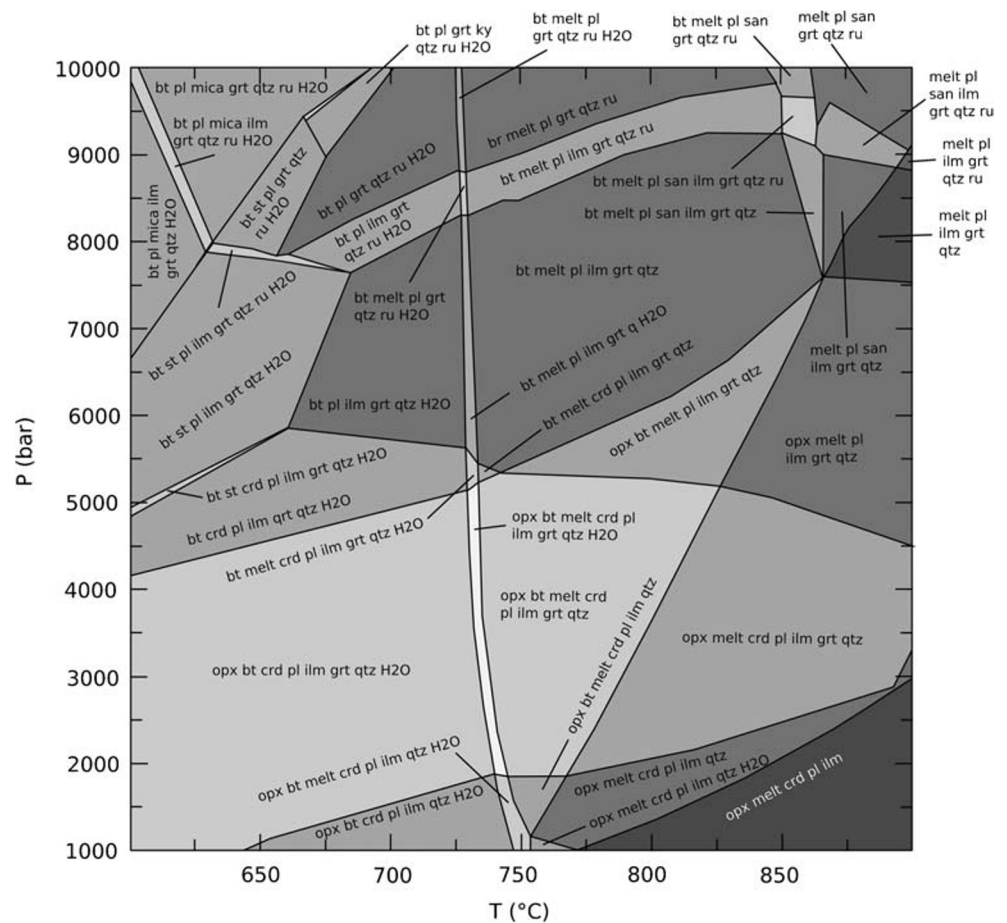
pseudosection, gave a pressure of 5 kbar and a temperature of 740 °C. This assemblage was later regressively metamorphosed to greenschist facies metamorphic conditions. The retrograde metamorphism is observed in thin sections where the paragenesis garnet – cordierite – sillimanite + melt is overprinted by chlorite – muscovite – epidote paragenesis. The peak temperature in graphite, based on the Raman spectroscopy measurements, was obtained using the calibration by Rahl et al. (2005). The obtained peak temperature of 737 °C is for samples lacking the D band, but peak temperature based on the mean values is 719 °C. We argue that 737 °C indicate the minimum temperature of the metamorphism, because this is the maximum temperature for the calibration, and measurements lacking the D band directly give this
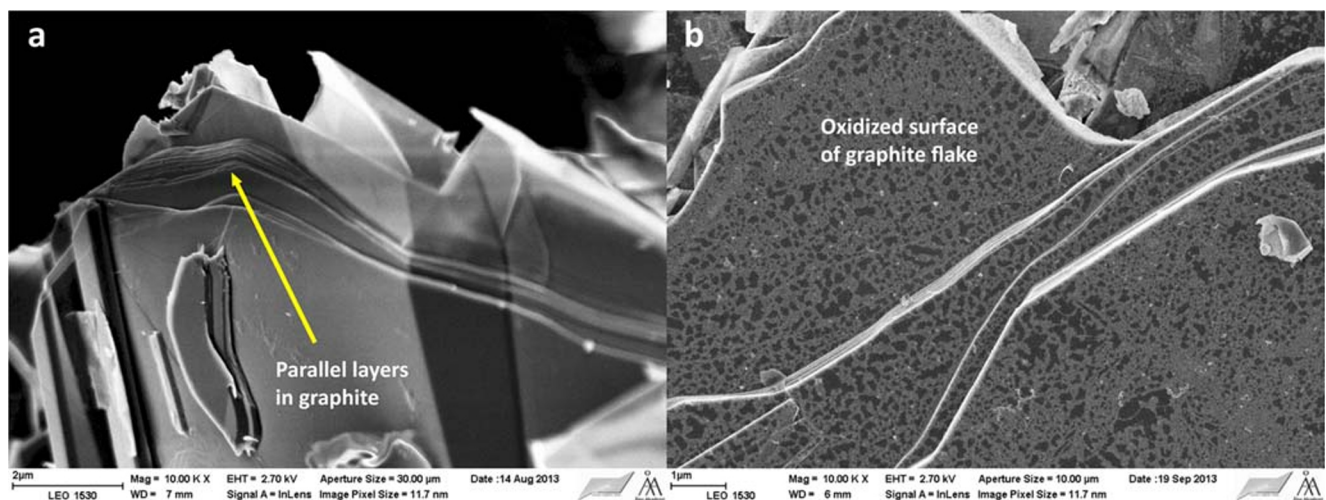
Fig. 10 SEM images showing parallel layers in graphite indicated by the arrow (a) and oxidized surfaces of graphite (b)

temperature. The observed mineral assemblages indicate slightly higher temperatures. No Raman geothermometer estimates in this study indicate any retrograde temperatures, which points to the graphitization process being irreversible. Further research is needed to study to what extent graphite is resistant to retrograde metamorphism. This result is promising for further graphite exploration, as even retrograde metamorphic areas may still contain high-quality flake graphite deposits.

The Raman spectra obtained from graphite grains show characteristic G and 2D bands, and low intensity D bands. This indicates that the graphitic structure lacks defects and is highly symmetric. The weak D bands, which are visible in some samples, can arise from the laser hitting an edge in the sample, or indicate minor defects such as inorganized carbon or other defects that break up the carbon structure. Measurements made directly on graphite in thin section show several D bands in the spectra and a new peak at 2900 cm^{-1} compared with the spectra measured from the grains. The difference between the measurements on hand-picked grains and thin sections was apparent. The polishing of thin sections probably damaged the graphitic structure, and therefore damaged graphite sheet edges were easily recorded, resulting in these D bands (Katagiri 1988; Wopenka and Pasteris 1993). The results from measurements on separated graphite grains are therefore considered reliable.

The results from the XRD measurements imply that the graphite materials mainly consist of large and highly oriented flake-like crystals, although there are small variations between the samples. The impurity reflections in sample 404804 and 404805 probably originate from mica, quartz, and feldspar that are present in small amounts. The lack of additional peaks in sample 404812 correlates well with the fact that the carbon content in the sample from Kärpälä is higher than in those from Piippumäki. The spacing between the graphene layers in the samples is calculated to be 0.334–0.335 nm, which is the expected distance in highly ordered graphite (Pierson 1993).

Comparison with other graphite occurrences in Fennoscandia

Similar graphite deposits as Piippumäki have been studied in Fennoscandia recently, Palosaari et al. (2016a) studied the flake graphite deposit in Vesterålen, Northern Norway, and Pearce et al. (2015) and Lynch et al. (2018) have studied the Nunasvaara graphite deposit and the surrounding geology in Northern Sweden. Graphite occurrences in Finland have been studied widely within the FennoFlakes project at Åbo Akademi University.

The flake graphite occurrence in Vesterålen has been derived from sedimentary carbonaceous material and is hosted by rocks metamorphosed in lower amphibolite granulite

facies. Palosaari et al. (2016a) conclude that the graphite flakes are up to 1 mm in size, of high quality, and low in impurities. Results from Raman spectroscopy measurements were used to determine the peak metamorphic temperature in graphite; however, the results indicate temperatures between 575 and 620 °C that are below the observed amphibolite-lower granulite facies (Palosaari et al. 2016a). The flake graphite in Vesterålen resembles the flake graphite in Piippumäki both being formed during the Svecofennian orogeny and being of high quality.

The graphite occurrence in Nunasvaara, northern Sweden has been studied by Pearce et al. (2015) and Lynch et al. (2016, 2018). It is Sweden's largest known metamorphic graphite occurrence with an indicated resource of approximately 5.6 Mt of 24.6% Cg (Lynch et al. 2016). The graphite in Nunasvaara has been interpreted to originate primarily from organic sedimentary material, but also graphite precipitated from fluids (Pearce et al. 2015). Compared with Piippumäki, the Nunasvaara graphite occurrence is roughly of the same age. The main differences between these occurrences are in the size of the graphite flakes and the amount of graphitic carbon; the Nunasvaara graphite is microcrystalline, while the Piippumäki graphite consists of large flakes. For Nunasvaara, the peak temperature based on Raman geothermometry is between 400 and 500 °C (Pearce et al. 2015), while it peaks at 737 °C in Piippumäki.

Nygård (2017) studied the quality of the graphite occurrence in Haapamäki, Northern Savo. There, graphite is found as flakes in graphite-bearing migmatite and metamorphosed black shale, and as massive graphite in shear zones. The area is strongly folded and the metapelitic sediments reached upper amphibolite facies during metamorphism. The Raman spectroscopy measurements indicate that the flake graphite in Haapamäki is of good quality with large flakes and only minor defects. Kujanpää (2017) studied the graphite occurrence in the Viistola-Hyypiä area, Eastern Finland, whose suitability for energy production was defined earlier (Sarapää and Kukkonen (1984a). The metamorphic degree in the area is lower amphibolite facies. This is evident as fine-grained graphite of low quality, which is the main difference compared with the graphite in Piippumäki.

Conclusions

The metamorphism in Piippumäki was of both granulite and greenschist facies. The observed granulite facies paragenesis observed (garnet – cordierite – sillimanite + melt) indicates metamorphic conditions at ca 5 kbar and 750 °C. This paragenesis is overprinted retrograde by chlorite – muscovite – epidote, which indicates temperatures not higher than 400 °C. The pseudosection based on whole-rock chemical composition indicates metamorphic conditions at ca 5 kbar and 740 °C. The peak temperature in graphite was determined

from Raman spectroscopy measurements with the calibration of Rahl et al. (2005) to 737 °C, which is the highest mathematical temperature for this calibration.

Overall, the composition and metamorphic degree of the metasedimentary rocks in the Southern Finland Subprovince of the Svecofennian province are suitable for exploration of high-quality graphite. The graphite content in the Piippumäki area varies between 2.29 and 14.7 wt% Cg (average 6.4 wt% Cg), and the sulfur content varies between 0.06 and 1.66 wt% S (average 0.33 wt% S). The graphite occurrence was located with a Slingram survey.

Based on our results, the flake graphite is of good quality with high order in the graphitic structure. The carbon structure is affected only to a minor extent, probably by O-bearing groups on the surface of graphene layers, causing defects in the graphitic structure and unorganized carbon. D bands could also be related to the laser, hitting an edge in the sample. The highly ordered structure was not affected by the retrograde metamorphism in the area, indicating that high-quality graphite deposits should also be explored within terrains that have experienced retrograde metamorphism.

References

Ahtola T, Kuusela J (2015) Esiselvitys Suomen grafiittipotentiaalista. Archive report, 88/2015. Geological Survey of Finland

Arkimaa H, Hyvönen E, Lerssi J, Loukola-Ruskeeniemi K, Vanne J (2000) Suomen Mustaliuskeet aeromagneettisella kartalla – Proterozoic black shale formations and aeromagnetic anomalies in Finland 1:1 000 000. Geological Survey of Finland

Auzanneau E, Schmidt MW, Vielzeuf D, Connolly JAD (2010) Titanium in phengite: a geobarometer for high temperature eclogites. Contrib Mineral Petrol 159:1–24

Beowulf Mining plc (2019) Strategy. https://beowulfminingcom/about-us/strategy/ Accessed 27 October 2019

Beyssac O, Goffé B, Chopin C, Rouzaud JN (2002) Raman spectra of carbonaceous material in metasediments: a new geothermometer. J Metamorph Geol 20:859–871

Beyssac O, Rumble D (2014) Graphitic carbon: ubiquitos, diverse and useful geomaterial. Elements 10:415–420

Coggon R, Holland TJB (2002) Mixing properties of phengitic micas and revised garnet-phengite thermobarometers. J Metamorph Geol 20: 683–696

DigiKP, Geological Survey of Finland (2017) Digital map database of the bedrock of Finland. https://gtkdatagtkfi/Kalliopera/indexhtml Accessed 25 October 2019

Eckmann A, Felten A, Mishchenko A, Britnell L, Krupke R, Novoselov KS, Casiraghi C (2012) Probing the nature of defects in graphene by Raman spectroscopy. Nano Lett 12:3925–3930

European Commission (2017a) Study on the review of the list of critical raw materials. Executive summary 9pp https://publicationseuropaeu/en/publication-detail/-/publication/08fdab5f-9766-11e7-b92d-01aa75ed71a1/language-en Accessed 21 June 2018

European Commission (2017b) Communication from the Commission to the European Parliament, the Council, the European Economic and Social Committee and the Committee of the Regions on the 2017 list of Critical Raw Materials for the EU 8pp https://eceuropaeu/transparency/regdoc/rep/1/2017/EN/COM-2017-490-F1-EN-MAIN-PART-1PDF Accessed 21 June 2018

Ferrari AC (2007) Raman spectroscopy of graphene and graphite: disorder, electron-phonon coupling, doping and nonadiabatic effects. Solid State Commun 143:47–57

Ferrari AC, Basko DM (2013) Raman spectroscopy as a versatile tool for studying properties of graphene. Nat Nanotechnol 8:235–246

Ferrari AC, Meyer JC, Scardaci V, Casiraghi C, Lazzeri M, Mauri F, Piscanec S, Jiang D, Novoselov KS, Roth S, Geim AK (2006) Raman spectrum of graphene and graphene layers. Phys Rev Lett 97:187401

Gautneb H (2016) Graphite in Fennoscandia. Presentation at Nordic Mining Day PDAC 2016 https://wwwnguno/sites/default/files/05_Gautneb_Graphitepdf Accessed 27 October 2019

Gautneb H, Tveten E (2000) Geology, exploration and characterization of graphite in the Jennestad area, Vesterålen, northern Norway. NGU-Bull 436:67–74

Holland T, Powell R (1996) Thermodynamics of order-disorder in minerals. 2. Symmetric formalism applied to solid solutions. Am Mineral 81:1425–1437

Holland TJB, Powell R (1998) An internally consistent thermodynamic data set for phases of petrological interest. J Metamorph Geol 16: 309–343

Holland T, Powell R (2001) Calculation of phase relations involving haplogranitic melts using an internally consistent thermodynamic dataset. J Petrol 42:673–683

Hyvönen E, Airo M-L, Arkimaa H, Lerssi J, Loukola-Ruskeeniemi K, Vanne J, Vuoriainen S (2013) Airborne geophysical, petrophysical and geochemical characteristics of Paleoproterozoic black shale units in Finland: applications for exploration and environmental studies. In: Hölttä P (ed) Geological Survey of Finland, Report of Investigation, vol 198, pp 59–61

Hölttä P, Heilimo E (2017) Metamorphic Map of Finland in bedrock of Finland at the scale 1:1 000 000 – major stratigraphic units,

metamorphism and tectonic evolution. In: Nironen M (ed) Geological Survey of Finland, Special Paper, pp 6075–6126

Kähkönen Y (2005) Svecofennian supracrustal rocks. In: Lehtinen M, Nurmi PA, Rämö OT (eds) Precambrian Geology of Finland. Dev in Precambrian Geol, vol 14. Elsevier, Amsterdam, pp 343–405

Katagiri G, Ishida H, Ishitani A (1988) Raman spectra of graphite edge planes. Carbon 26:565

Kujanpää P (2017) Kvalitetsbestämning av flakgrafit i norra Viistola-Hyypiäområdet, östra Finland. Master's thesis. Åbo Akademi University, Turku 60 pp

Leading Edge Materials (2018) Woxna graphite. https://leadingedgematerialscom/woxna-graphite/ Accessed 27 October 2019

Lynch EP, Hellström FA, Huhma H (2016) The Nunasvaara graphite deposit, northern Sweden: new geochemical and U-Pb zircon age results from the host greenstones. Conference abstract, Nordic Geological Winter Meeting 13–15 January 2016, Helsinki http://www.geologinenseura.fi/winter_meeting/abstracts_newnum_pdf/S2_1_365.pdf Accessed 27 October 2019

Lynch EP, Hellström FA, Huhma H, Jönberger J, Persson P-O, Morris GA (2018) Geology, lithostratigraphy and petrogenesis of c. 2.14 Ga greenstones in the Nunasvaara and Masugnsbyn areas, northernmost Sweden. In: Bergman S (ed) Geology of the Northern Norrbotten ore province, northern Sweden, Rapporter och meddelanden, Sveriges geologiska undersökning, vol 141, pp 19–77

Mineral Deposits and Exploration (n.d.) Geological Survey of Finland. https://gtkdata.gtk.fi/mdae/index.html Accessed 25 October 2019

Nemanich RJ, Solin SA (1979) First- and second-order Raman scattering from finite-size crystals of graphite. Phys Rev B 20:392–401

Newton RC, Charlu TV, Kleppa OJ (1980) Thermochemistry of the high structural state plagioclases. Geochim Cosmochim Acta 44:933–941

Nironen M (2017) Guide to the geological map of Finland – bedrock 1:1 000 000. In: Nironen M (ed) Bedrock of Finland at the scale 1:1 000 000 – major stratigraphic units, metamorphism and tectonic evolution. Geol Surv Finland Spec Pap, vol 60, pp 41–76

Nironen M, Kousa J, Luukas J, Lahtinen R (2016) Geological map of Finland – bedrock 1:1 000 000. Geological Survey of Finland

Northern Graphite (2019) Graphite pricing. http://northerngraphitecom/about-graphite/graphite-pricing/ Accessed 20 October 2019

Nurmela P (1989) Katsaus Suomen grafiittiesiintymiin. Report M81/1989/1, Geological Survey of Finland

Nygård H (2017) Kvalitetsbestämning av flakgrafit i Haapamäki, Leppävirta, Norra Savolax. Master's thesis. Åbo Akademi University, Turku

Palosaari J, Latonen R-M, Smått J-H, Blomqvist R, Eklund O (2016a) High-quality flake graphite occurrences in a high-grade metamorphic region in Sortland, Vesterålen, northern Norway. Nor J Geol 96:19–26

Palosaari J, Eklund O, Raunio S, Lindfors T, Latonen R-M, Peltonen J, Smått J-H, Kauppila J, Lund, S, Sjöberg-Eerola P, Blomqvist R, Marmo J (2016b) FennoFlakes: a project for identifying flake graphite ores in the Fennoscandian shield and utilizing graphite in different applications. Geophysical Research Abstracts 18. EGU General Assembly 2016

Pearce JA, Godel BM, Thompson M (2015) Microstructures and mineralogy of a world-class graphite deposit. Society of Economic Geologists, Annual Conference 2015 Hobart, Australia. Program and abstracts

Pierson HO (1993) Handbook of carbon, graphite, diamond and fullerenes. Noyes Publications, Saddle River

Puustinen K (2003) Suomen kaivosteollisuus ja mineraalisten raaka-aineiden tuotanto vuosina 1530-2001, historiallinen katsaus erityisesti tuotantolukujen valossa Geological Survey of Finland Archive report, M101/2003/3 Web-version: http://weppigtkfi/aineistot/kaivosteollisuus/Grafiittikaivoksethtm Accessed 20 June 2018

Rahl JM, Anderson KM, Brandon MT, Fassoulas C (2005) Raman spectroscopic carbonaceous material thermometry of low-grade metamorphic rocks: calibration and application to tectonic exhumation in Crete, Greece. Earth Planet Sci Lett 240:339–354

Rankama K (1948) New evidence of the origin of pre-Cambrian carbon. Bull Geol Soc Am 59:399–416

Rønning JS, Gautneb H, Larsen BE, Knežević J, Baranwal VC, Elvebakk H, Gellein J, Ofstad F, Brönner M (2018) Geophysical and geological investigations of graphite occurrences in Vesterålen and Lofoten, Northern Norway 2017. NGU report 2018.011. Geological Survey of Norway

Sarapää O, Kukkonen I (1984a) Grafiittitutkimukset Kiihtelysvaaran Hyypiässä vuosina 1981-1983. Report M 81/4241/−84/2. Geological survey of Finland

Sarapää O, Kukkonen I (1984b) Grafiittiesiintymistä ja niiden energiakäyttömahdollisuuksista. Report M 81/1984/3. Geological survey of Finland

Simonen A (1982) Mäntyharjun ja Mikkelin kartta-alueiden kallioperä. Summary: pre-quaternary rocks of the Mäntyharju and Mikkeli map-sheet areas. Geological map of Finland 1:100 000, explanation to the maps of pre-quaternary rocks, sheets 3123 and 3142. Geological Survey of Finland

Tajčmanová L, Connolly JAD, Cesare B (2009) A thermodynamic model for titanium and ferric iron solution in biotite. J Metamorph Geol 27:153–164

Waldbaum DR, Thompson JB (1968) Mixing properties of sanidine crystalline solutions: 2. Calculations based on volume data. Am Mineral 53:2000–2017

Wall M (2012) Raman spectroscopy optimizes graphene characterization. Adv Mater Process 170:35–38

White RW, Powell R, Holland TJB, Worley BA (2000) The effect of TiO_2 and Fe_2O_3 on metapelitic assemblages at greenschist and amphibolite facies conditions: mineral equilibria calculations in the system K_2O-FeO-MgO-Al_2O_3-SiO_2-H_2O-TiO_2-Fe_2O_3. J Metamorph Geol 18:497–511

White RW, Powell R, Holland TJB (2001) Calculation of partial melting equilibria in the system Na_2O-CaO-K_2O-FeO-MgO-Al_2O_3-SiO_2-H_2O (NCKFMASH). J Metamorph Geol 19:139–153

Wopenka B, Pasteris JD (1993) Structural characterization of kerogens to granulite-facies graphite: applicability of Raman microprobe spectroscopy. Am Mineral 78:533–557